FUEL INSPECTION REPORT
REC'D W/LTR DTD 8-10-76
CN# 8244 docket No. 50-247

— NOTICE —

THE ATTACHED FILES ARE OFFICIAL RECORDS OF THE DIVISION OF DOCUMENT CONTROL. THEY HAVE BEEN CHARGED TO YOU FOR A LIMITED TIME PERIOD AND MUST BE RETURNED TO THE RECORDS FACILITY BRANCH 016. PLEASE DO NOT SEND DOCUMENTS CHARGED OUT THROUGH THE MAIL. REMOVAL OF ANY PAGE(S) FROM DOCUMENT FOR REPRODUCTION MUST BE REFERRED TO FILE PERSONNEL.

DEADLINE RETURN DATE _____

RETURN TO REGULATORY CENTRAL FILES
ROOM 016
REGULATORY DOCKET FILE COPY

RECORDS FACILITY BRANCH

8110210187 760831
PDR ADOCK 05000247
Q PDR

INDIAN POINT UNIT NO. 2

FUEL INSPECTION

This Report was prepared
with the participation of
Nuclear Assurance Corporation
of Atlanta, Georgia

Docket # 50-247
Control # 8244
Date Recvd. 8-10-76
Regulatory Docket File

CONSOLIDATED EDISON COMPANY OF NEW YORK, INC.

AUGUST, 1976

Indian Point Unit No. 2

Fuel Inspection

TABLE OF CONTENTS

		Page No.
1	Summary	1-1
2	System Qualification Results	2-1
3	Visual Examination	3-1
4	Assembly Bow	4-1
5	Assembly Twist	5-1
6	Rod Length	6-1
7	Rod Bow	7-1

SUMMARY AND CONCLUSIONS

A visual fuel inspection of the two lead burnup assemblies of each region of the core at Indian Point Unit No. 2 was completed on May 3, 1976 during our first refueling outage. The following assemblies along with their burnups at end-of-cycle 1 were inspected:

Assembly	Burnup (MWD/MTU)
A04	18792
A44	18475
B16	20072
B17	20096
C02	18045
C10	17975

The television examination of the peripheral rods of these fuel assemblies indicated that the overall condition was excellent, with light to medium patchy oxide covering the active fuel cladding surfaces. The crud layer on the peripheral rods surfaces appeared to be thin; however, crud spalling was noticed on some of the rods. In addition, some very small particles were identified in a few flow channels between the peripheral rods at the lower nozzle and in the spacer springs of the grid. Due to the minute size of these particles, their effect on fuel performance is insignificant.

Dimensional measurements were performed on all six assemblies inspected employing a camera capable of high magnification mounted on a movable carriage. The carriage moved vertically up-and-down the inspection stand which held the assembly in an open-sided basket. The camera position was monitored by electronic encoders that travel with the camera along pre-calibrated tracks. Figure 1 shows the inspection stand,

Minimal bowing of the peripheral rods was seen; dimensional measurements were performed on all areas that rod bowing appeared to have occurred. Dimensional measurements of rod length, rod bow, assembly bow and assembly twist were made. Analysis of the dimensional results indicated that (1) average rod growth of "A", "B" and "C" assemblies were 0.415, 0.642 and 0.588 inches respectively; (2) the maximum assembly bow was 0.177 inches; (3) maximum rod bow was 0.047 inches corresponding to a 33% rod to rod gap closure; (4) the maximum assembly twist was 2.69°. In general, no evidence of fuel cladding failure or any other condition (such as clad flattening) that could lead to unacceptable fuel performance was observed.

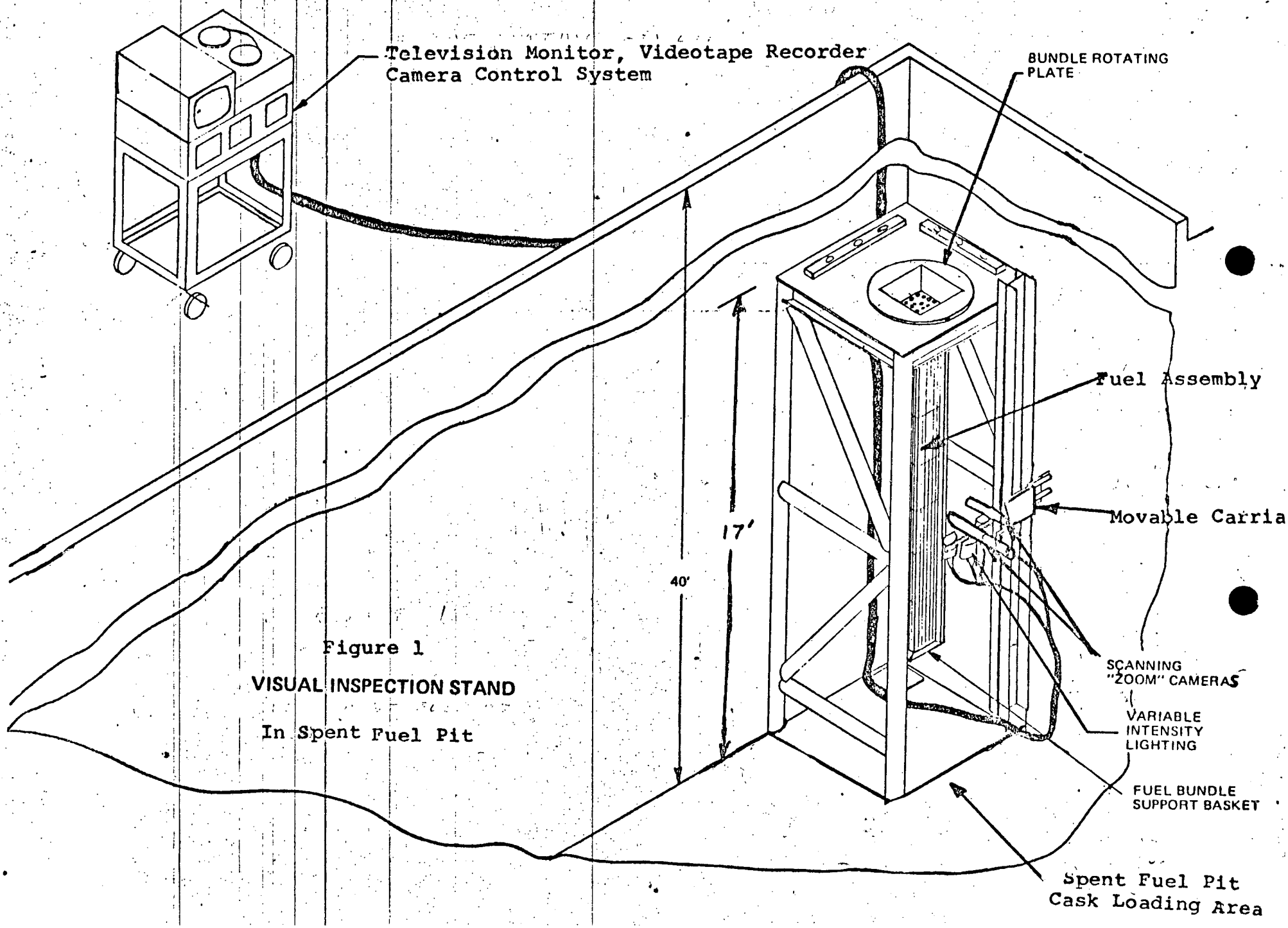

Figure 1

VISUAL INSPECTION STAND

In Spent Fuel Pit

SYSTEM QUALIIFICATION

The visual inspection system was qualified at Indian Point during April 14 and 15, 1976 for width, length and bow system runout. Table 1 is a summary of the system's bias and precise results.

TABLE 1

SYSTEM QUALIFICATION SUMMARY

	Bias (Inches)	Precision (Inches) One Sigma	Two Sigma
Length	-0.0001	±0.0048	±0.0096
Width	0.0000	±0.0023	±0.0046
System Runout	0.0010	±0.0107	±0.0214

The precision of system runout is limited by the degree of polynomial fit. The precision could be improved by increasing (1) the number of data points taken and (2) the degree of polynomial regression analysis available. The system runout precision should approach that of the width precision. However, because of the way the system runout is calculated, the system runout precision will be greater than the width precision.

The fuel inspection stand was set up in a vertical position and the legs leveled by adjusting the (stand) feet. Using a bubble level, the television carriage (vertical) tracks were made vertical by adjusting the stand's feet. After the stand was

properly aligned, the fuel assembly support basket was then leveled. At this time, the calibration standard was installed into the basket and also made vertical by adjusting it's feet.

The first step to qualify the system was to determine the relationship of the vertical encoder to the standard's vertical scale. Encoder readings were taken at various positions over the entire length of the scale and then reduced using a calculation program to determine the bias and precision of the system. These measurements are shown in Table 2. A linear least squares fit of the data was first performed to determine the relationship between the scale and encoder readings. This fit (Figure1A) indicated the vertical encoder readings had to be multiplied by 1.0006 to correct the reading of the vertical position in inches. The data in Table 2 were reduced to determine the reading bias, if any, and precision. This was accomplished by taking incremental scale and corrected encoder readings, then subtracting the delta values from each other to determine the measurement error. Figure 2 is a frequency histogram of the measurement errors incurred during the length qualification. The data reduction showed a -0.001 inches system bias and a precision of ± 0.0048 inches at the one sigma level.

Using the same calculator program as for length qualification, encoder width measurements were qualified. Multiple measurements shown in Table 3 were made to determine to the encoder correction factor, bias, and precision of the system.

The first stage of the data reduction, Figure 3, showed a 1 to 1 correlation between the encoder reading and scale position, this indicating that no correction factor was required for the width encoder readings. Further data reduction, Figure 4, showed a 0.0000 inches bias and a precision of ± 0.0023 inches at the one sigma level.

After both encoders were calibrated for length and width measurements, the system for bow measurement was qualified. Qualification of the system was done in two steps; one to determine the runout of the mechanical system, and the other to determine the reading bias and precision. Incorporated within the standard is a 0.012 inch thick multiple strand wire stretched over the length to be measured for bow. Horizontal and vertical readings were taken at various points along this stretched wire to determine the system runout. These measurements (shown in Table 4) were taken by aligning the right side of the vertical crosshair imposed on the vertical television screen with the left side of the stretched wire and then recording the x and y positions. A polynomial regression analysis was used to best fit the data points. A 9th degree polynomial equation (shown in Figure 5) best represented the data points for system runout. Since it was highly improbable that the wire was vertical, a linear least squares fit was performed on the data to determine the vertical tilt of the wire. For a given vertical position, the difference between the 9th degree polynomial and linear equations was determined to be the system runout. The equation for the

system runout, X_s, is shown below:

$$X_s=a+a_1y+a_2y^2+a_3y^3+a_4y^4+a_5y^5+a_6y^6+a_7y^7+a_8y^8+a_9y^9$$

where $a = 5.4836 \times 10^{-2}$
$a_1=-1.38073\times10^{-3}$
$a_2= 2.17615\times10^{-4}$
$a_3=-1.95168\times10^{-5}$
$a_4= 6.3853 \times10^{-7}$
$a_5=-1.03668\times10^{-8}$
$a_6= 9.11857\times10^{-11}$
$a_7=-4.30390\times10^{-13}$
$a_8= 9.73497\times10^{-16}$
$a_9=-7.17425\times10^{-19}$

To determine the bias and the precision of the system runout, the data points tabulated in Table 4 were converted to inches and compared with the 9th degree polynomial equation. Figure 6 is a frequency histogram of the difference between the actual data points and calculated data points. The data reduction of error readings for bow runout correction showed a 0.0010 inch bias and a precision of $\pm$0.0107 inches at the one sigma level. This bias and precision included the width and system runout error.

TABLE 2

QUALIFICATION DATA - LENGTH MEASUREMENT

Run 1		Run 2		Run 3	
Scale (Inches)	Encoder	Scale (Inches)	Encoder	Scale (Inches)	Endcoder
1.000	.9965	140.000	139.9150	10.000	9.9905
15.000	14.9865	135.000	134.9165	15.000	14.9875
30.000	29.9725	115.000	114.9190	20.000	19.9810
45.000	44.9740	100.000	99.9320	50.000	49.9655
60.000	59.9595	85.000	84.9510	65.000	64.9590
75.000	74.9540	60.000	59.9615	80.000	79.9485
90.000	89.9480	50.000	49.9695	95.000	94.9360
105.000	104.9295	40.000	39.9735	110.000	109.9260
120.000	119.9240	30.000	29.9785	125.000	124.9200
130.000	129.9185	20.000	19.9865	135.000	134.9060
140.000	139.9150	10.000	9.9905	140.000	139.9050

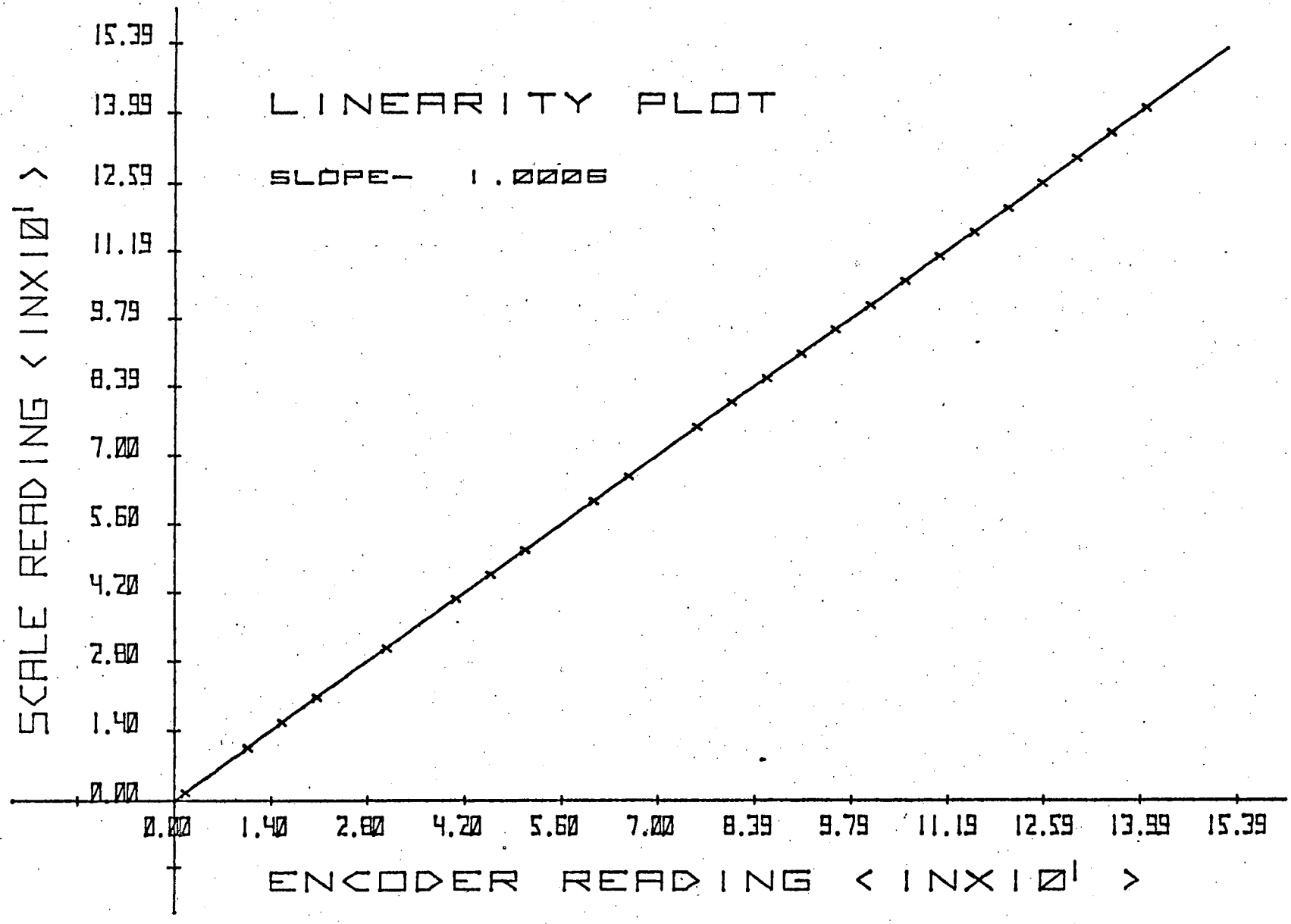

Figure 1A Length Measurement Linearity

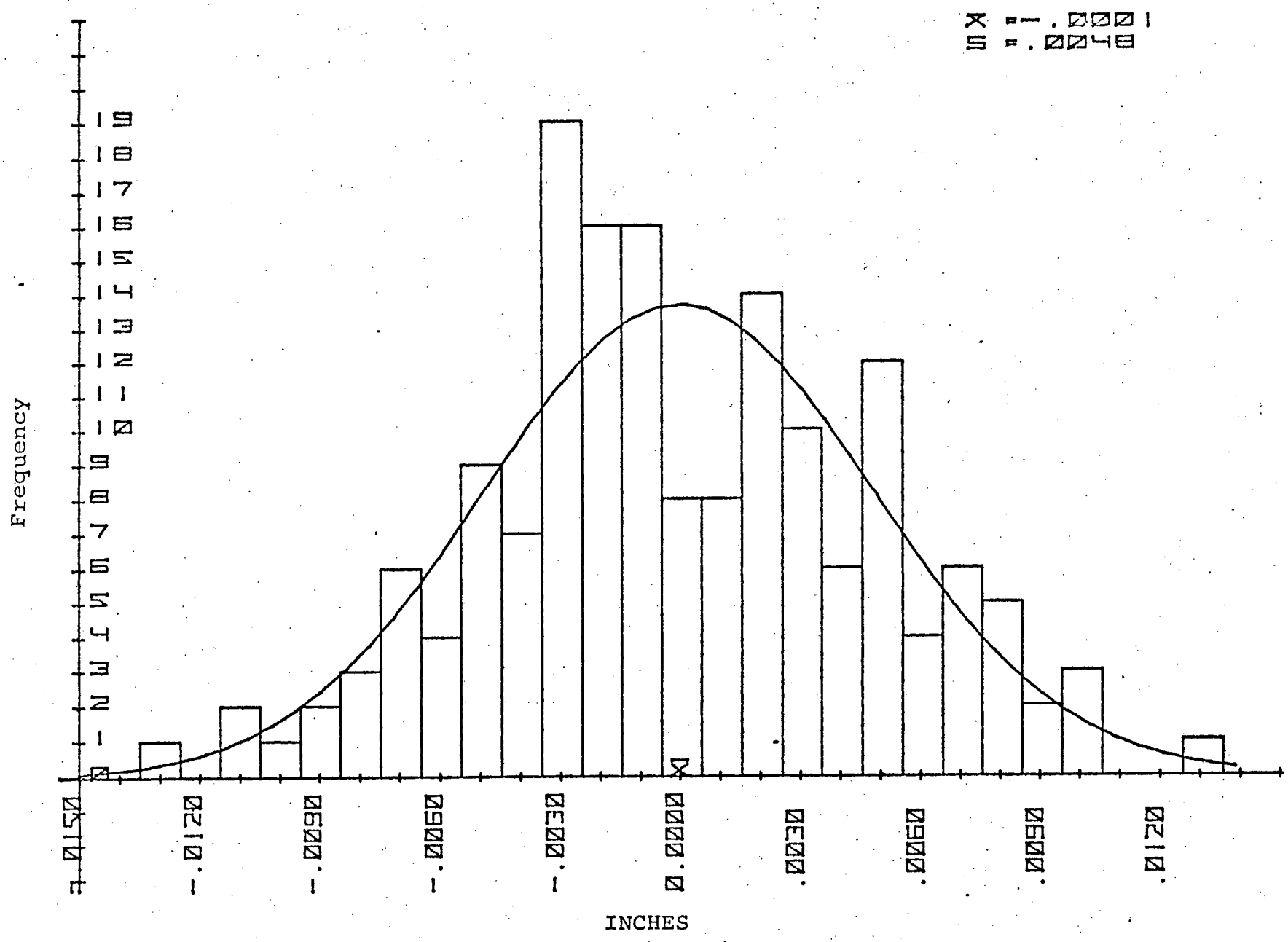

Figure 2 Length Qualification Bias & Standard Deviation

TABLE 3

QUALIFICATION DATA - WIDTH MEASUREMENT

Run 1		Run 2	
Scale (Inches)	Encoder	Scale (Inches)	Encoder
1.015	1.0000	10.750	10.7338
2.000	1.9855	9.000	8.9836
3.030	3.0141	8.125	8.1079
3.985	3.9680	7.250	7.2325
5.000	4.9803	6.025	6.0082
6.060	6.0415	5.500	5.4817
7.560	7.5422	4.000	3.9838
8.000	7.9825	2.505	2.4890
9.250	9.2375	1.750	1.7329
10.750	10.7338	1.000	0.9825

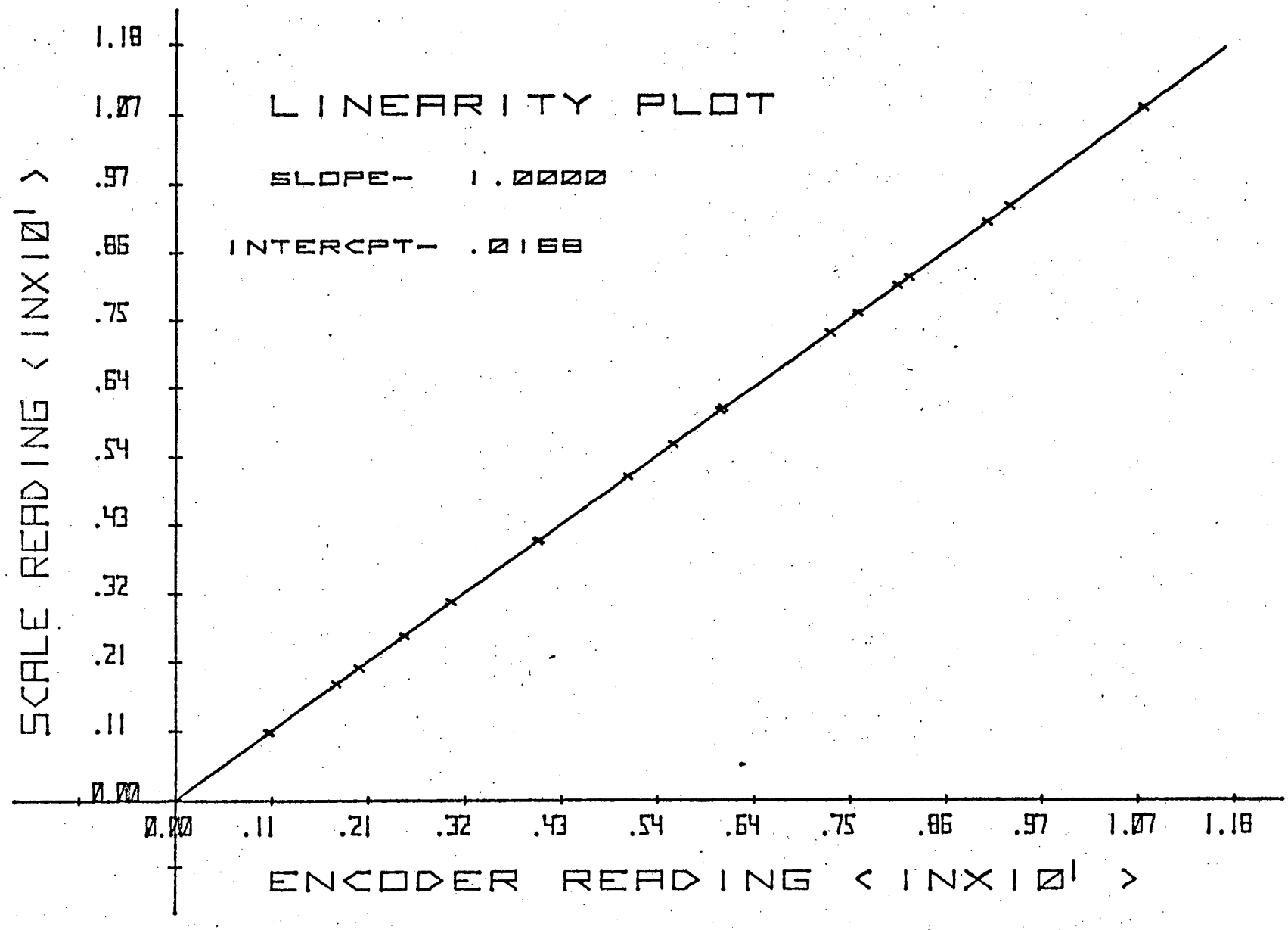

Figure 3. WIDTH MEASUREMENT LINEARITY

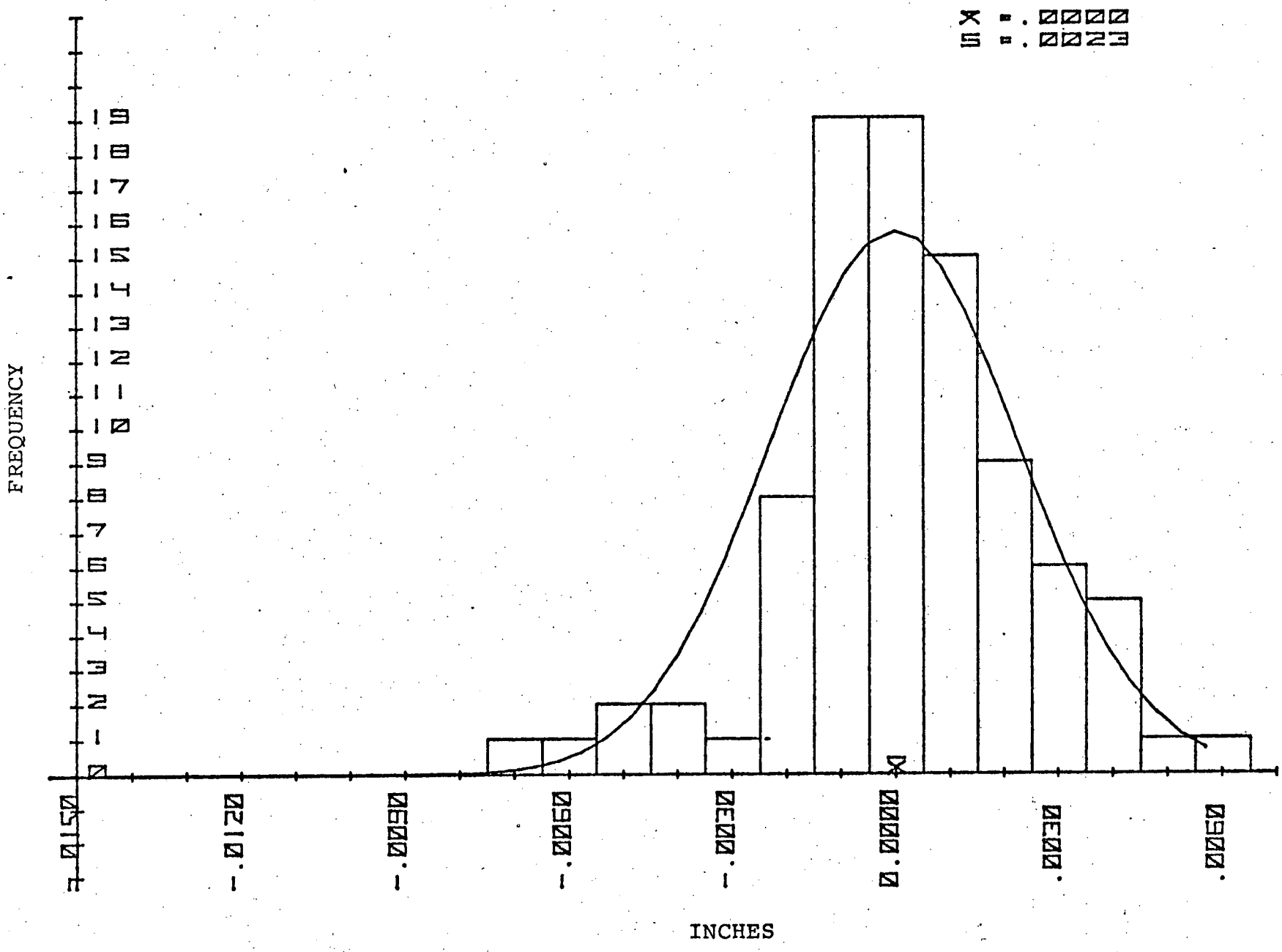

Figure 4. WIDTH QUALIFICATION BIAS & STANDARD DEVIATION

TABLE 4

BOW QUALIFICATION

Run 1		Run 2	
X (Inches)	Y (Inches)	X (Inches)	Y (Inches)
.3226	1.8030	.3174	1.8175
.3198	5.014	.3198	2.7625
.3207	7.0140	.3117	4.9390
.3133	10.3715	.3037	9.0470
.3120	17.0135	.3104	13.8246
.3101	25.0158	.3044	19.7410
.3273	37.000	.3117	29.9980
.3290	48.675	.3118	44.9675
.3268	50.8335	.3043	54.7040
.3238	60.145	.2889	64.8530
.2891	70.003	.2713	75.2500
.2890	80.0005	.2766	85.4585
.2937	84.442	.2653	97.1335
.3027	90.173	.2552	100.0565
.2852	94.276	.2345	108.5935
.2711	100.475	.1937	115.7088
.2574	105.521	.1382	127.4280
.2383	109.461	.0753	136.466
.2176	114.911	.0367	141.2325
.1969	120.234	.0112	144.2400
.1536	127.183	-.0208	148.3205
.1104	134.175	-.0405	150.4035
.0623	141.051		
.0320	146.25		
-.0045	150.61		

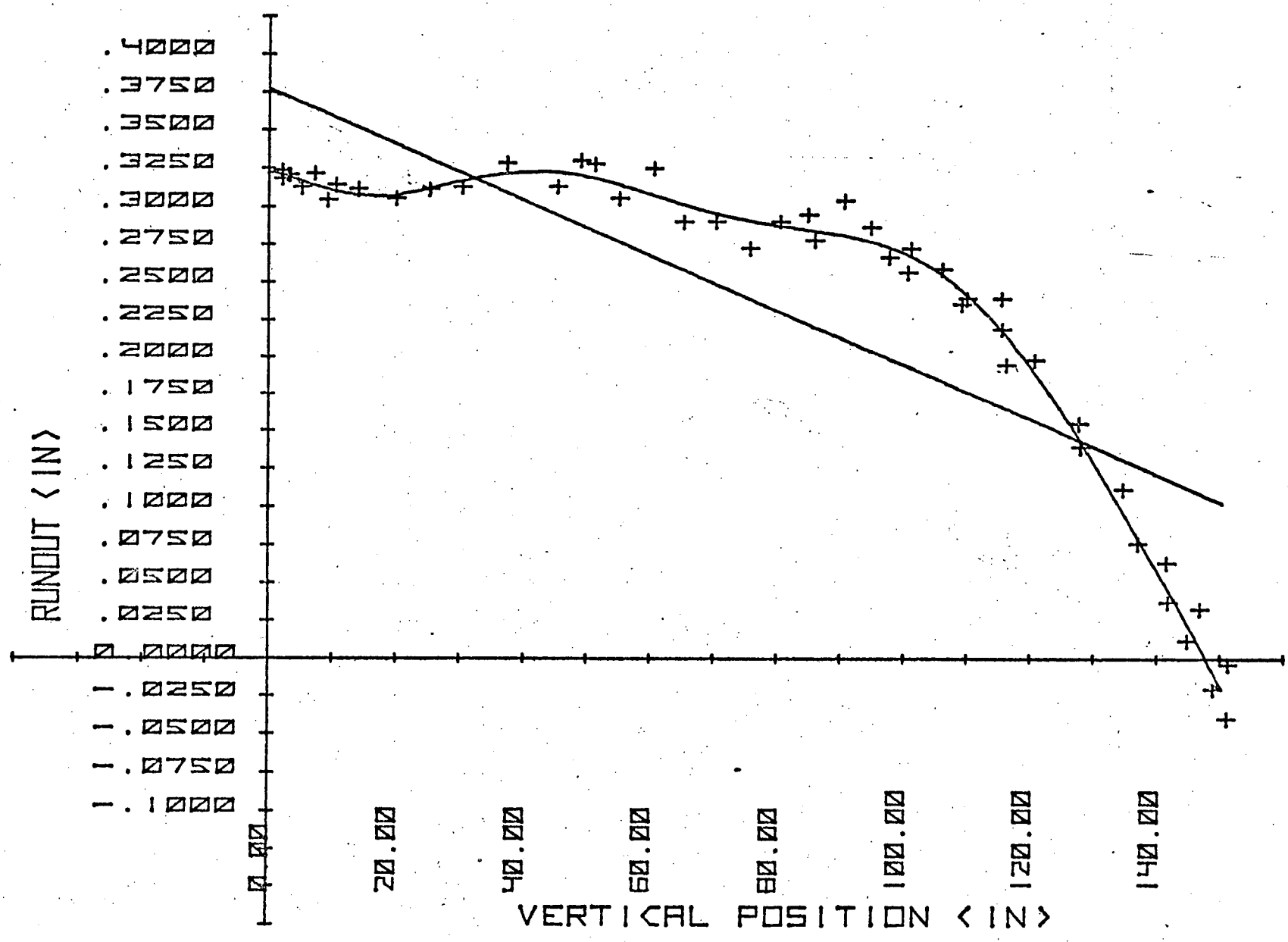

Figure 5. Bow Qualification for System Runout

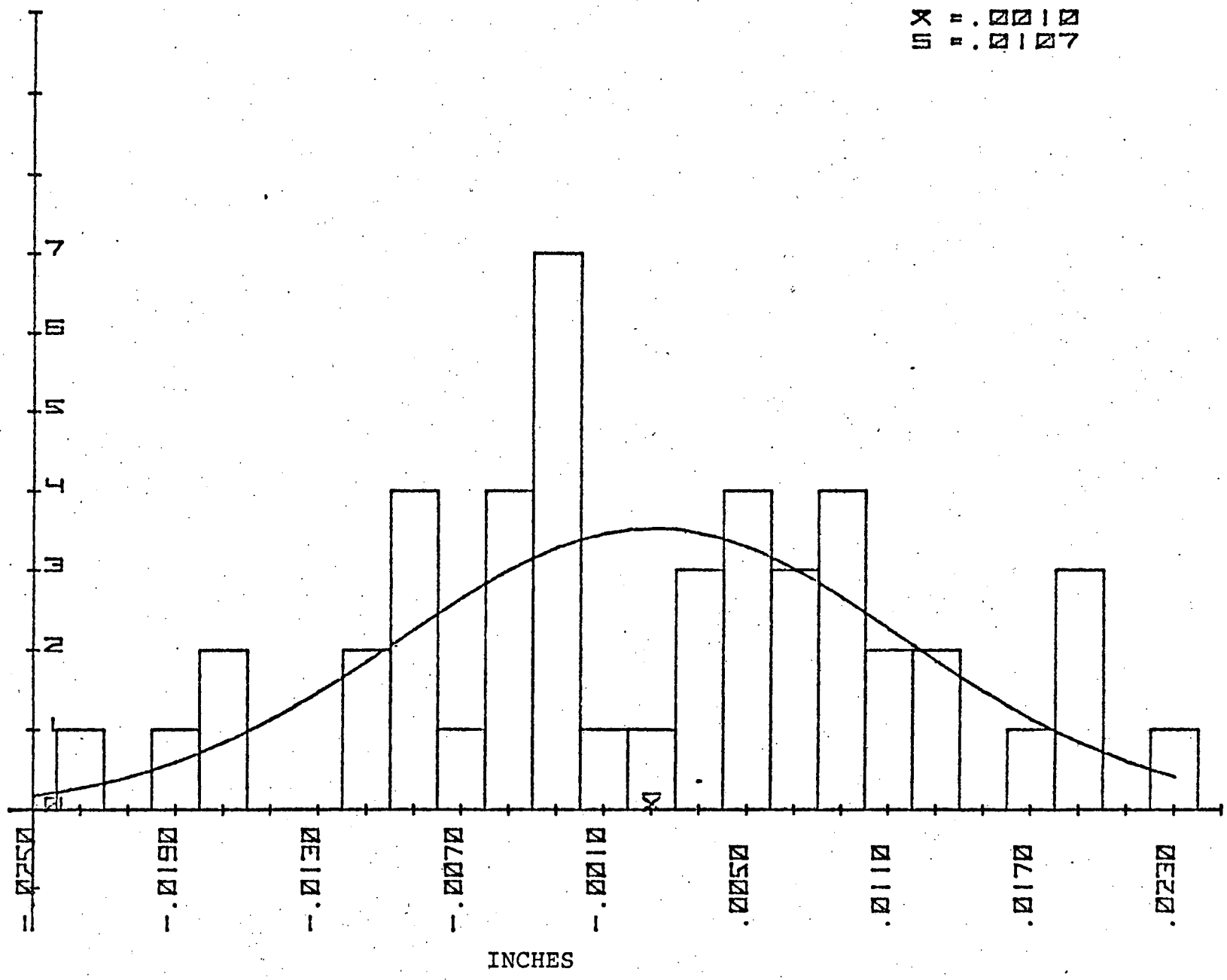

Figure 6 Runout Qualification Bias & Standard Deviation

RESULTS

Visual Examination

The peripheral rods examined in the six 15 x 15 Indian Point #2 fuel assemblies specified as the two highest burnup per region appeared to be in excellent condition with light to medium patchy oxide covering the active fuel cladding surfaces. The crud layer on the peripheral rods surfaces appeared to be thin; however, slight crud spalling was noticed on some of the rods. In addition, some very small particles were identified in the flow channels between a few peripheral rods. The majority of the particles were either resting or lodged between the lower nozzle and the bottom of the fuel rods. The remaining particles appeared to be lodged in the peripheral spacer springs or on the spacer tabs of the grids.

The only other major generic item noticed during this examination was that a majority of the rods had a shiny region approximately 0.5 inches above the lower end plug. After further investigation, this region appears to correspond to the weld location of the lower end plug to the zircaloy tubing. A possible explanation of this would be that during welding, the surface of the rod was sensitized.

Two other specific items were seen during this inspection: (1) a fuel rod in Assembly A-04 was touching both the upper and lower nozzle

(2) The bottom nozzle of assembly A44 was observed to have a small area of high reflectivity.

An apparently metallic, very small particle was found lodged diagonally on the top surface of the lower nozzle of fuel assembly B-17 between the endplugs of rods 4 and 5 of face 1. The effect on fuel performance of this paricle was evaluated to be insignificant and the assembly was returned to the core after being vacuum cleaned underwater.

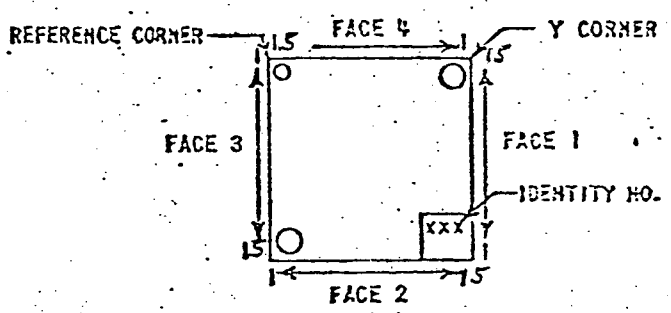

Figure 7 Assembly Face Orientation and Rod Numbering System

Complete video tapes were made of the visual examination of these six fuel assemblies. Figure 7 shows the face orientation for the Indian Point #2 fuel assemblies.

The visual examination of an individual face was carried out in two stages. The first half of the peripheral rods were examined by starting at the lower left side of the assembly and scanning upward at approximately 2½ to 3 feet/min. The second half of the rods were examined by starting from the upper right side of the assembly and scanning downward at the same rate. The elapsed time to scan a complete face for visual examination was approximately 15 to 20 minutes.

Table 5 lists the observations made on the peripheral rods of the six Indian Point #2 fuel assemblies.

TABLE 5

List of Visual Observations
made on the six Indian Point #2 Assemblies

Assembly A-04

Face	Rod	Location (inches)	Observation
1		88	crud particles
3	2,8,9,10,11,12,15	0.5	shiny areas near lower end plug
3	"	1.5	crud hole with spalling
4	"		rod touching both end nozzles
4	1,2,3,4,6,7,9,13,14	0.5	shiny areas near lower end plug

Assembly A-44

Face	Rod	Location (inches)	Observation
1	all	0.5	shiny areas near lower end plug
2	12,13		crud spot on spacer tabs between rods 12 & 13
2	2	63	crud hole with spalling
3	all	0	crud particles located on lower nozzles
4	1	41	crud hole with spalling
4	1	129	crud particle lodged in Grid 3 at corner of Faces 3 & 4

Assembly B-16

Face	Rod	Location (inches)	Observation
1			Normal - nothing unusual with exception of particles in spacers
2			Clean - little or no crud
3	all	0.5	shiny area near lower end plug
4	all	0.5	shiny area near lower end plug

Assembly B-17

Face	Rod	Location (inches)	Observation
1	all	0	crud particles located on bottom nozzles
1	4 & 5	0	particle appears to be lodged in a diagonal in a gap between rods 4 & 5
2			nothing unusual seen
3	all	.05	shiny spots near lower end plug
4			nothing unusual seen

Assembly C-02

Face	Rod	Location (inches)	Observation
1	all	0.5	shiny spots near lower end plug
3	1	13	crud hole with spalling
4	all	0	crud particles located on bottom nozzle

Assembly C-10

Face	Rod	Location (inches)	Observation
1	8	40	shiny spot
2	all		shiny spots near lower end plug
3			nothing unusual seen
4			nothing unusual seen

Assembly Bow

Assembly bow measurements were performed on two faces of the six specified assemblies. Bow measurements were made at the left hand edge of Face 1 and 2. These readings actually describe the bow of the face at 90° (Face 2 and 3 respectively) to the face being observed. The measurements involved first, aligning the right hand side of the television monitor with the center edge of the individual grids and then recording the position location. The locations were then converted to inches and the appropriate system runout for the particular vertical position added to the horizontal reading. The displacement of each grid or bow was then determined by correcting for tilt. This was done by assuming grids 1 and 9 were fixed points of the assembly, and determining the slope between them.

Table 6 is a summary of the maximum assembly bow of individual assemblies measured. Figures 8 through 19 show the assembly bow of the individual faces measured. Assembly B-16 appeared to have the most significant bow on each of the faces measured, 0.149 and 0.177 inches for Faces 2 and 3,respectively. This bow measurement would be typical of the bowing seen when the assembly is free standing, i.e. in storage racks or in reactor core. No problems were encountered during handling and reinsertion of the assembly into the reactor,

TABLE 6

Summary of Assembly Bow Measurements

Assembly	Face	Maximum Bow ($x10^{-3}$ inches)
A-04	1	96.0
	2	140.4
A-44	1	87.7
	2	91.9
B-16	1	149.2
	2	-177.3
B-17	1	65.7
	2	-41.9
C-02	1	36.7
	2	60.9
C-10	1	-34.1
	2	73.1

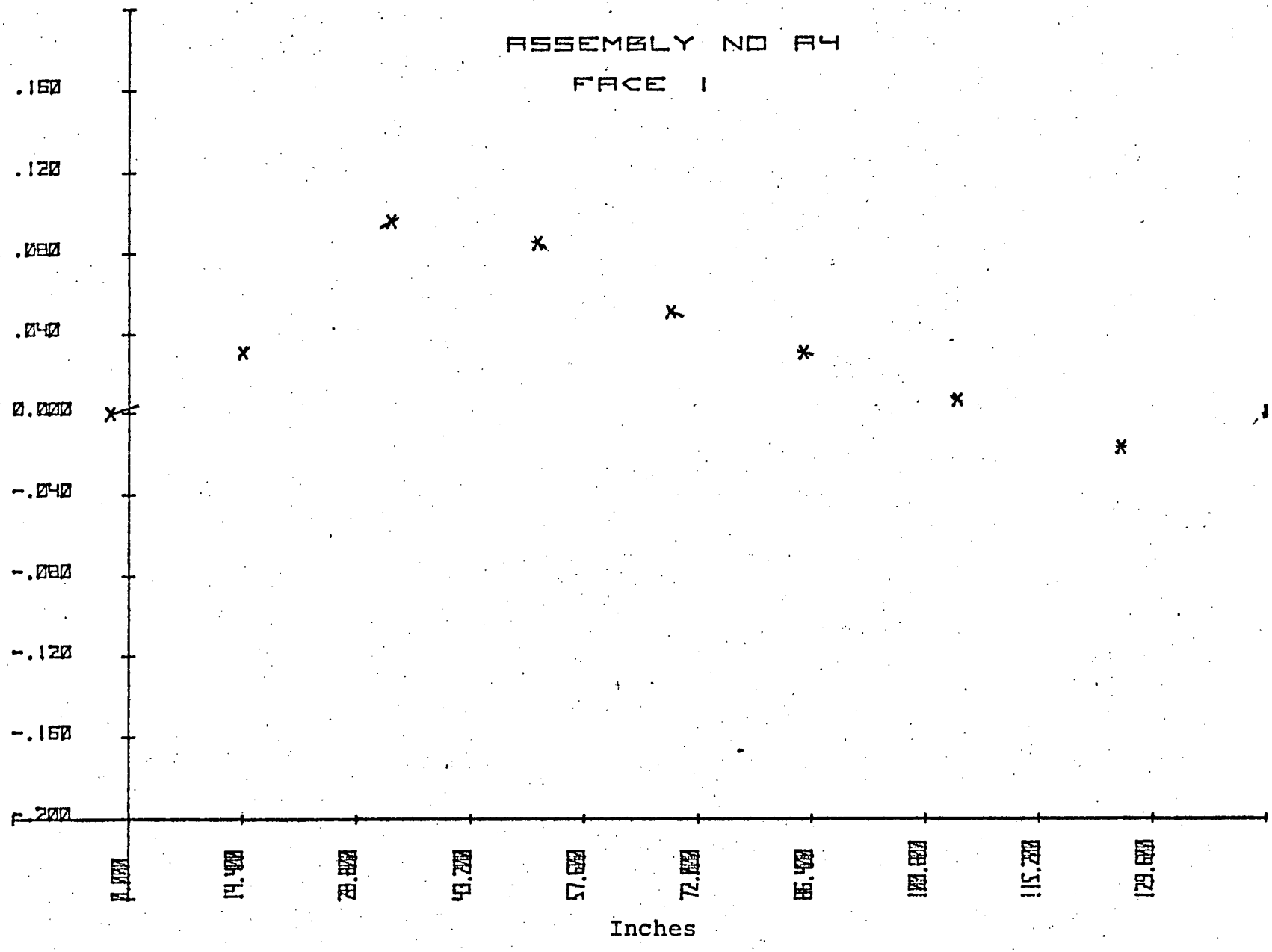

Figure 8 Assembly Bow of Face 1, Assembly A-04

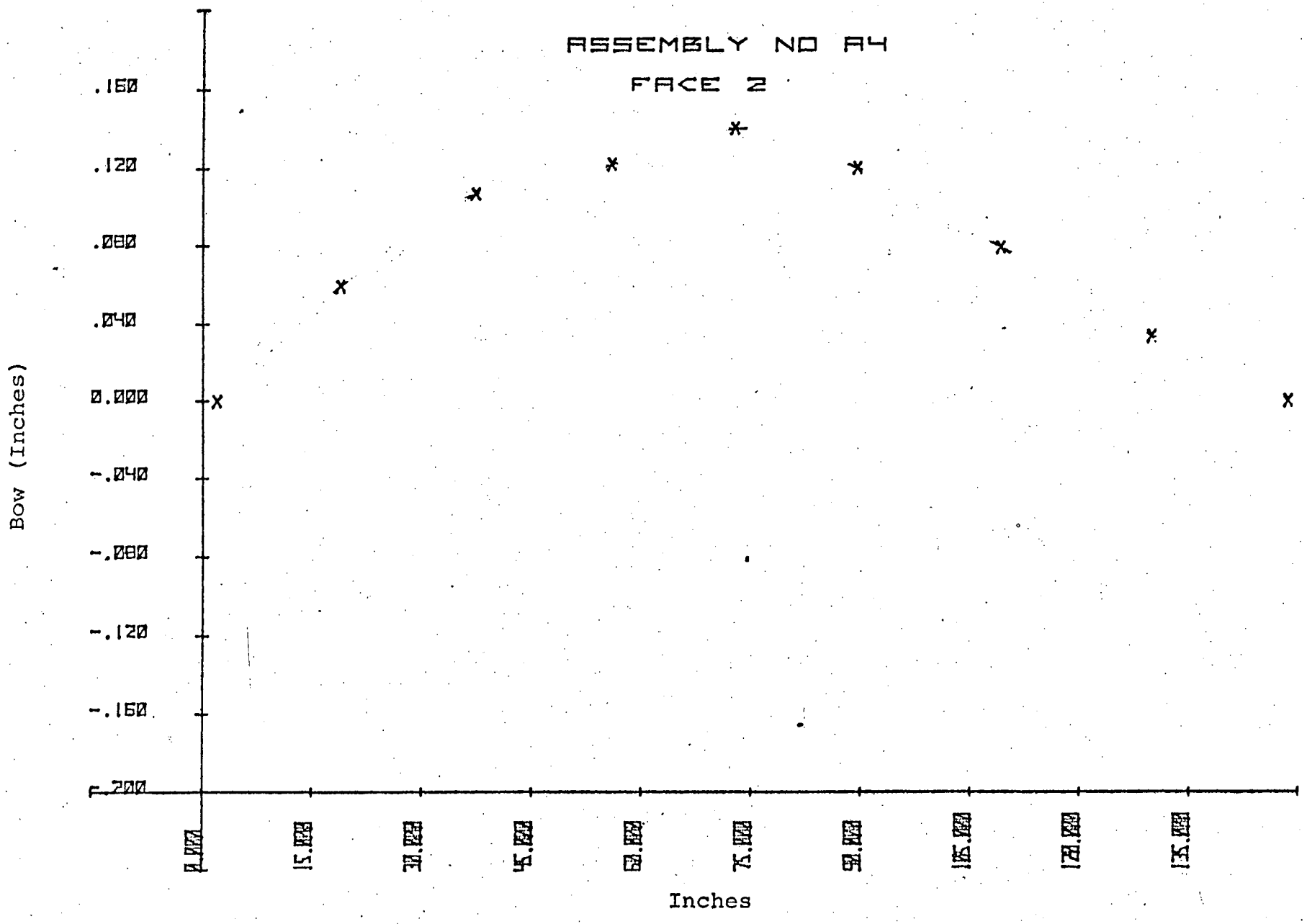

Figure 9 Assembly Bow of Face 2, Assembly A-04

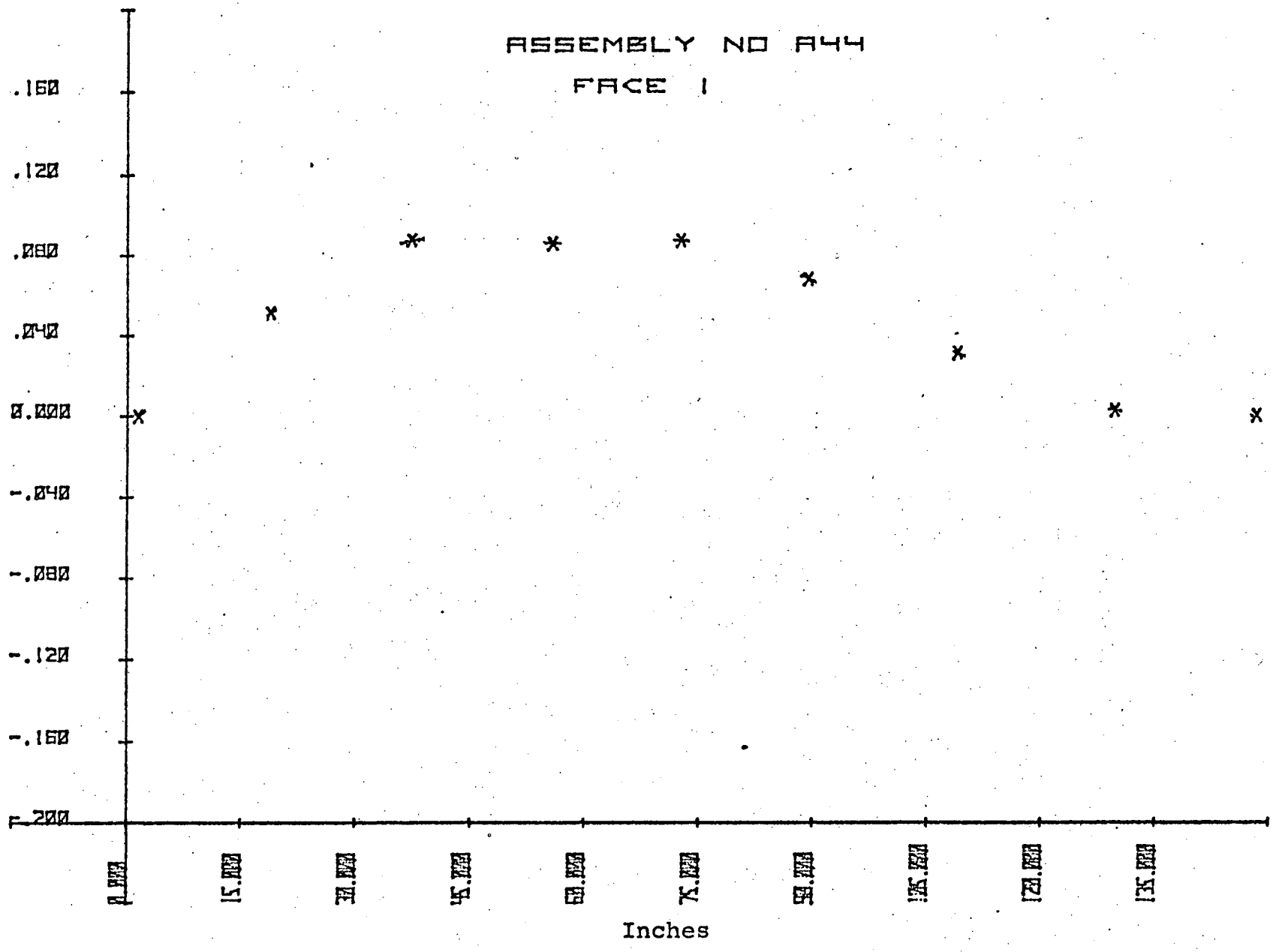

Figure 10 Assembly Bow of Face 1, Assembly A-44

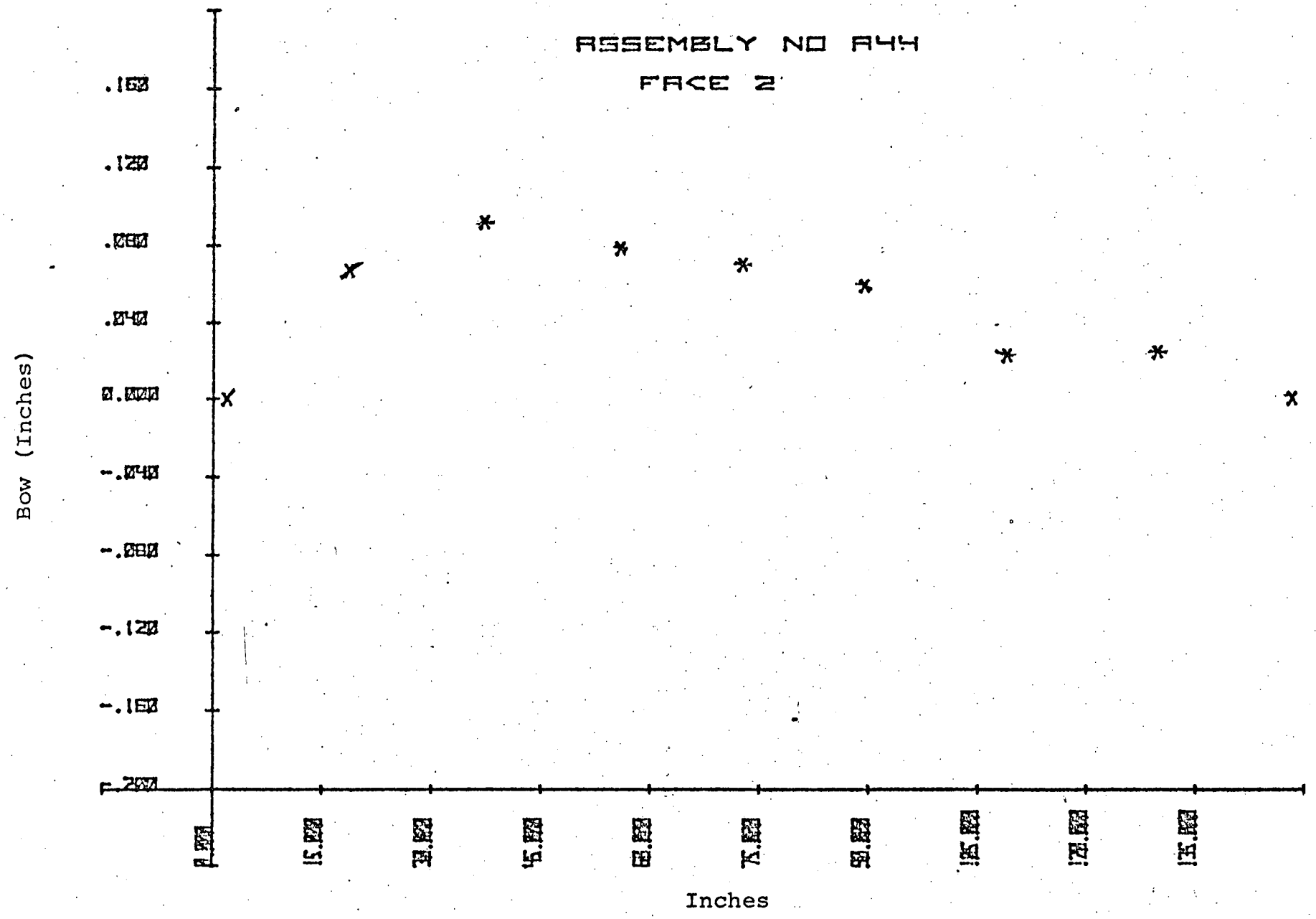

Figure 11 Assembly Bow of Face 2, Assembly A-44

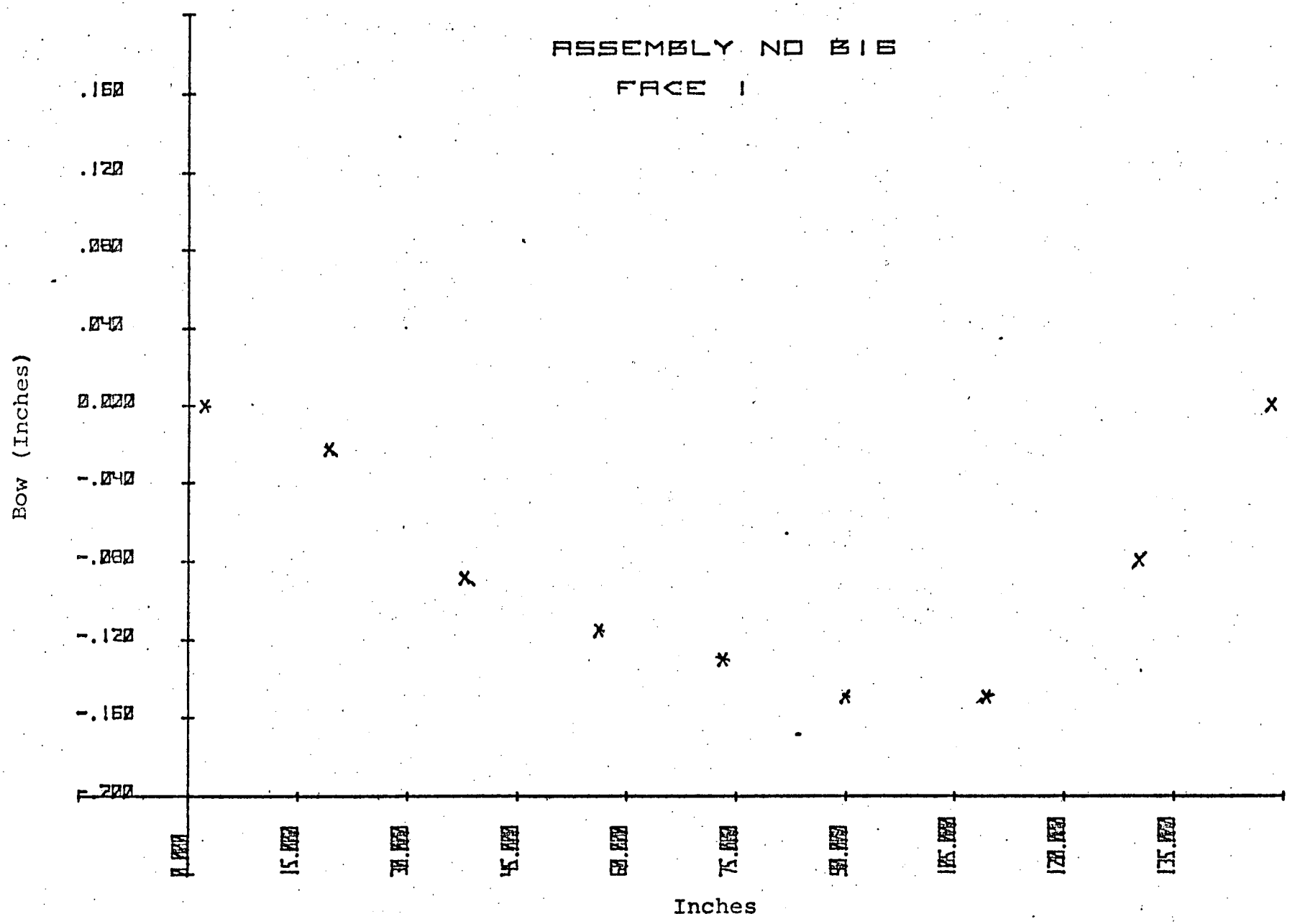

Figure 12 Assembly Bow of Face 1, Assembly B-16

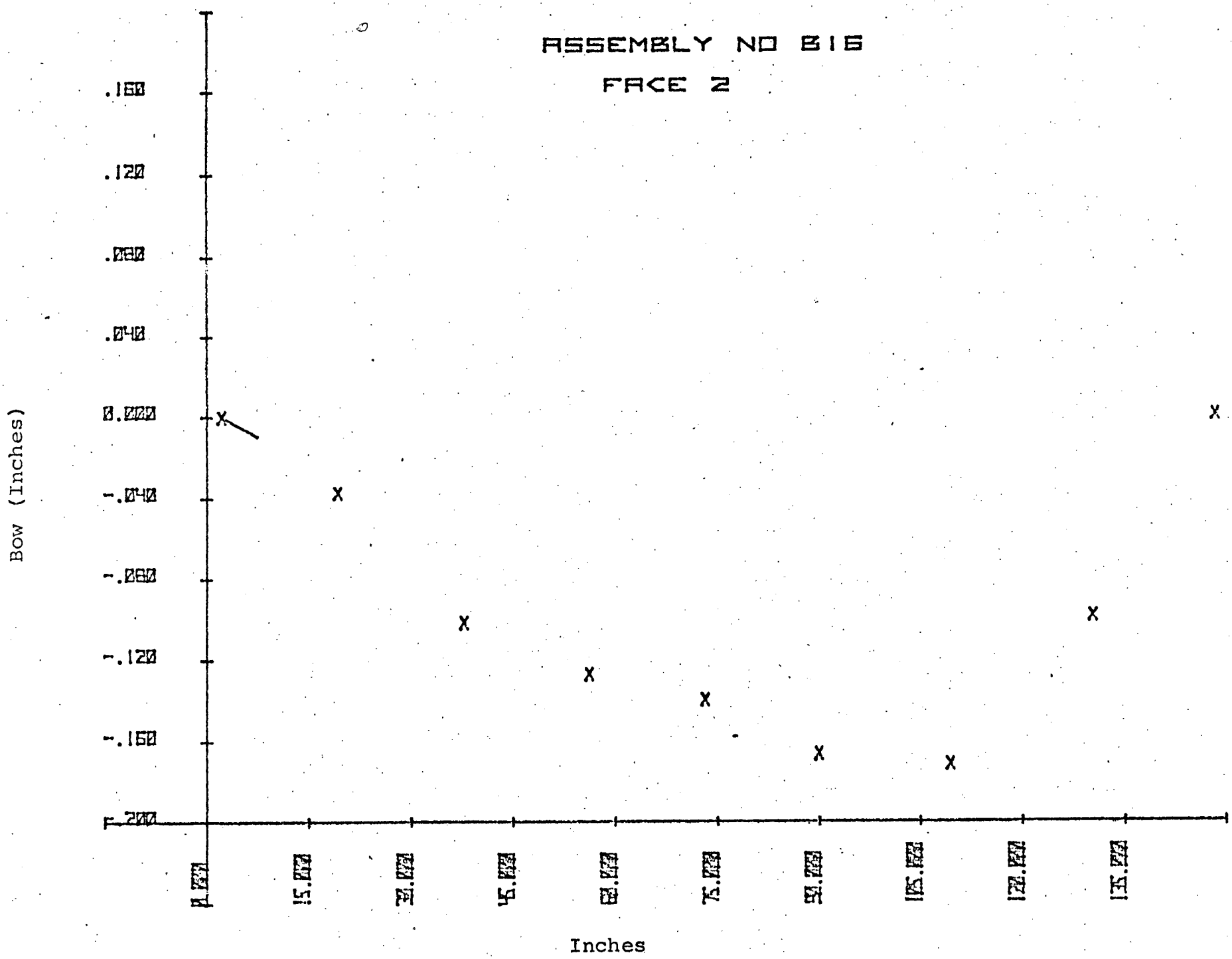

Figure 13 Assembly Bow of Face 2, Assembly B-16

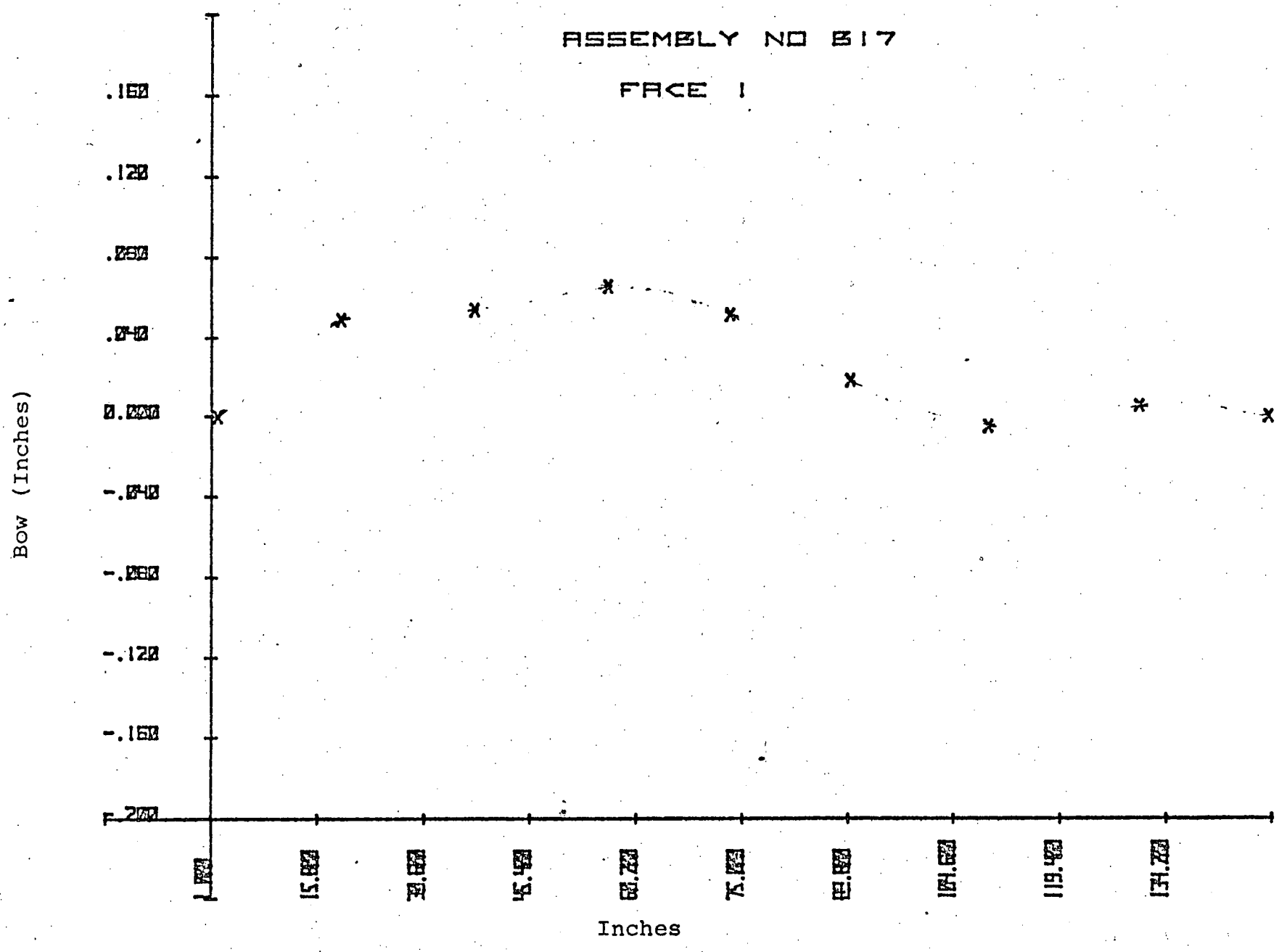

Figure 14 Assembly Bow of Face 1, Assembly B-17

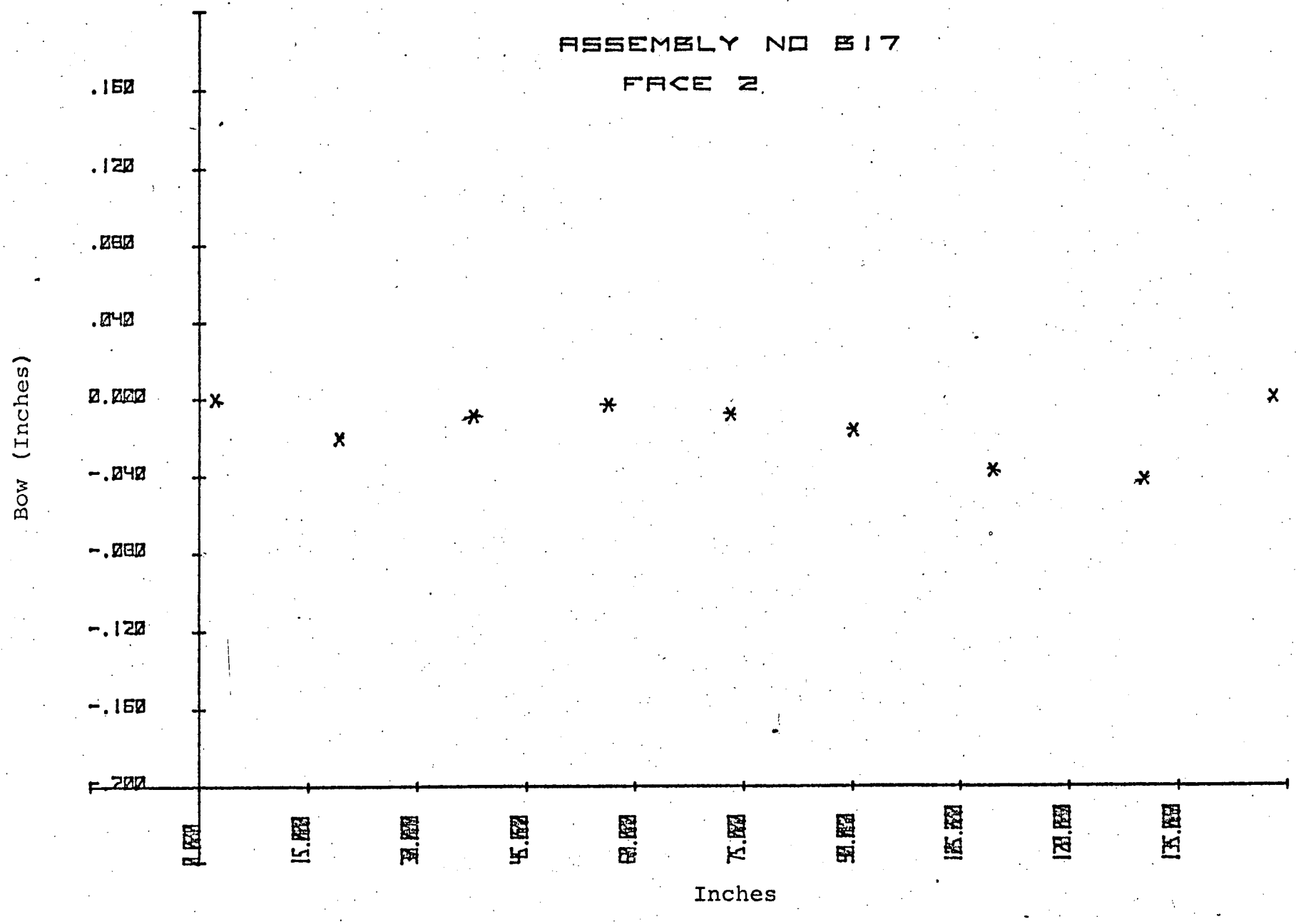

Figure 15 Assembly Bow of Face 2 of Assembly B-17

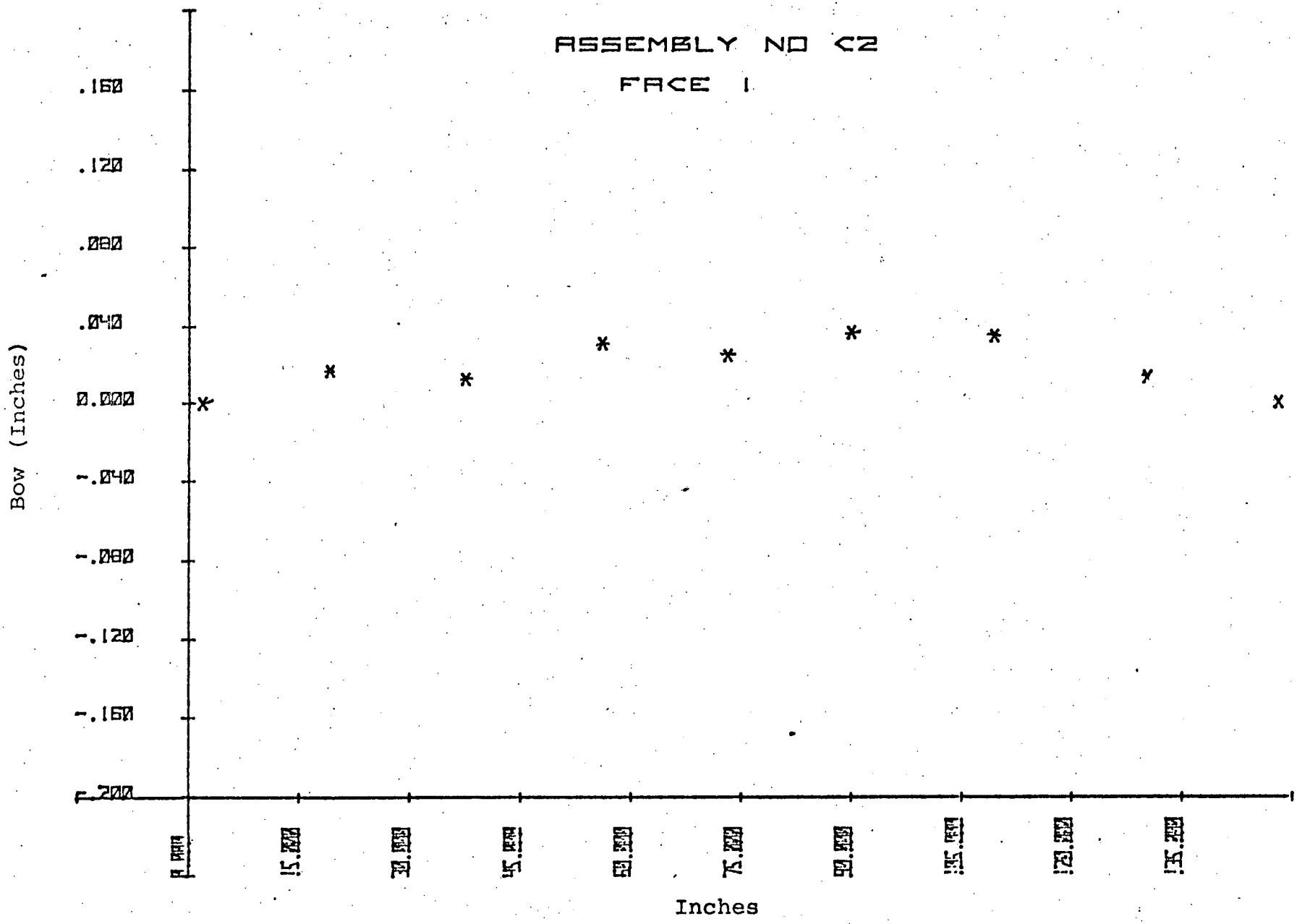

Figure 16 Assembly Bow of Face 1, Assembly C-02

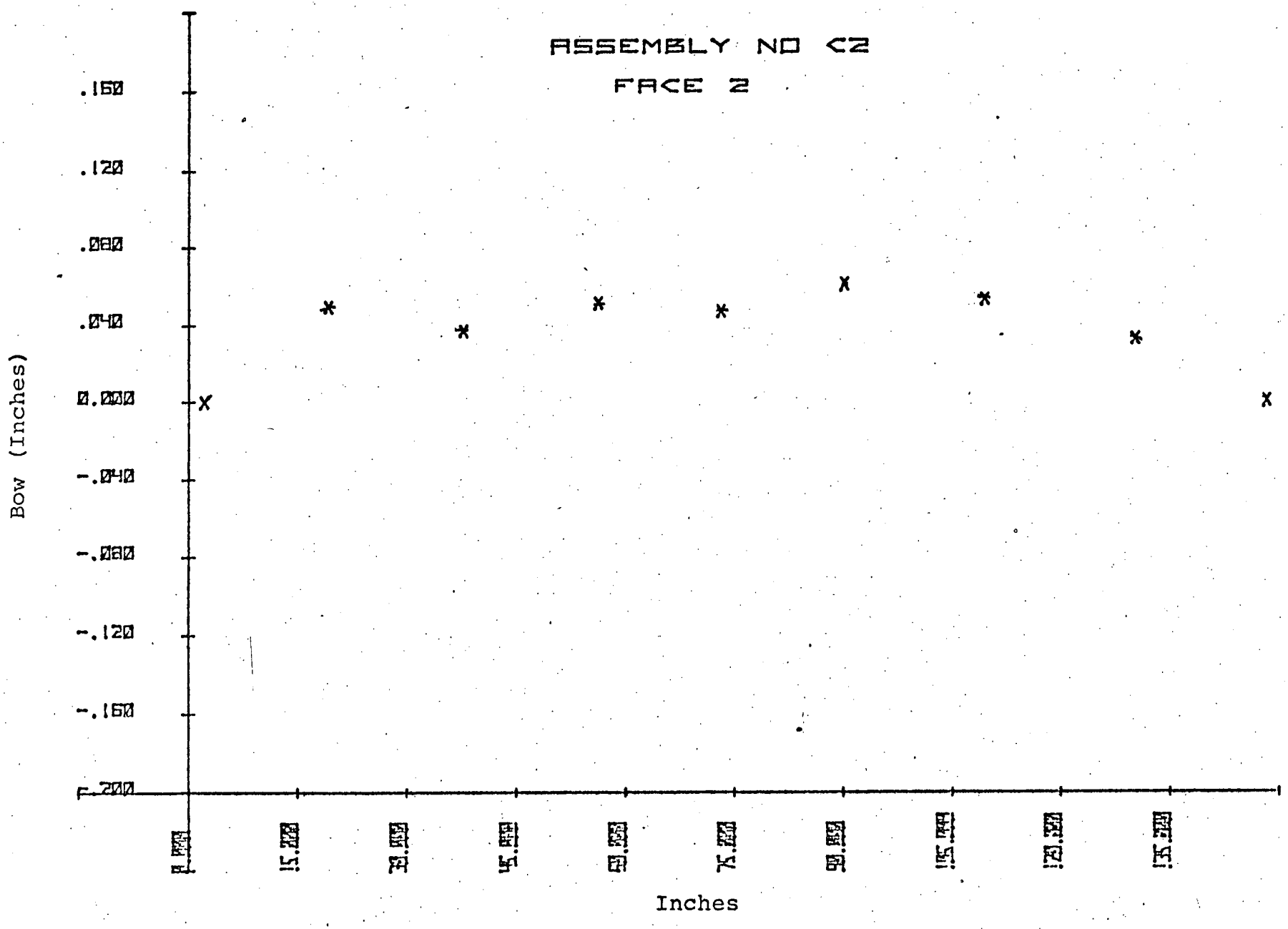

Figure 17 Assembly Bow of Face 2, Assembly C-02

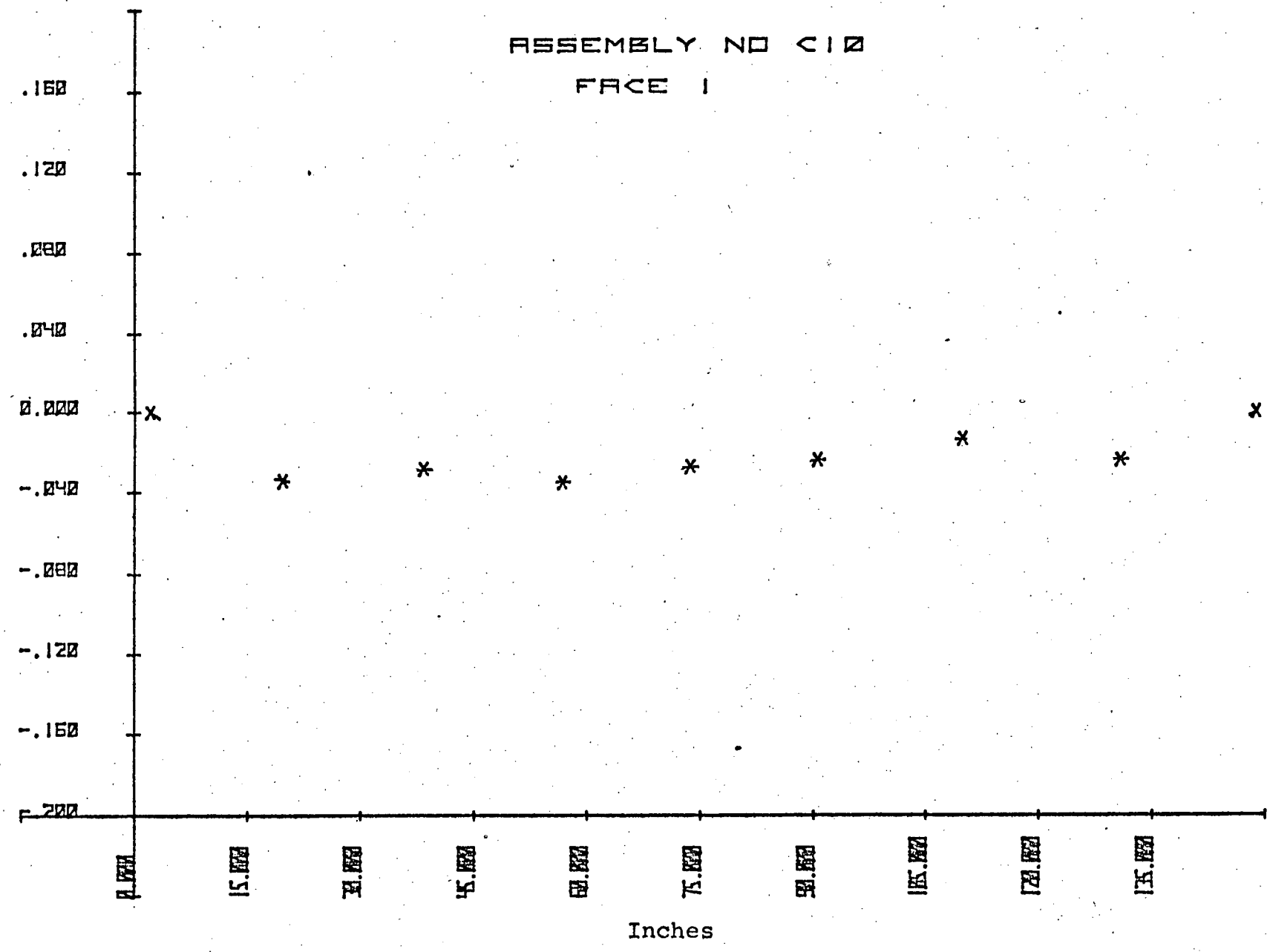

Figure 18 Assembly Bow of Face 1, Assembly C-10

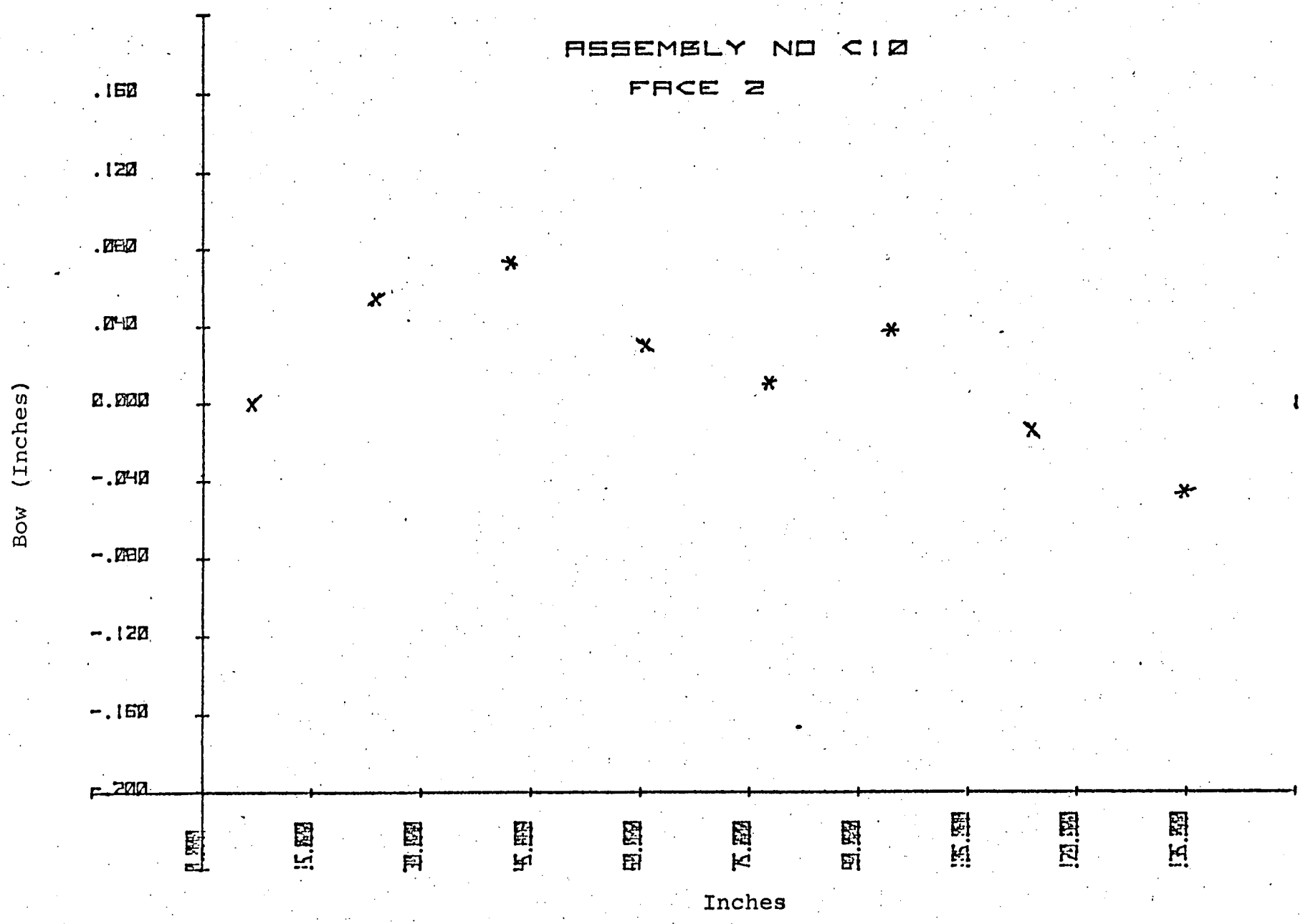

Figure 19 Assembly Bow of Face 2, Assembly C-10

Assembly Twist

Twist measurements were made by rotating the assembly to 45° to orientate the plane of the corner of the upper and lower nozzles to be perpendicular with respect to the camera axis. The location of the nozzle corners was then determined. These encoder readings, using a calculator program, were converted to inches and corrected for runout. By assuming the distance between the corners of the upper and lower nozzles in the axial direction is a chord of a circle with a radius of 5.95 inches (the radius of the fuel assembly), one can calculate the angle of the arc formed by the chord.

Six assembly twist measurements (one per assembly) were made during the examination. Table 7 summarizes these measurements.

TABLE 7

INDIAN POINT #2 FUEL ASSEMBLY TWIST

Assembly No.	Degrees Twist
A-04	2.28
A-44	2.69
B-16	0.83
B-17	2.33
C-02	1.67
C-10	0.09

Rod Length

Rod lengths were taken on each assembly face at specified locations. By predetermining which three rods were to be measured, the results should be interpreted as typical and not biased. The rod lengths measured for the six assemblies are summarized in Table 8 and shown in Table 9.

TABLE 8

Rod Length Statistical Results
Uncorrected for Temperature
Assembly (inches)

Item	"A"	"B"	"C"
X Max	149.9159	150.1625	150.0345
X Min	149.6863	149.7963	149.6933
Range	0.2296	0.3662	0.3412
Mean	149.8051	149.9790	149.9231
Variance	0.0033	0.0060	0.0108
Skewness	0.5131	0.2459	0.8352
Kurtosis	-414.149	124.3030	-115.9948
N	24	24	24

TABLE 9

INDIAN POINT #2 FUEL ROD LENGTHS

Uncorrected for Temperature

Rod No.	Face 1	Face 2	Face 3	Face 4
		Assembly A-04		
3	149.8318	149.7348	149.7593	149.8549
8	149.8639	149.7923	149.7968	149.8228
14	149.7348	149.8173	149.7638	149.8434
		Assembly A-44		
3	149.6863	149.7698	149.8293	149.9159
8	149.7383	149.7568	149.7748	149.8373
14	149.7903	149.9104	149.8213	149.8764
		Assembly B-16		
3	149.9294	150.0059	149.7963	149.9564
8	149.9544	149.9859	149.9014	149.9234
14	150.0810	150.0195	149.9589	150.0034
		Assembly B-17		
3	149.9069	150.0450	149.9494	149.9599
8	149.9514	150.0375	149.9939	149.9794
10	149.9934	150.1625	150.1210	149.8799
		Assembly C-02		
3	149.8874	150.0295	149.9409	150.0220
8	149.9544	149.9714	149.9499	150.0029
10	149.9404	149.9874	149.9979	149.9759
		Assembly C-10		
3	149.8609	150.0345	149.8278	149.7273
8	149.9059	149.9894	149.7723	149.6933
14	149.8729	150.0335	150.0330	149.7428

The rod length measurements were made by recording the bottom of the three individual rods, scanning half of the face and then reading the top of the three individual rods. The difference between two corrected readings was the actual rod length. The length measurements must be corrected for the temperature differential between the spent fuel pool coolant and 70°F (temperature at which system was calibrated). This would increase an average reading of 149.90 inches by 0.0010 inches for each °F above 70°F.

Using the average spent fuel pool temperatures at the time of inspection, leads to the following temperature correction factors:

Assembly	Spent Fuel Pool Temperature	Correction
A04	98°	.028
A44	102°	.032
B16	101°	.031
B17	105°	.035
C02	105°	.035
C10	105°	.035

The mean rod length corrected for temperature of the "A" assemblies was 149.835 inches. This indicated an average rod growth for "A" assemblies during the first cycle of .415 inches as compared with an initial rod length of 149.420 ± 0.035 inches. Figure 20 is a frequency histogram of the measured rod lengths of the "A" assemblies and shows the standard deviation at the one sigma level to be ± 0.057 inches. This standard deviation compares favorably with the standard deviation of the initial rod length. However, by examining the actual scanning of the "A" assemblies, it would appear that rod growth has a greater variance than indicated in the histogram. For example, rod 11 of assembly A-04 face 4 was touching both the upper and lower nozzles. Bowing measurements were taken on this particular rod to determine if additional rod growth beyond that which could be measured in the vertical plane took place. These measurements indicated that no significant bowing had occurred. It was expected that a certain percentage of the rods would be touching both lower and upper nozzles with high exposure "A" assemblies. This is basically due to the fact that unlike the Region 2 and 3 assemblies, Region 1 was fabricated with an axial clearance between rods and nozzles corresponding to the Zircaloy growth expected during only one cycle of operation.

The mean rod length for the "B" assemblies was 150.012 inches which indicated an average rod growth during the first cycle of .642 inches as compared with the initial rod length of 149.370 ± 0.035 inches. Figure 21 is a frequency histogram of the measured rod lengths of the "B" assemblies and shows the deviation at one sigma level to be ± 0.0775 inches. The mean rod length for the "C" assemblies (Figure 22) was 149.958 inches which indicated an average rod growth during the first cycle of 0.588 inches as compared with the initial fuel rod length of 149.370 ± 0.035 inches.

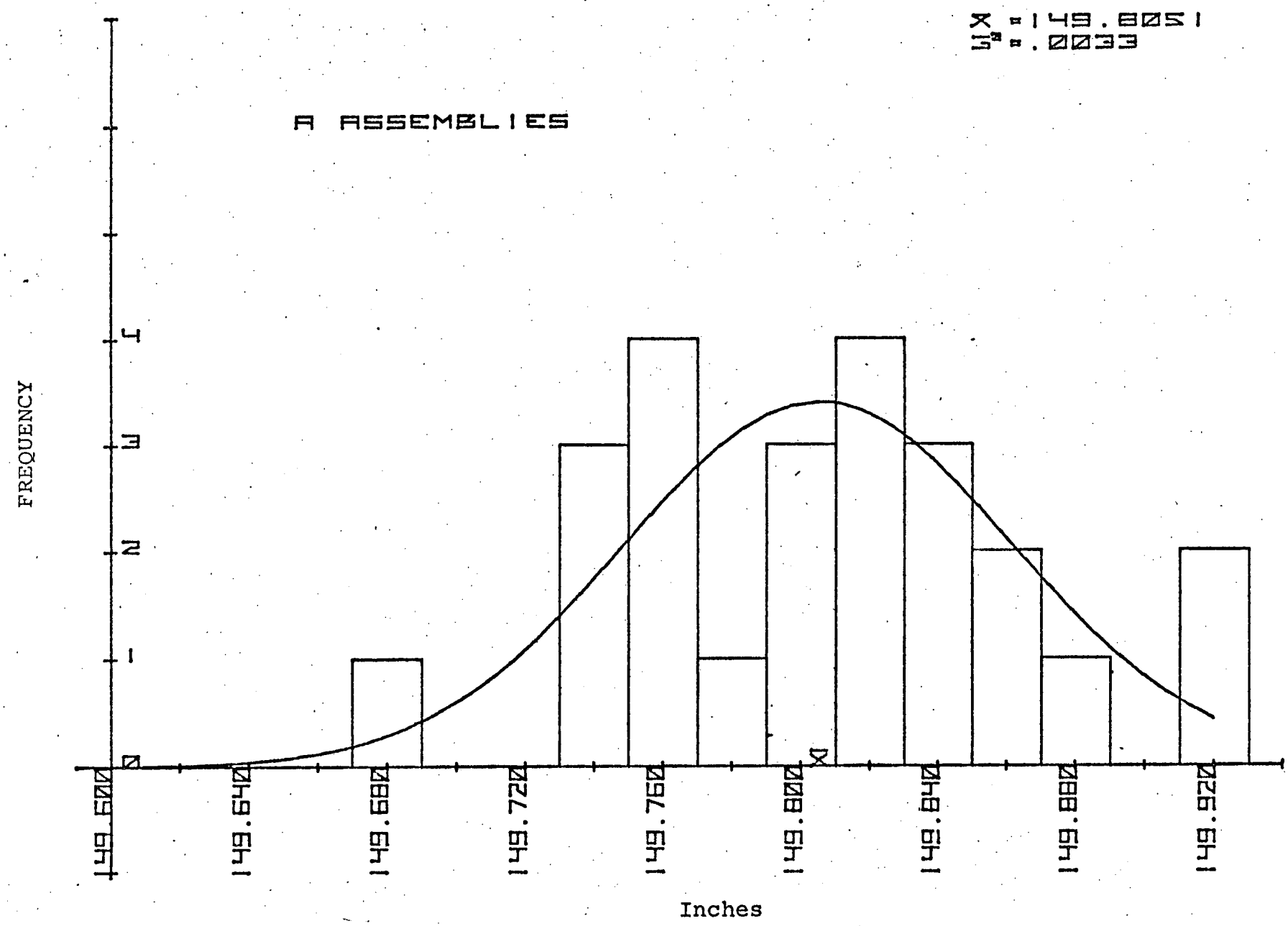

Figure 20 Rod Lengths of "A" Assemblies
Uncorrected for Temperature

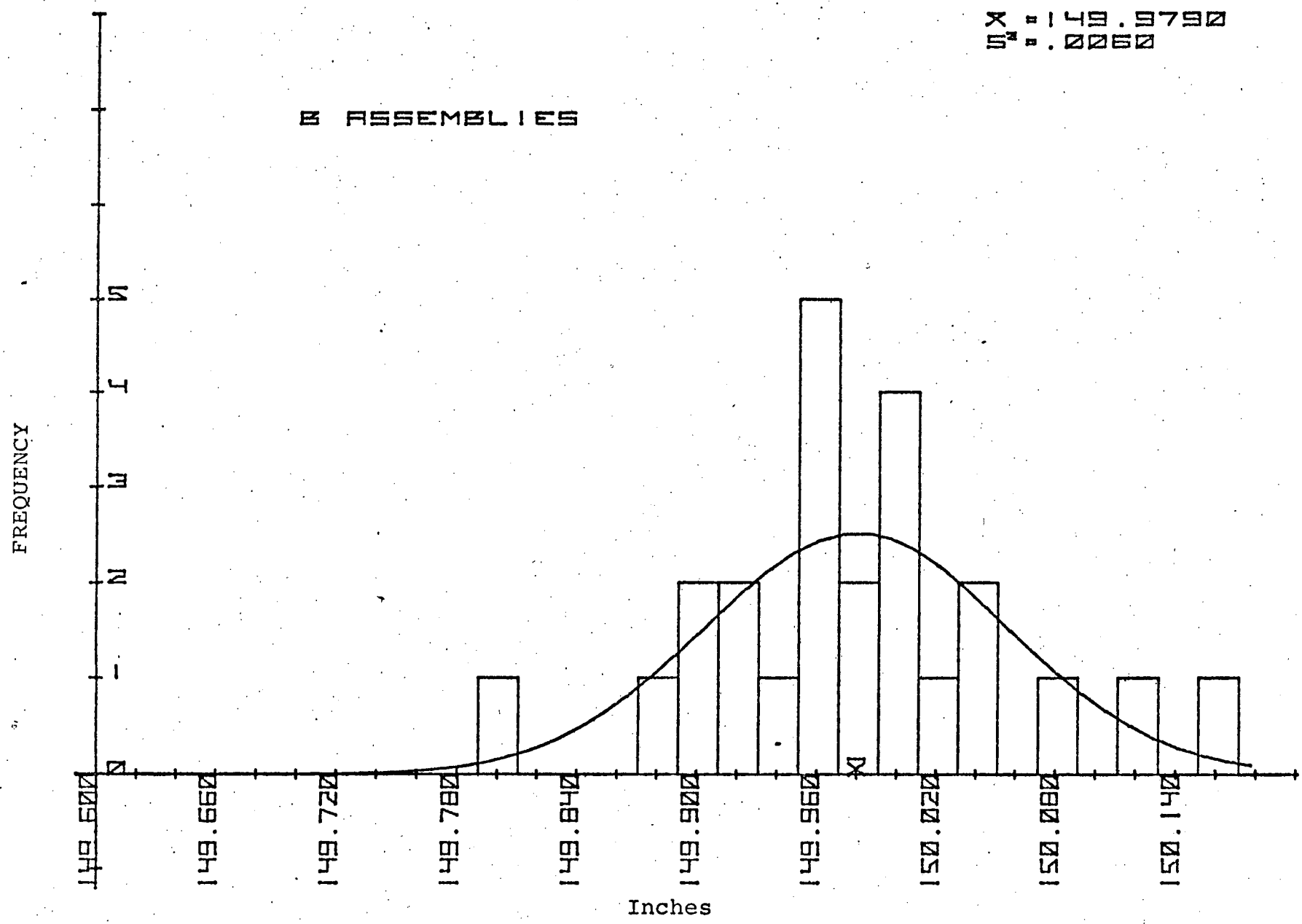

Figure 21 Rod Lengths of "B" Assemblies Uncorrected for Temperature

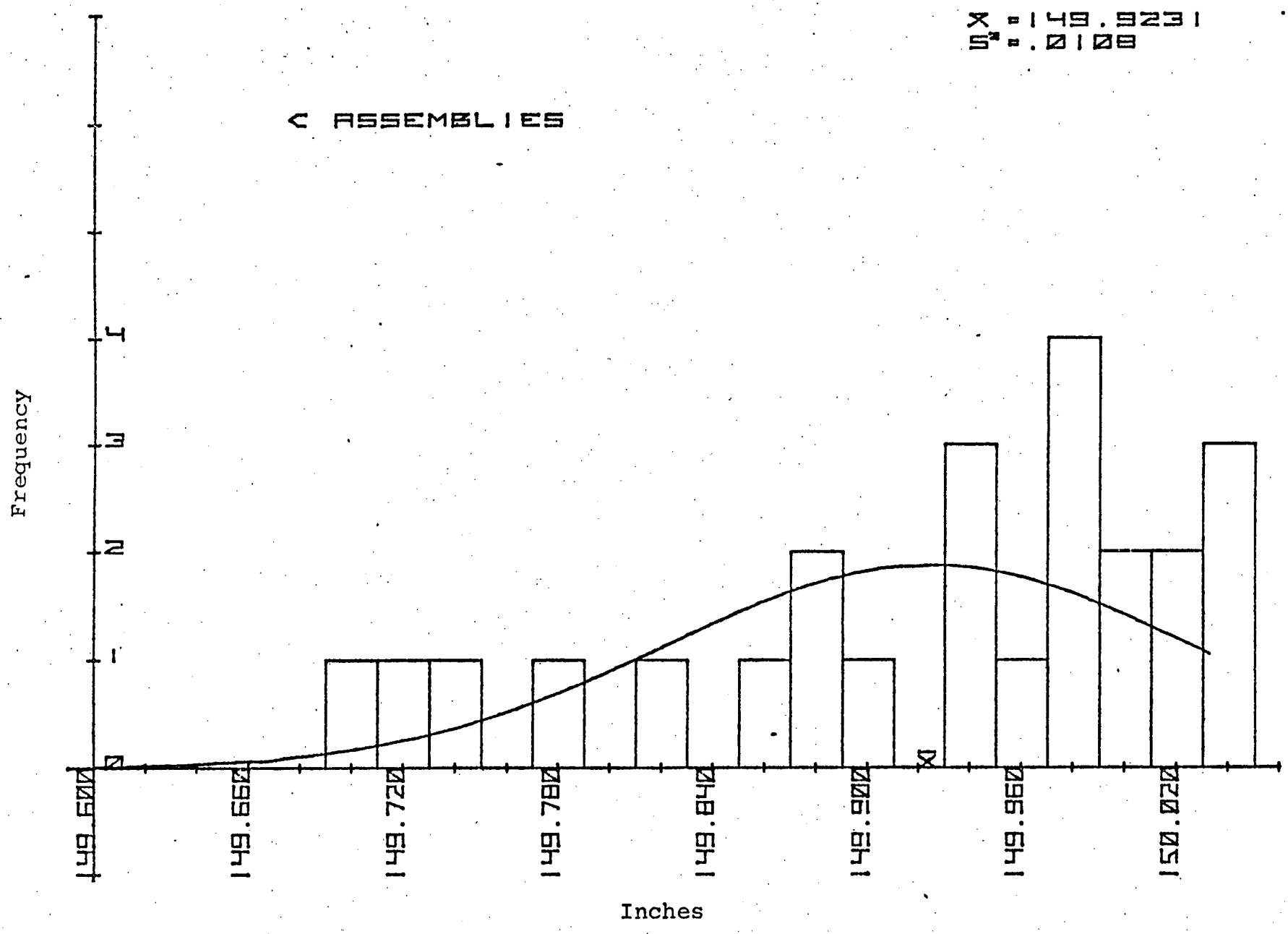

Figure 22 Rod Length of "C" Assemblies
Uncorrected for Temperature

Rod Bow

As specified by Consolidated Edison, two rod bow measurements were performed on each assembly face. In the process of visually scanning the asssmbly face, locations where measurable bowing occurred were identified. The two most pronounced rod bowing locations were chosen for the rod bow measurements. The rod bowing data between specific grids, as summarized in Tables 10 and 11, using this procedure, are biased and should not be construed as typical rod bowing seen in the assemblies examined. Of the 48 rods examined for bowing, only 11 rods had measurable rod bowing (greater than 0.0214 inches, or two sigma) as shown in Table 10.

TABLE 10

Relationship of Rod Bowing Measured to Standard Deviation of Calibration

Rod Bowing	No. of Occurrences	% of Total
> One Sigma	37	77
> Two Sigma	11	23
> Three Sigma	5	10.5

The individual rod bow measurements, Figures 23 through 70, were made by aligning the right hand edge of the rod with the left hand edge of the cross hair on the television monitor and recording the axial and vertical position. A minimum of six measurements were made on the rod between the grids of interest. These encoder readings, using a calculator program, were then converted to inches and corrected for runout. The corrected data were then compared with a straight line connecting the first and last measured points to determine the actual bow at a given point.

TABLE 11

Summary of Rod Bowing Measurements

Assembly	Face	Rod	Grid Location	Maximum Bow (x10-3 inches)
A-04	1	3	2&3	-15.1
		6	3&4	12.2
	2	11	4&5	-16.8
		3	5&6	-16.2
	3	12	1&2	13.3
	4	11	4&5	26.5
A-44	1	4	3&4	11.7
	2	7	3&4	14.3
	3	4	4&5	46.6
		11	5&6	-19.0
	4	11	5&6	17.7
B-16	1	2	2&3	14.8
	2	5	3&4	-14.3
		10	4&5	-40.4
	3	4	1&2	41.7
		6	3&4	19.8
	4	1	3&4	-10.8
		7	5&6	11.6
B-17		2	1&2	22.2
	1	4	2&3	-11.4
	2	6	2&3	15.9
		2	4&5	14.0
	3	10	4&5	15.8
	4	7	5&6	-19.5
C-02	1	8	4&5	12.4
	2	8	3&4	-23.9
	3	4	2&3	-32.0
		9	5&6	16.5
	4	9	5&6	-10.9
		4	6&7	33.4
C-10	1	12	1&2	17.5
	2	2	2&3	36.1
		11	3&4	16.1
	3	3	1&2	23.5
		7	2&3	-28.4
	4	5	2&3	-13.6
		12	4&5	-15.4

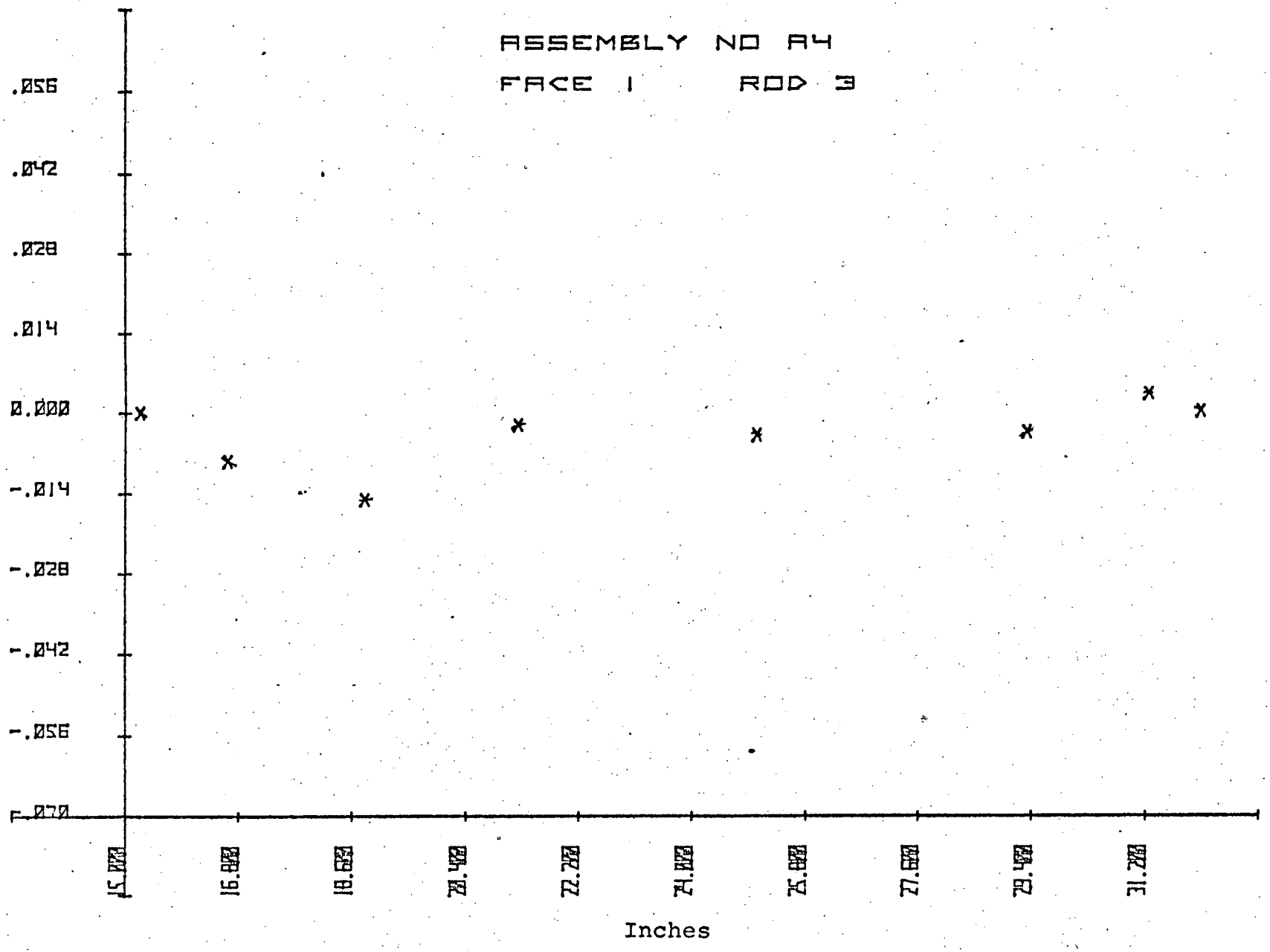

Figure 23 Bow of Rod 3, Face 1 of Assembly A-04 between Grids 2 and 3

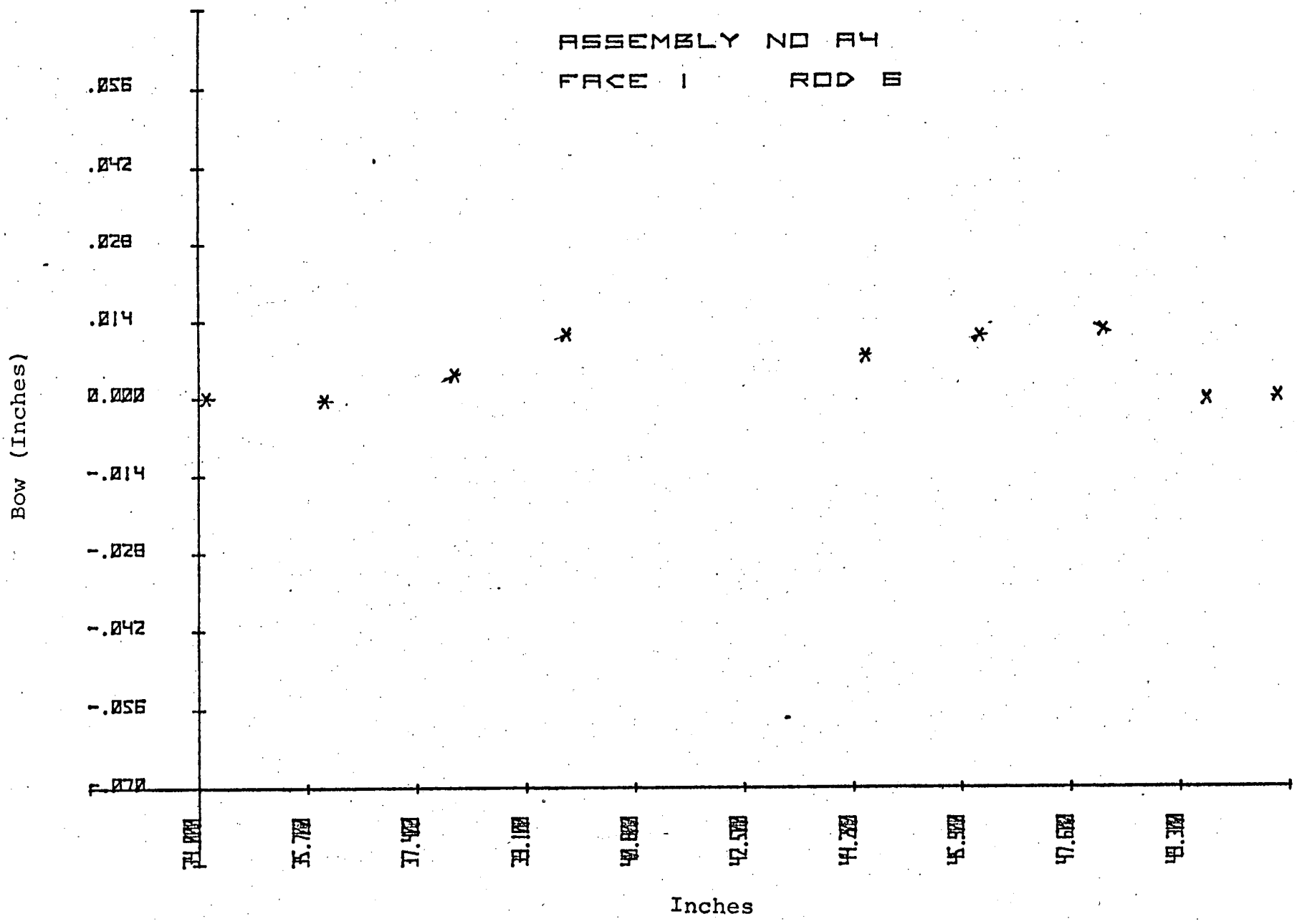

Figure 24 Bow of Rod 6, Face 1 of Assembly A-04 between Grids 3 and 4

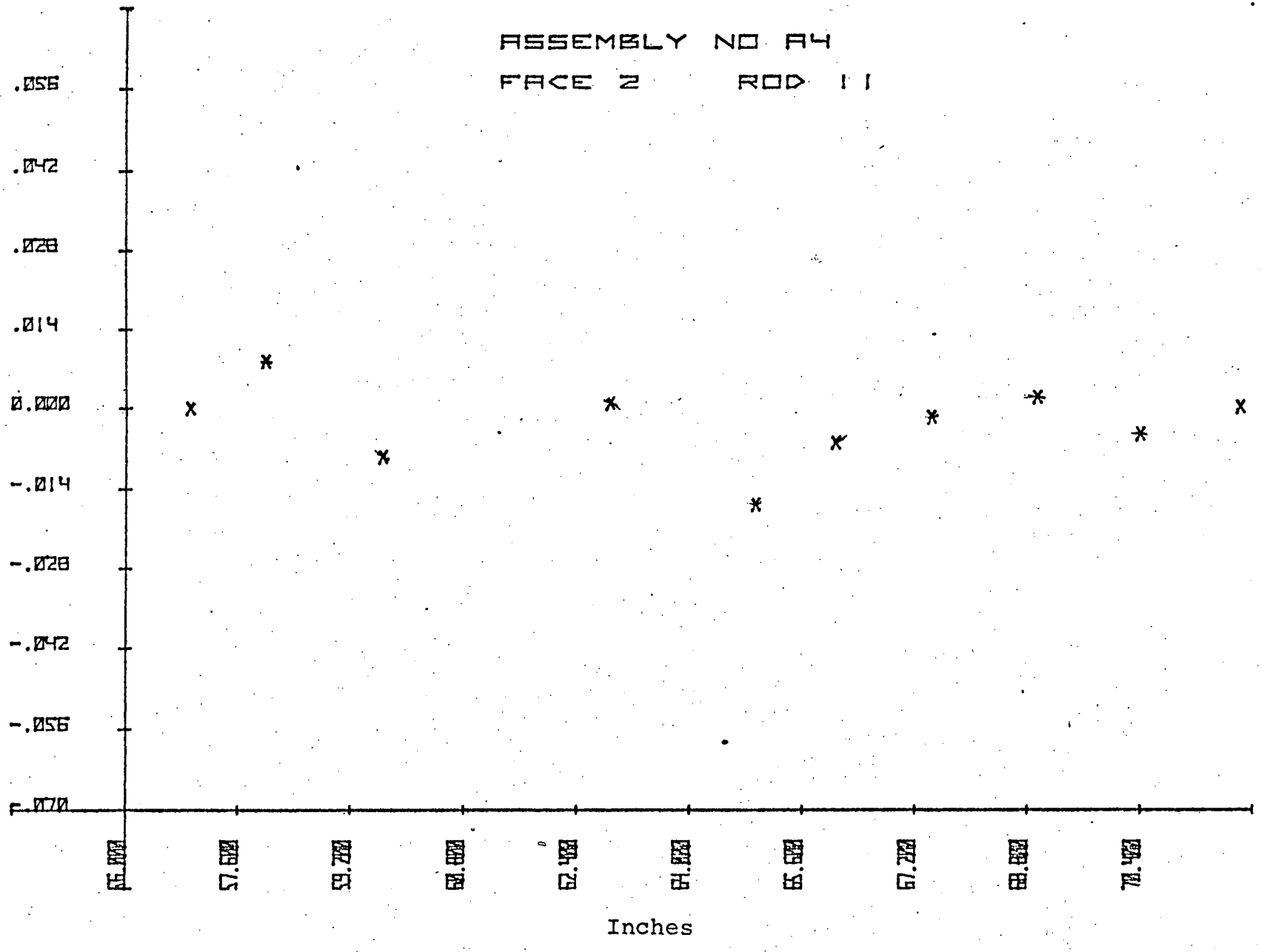

Figure 25 Bow of Rod 11, Face 2 of Assembly A-04 between Grids 4 and 5

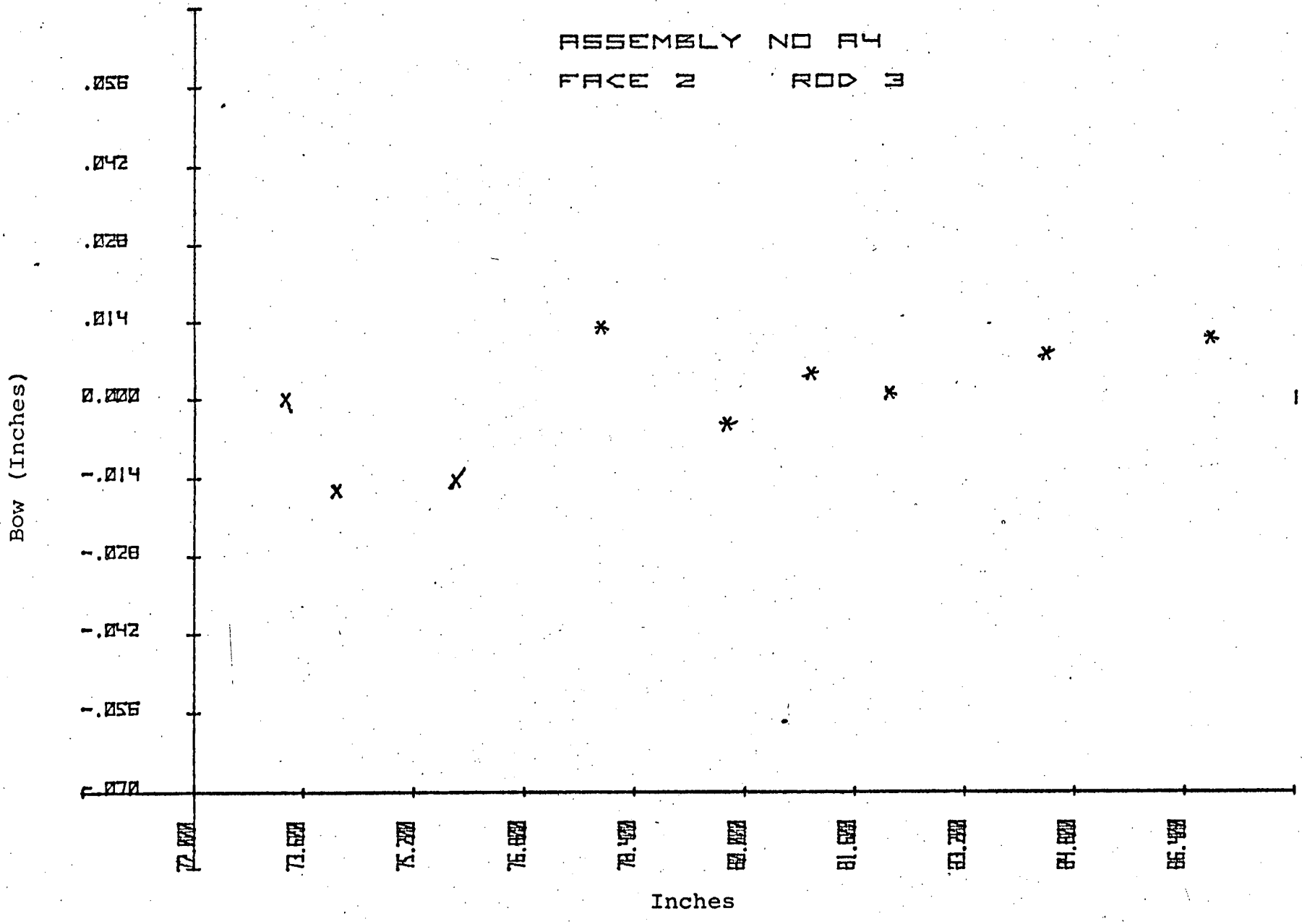

Figure 26 Bow of Rod 3, Face 2 of Assembly A-04 between Grids 5 and 6

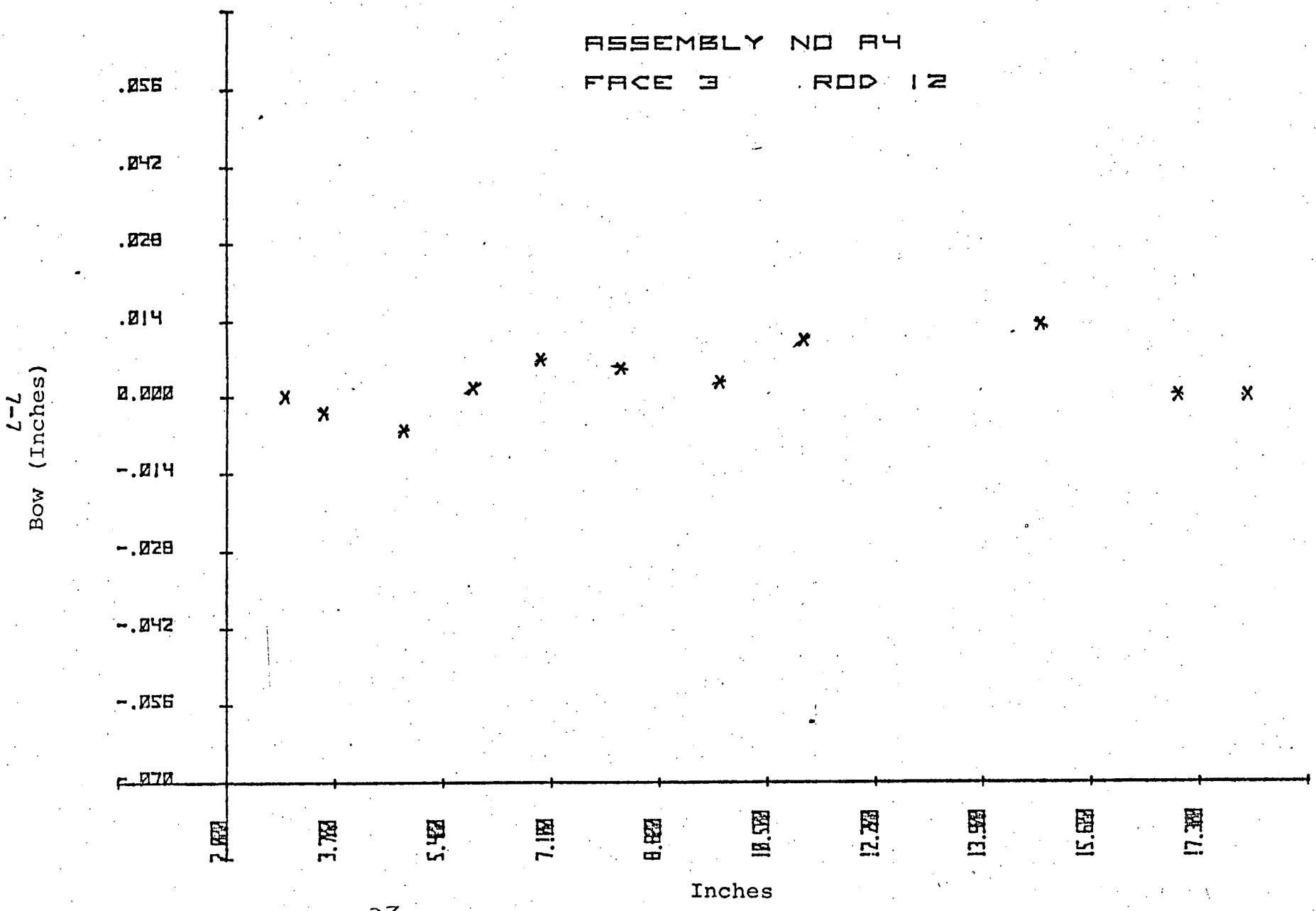

Figure 27 Bow of Rod 12, Face 3 of Assembly A-04 between Grids 1 and 2

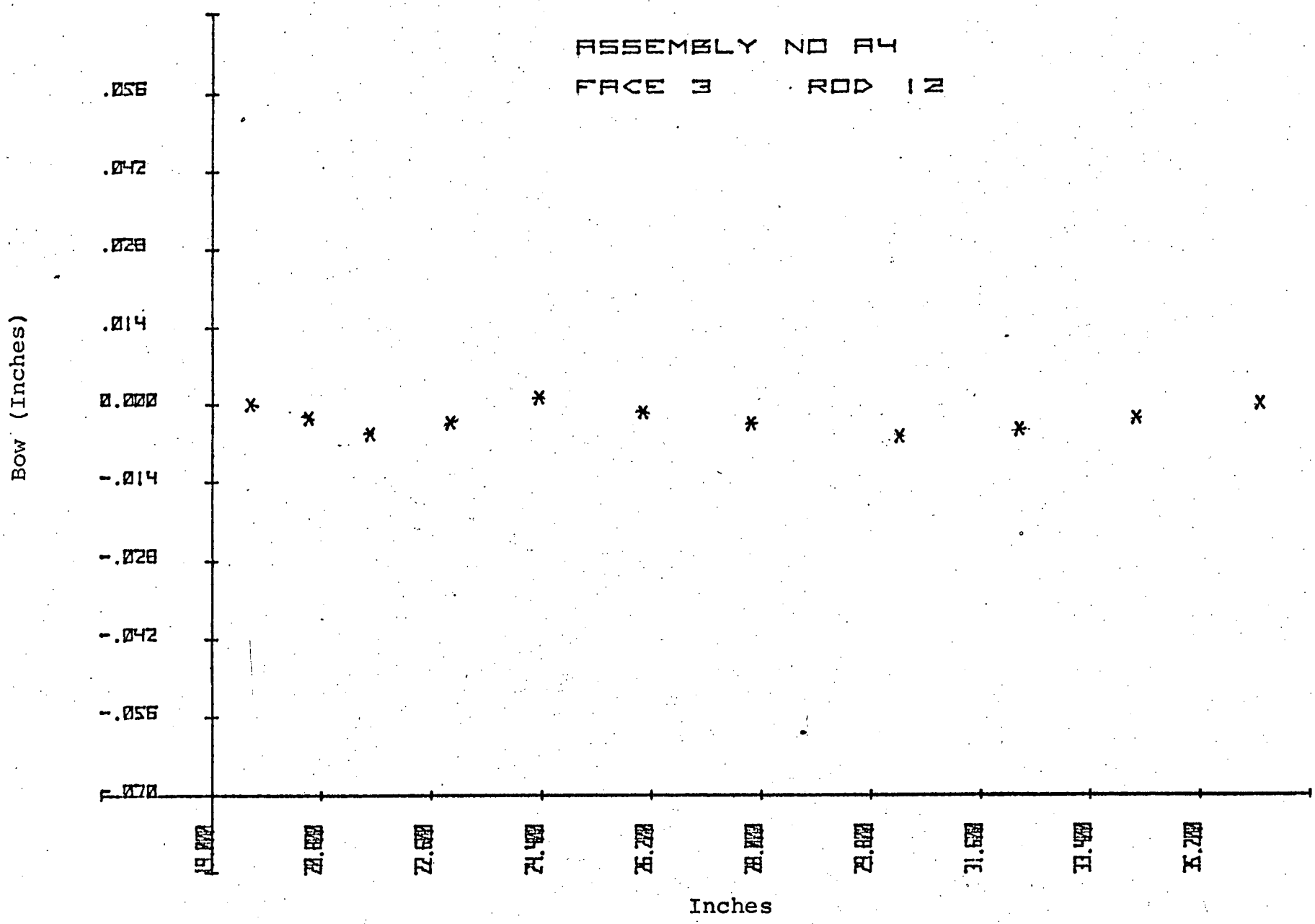

Figure 28 Bow of Rod 12, Face 3 of Assembly A-04 between Grids 2 and 3

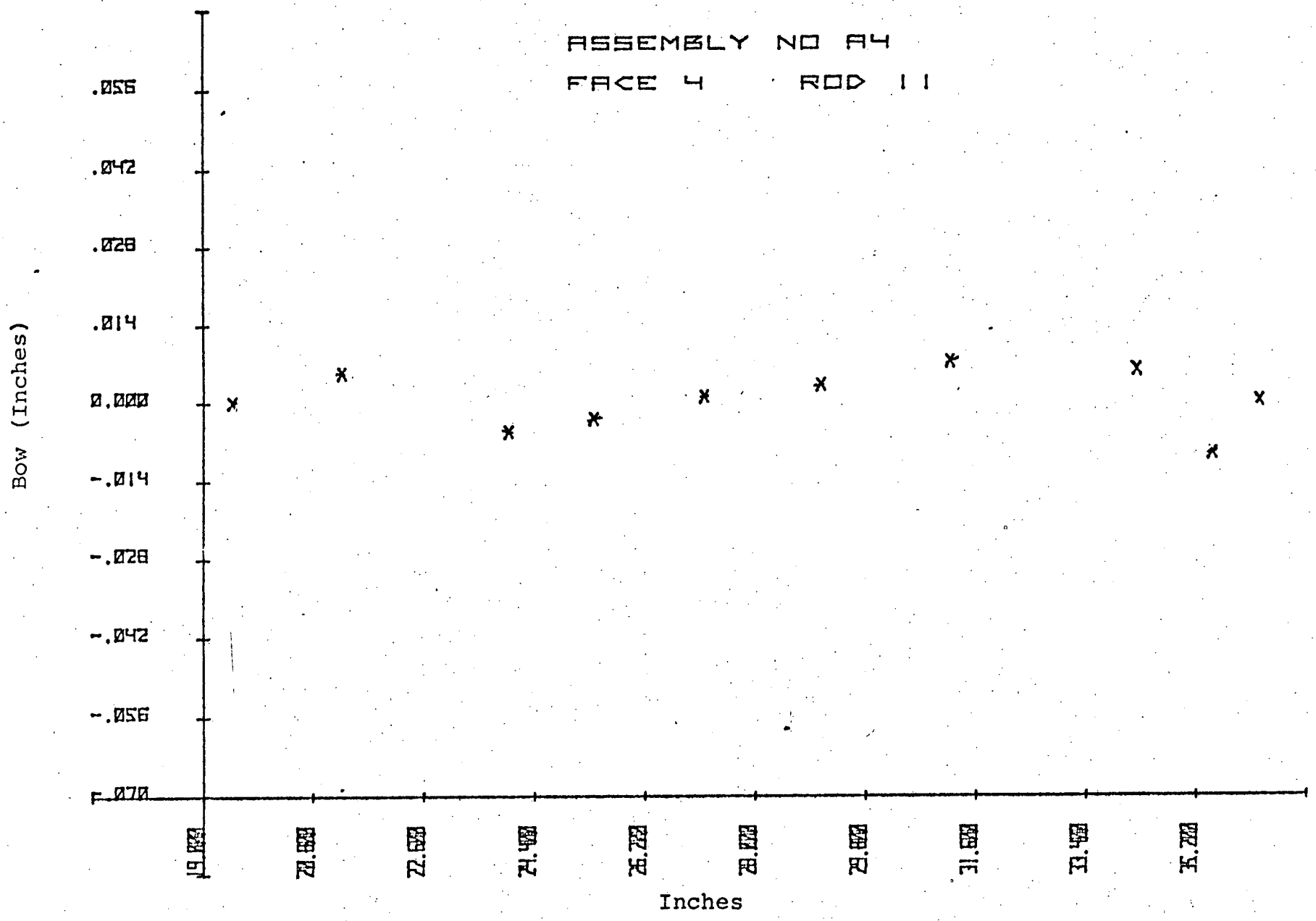

Figure 29 Bow of Rod 11, Face 4 of Assembly A-04 between Grids 2 and 3

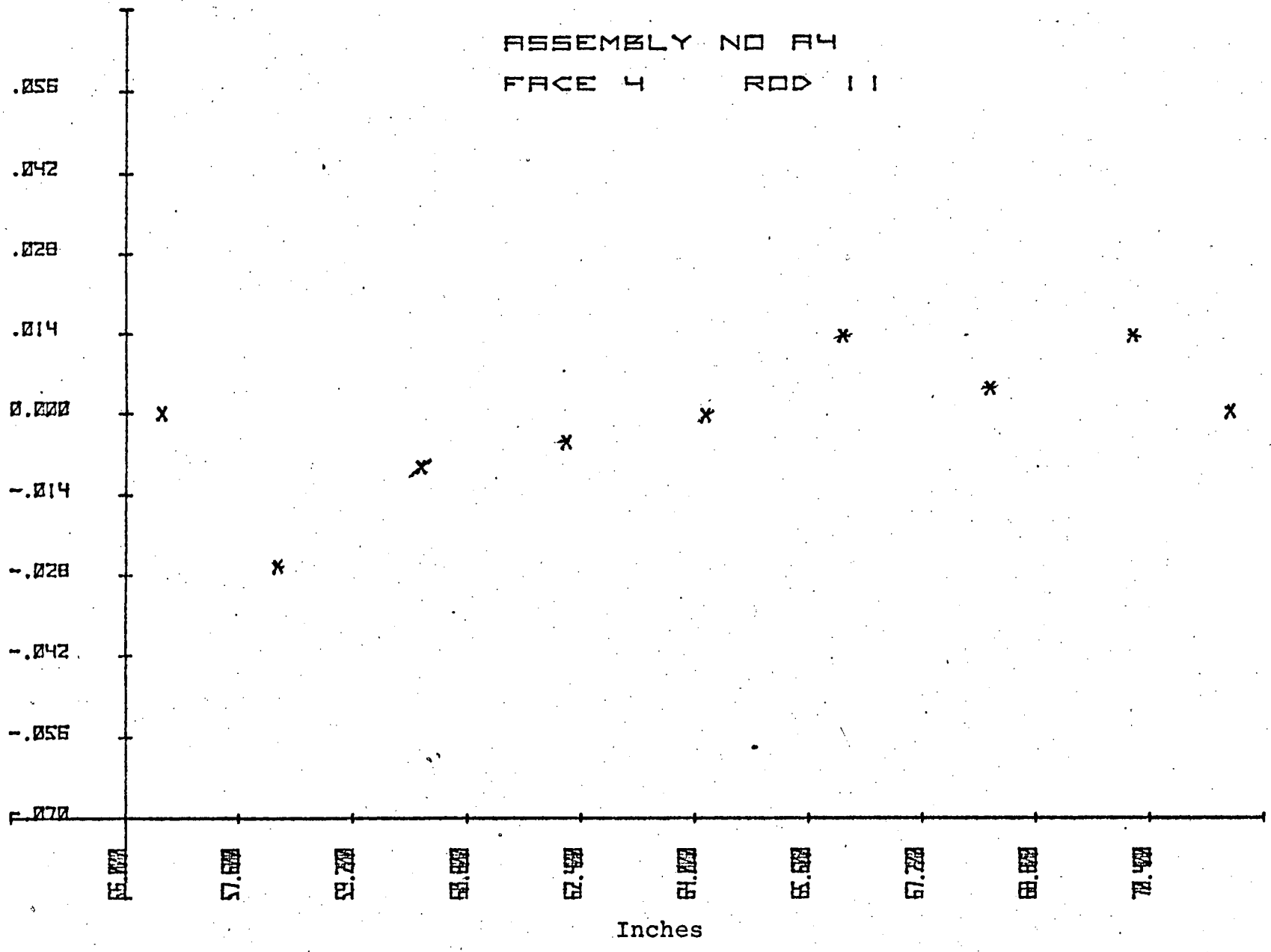

Figure 30 Bow of Rod 11, Face 4 of Assembly A-04 between Grids 4 and 5

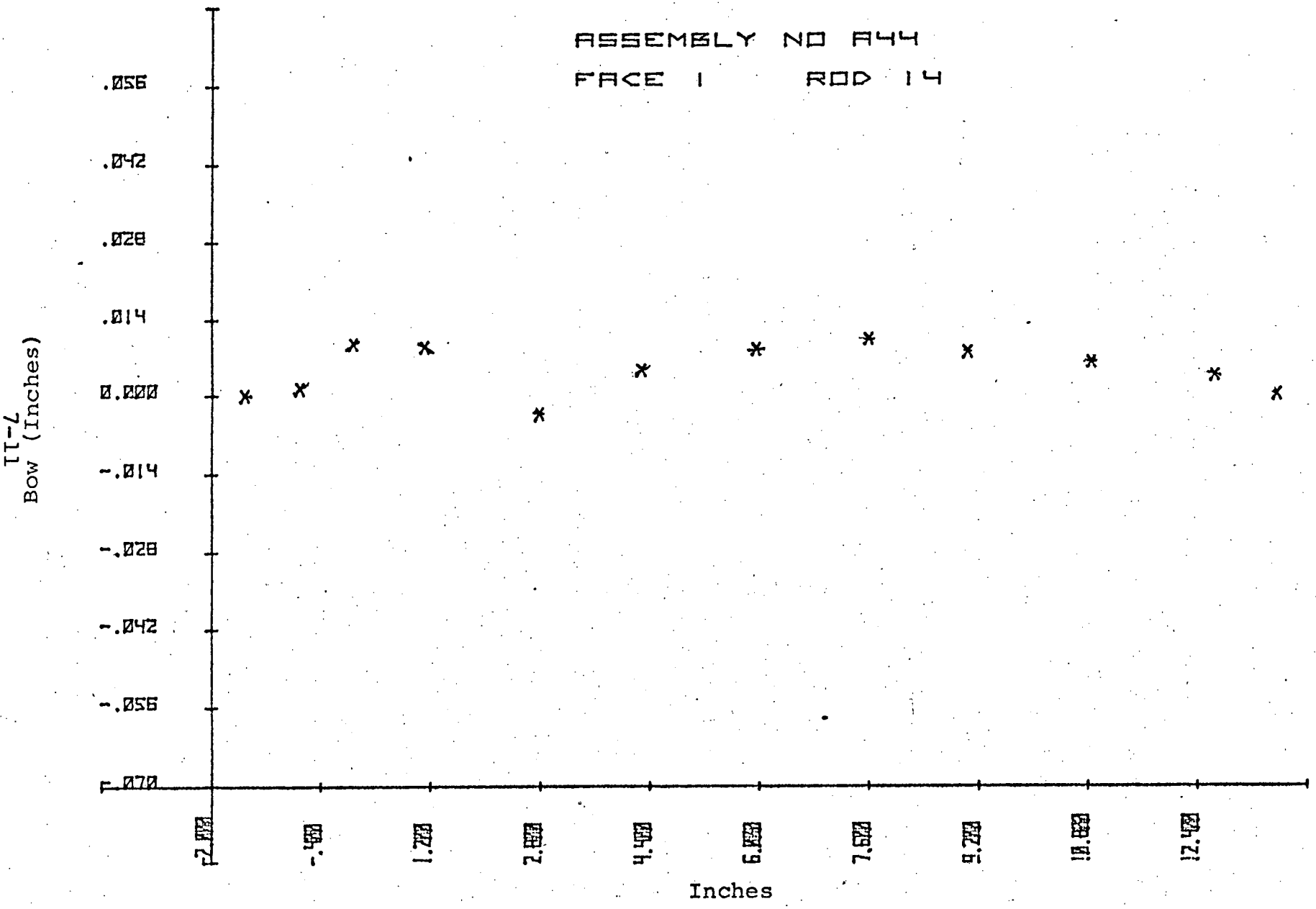

Figure 31 Bow of Rod 14, Face 1 of Assembly A-44 between Grids 1 and 2

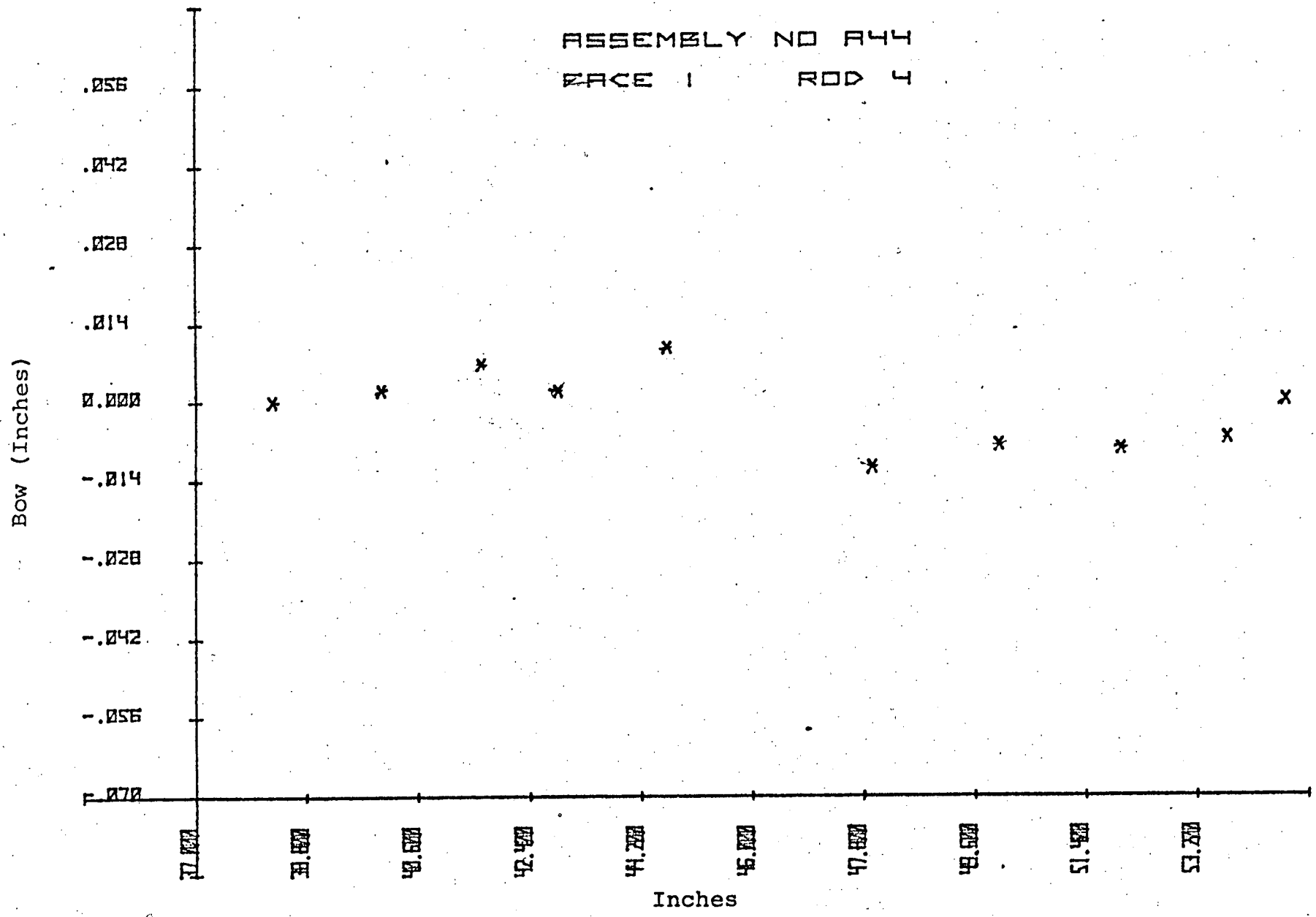

Figure 32 Bow of Rod 4, Face 1 of Assembly A-44 between Grids 3 and 4

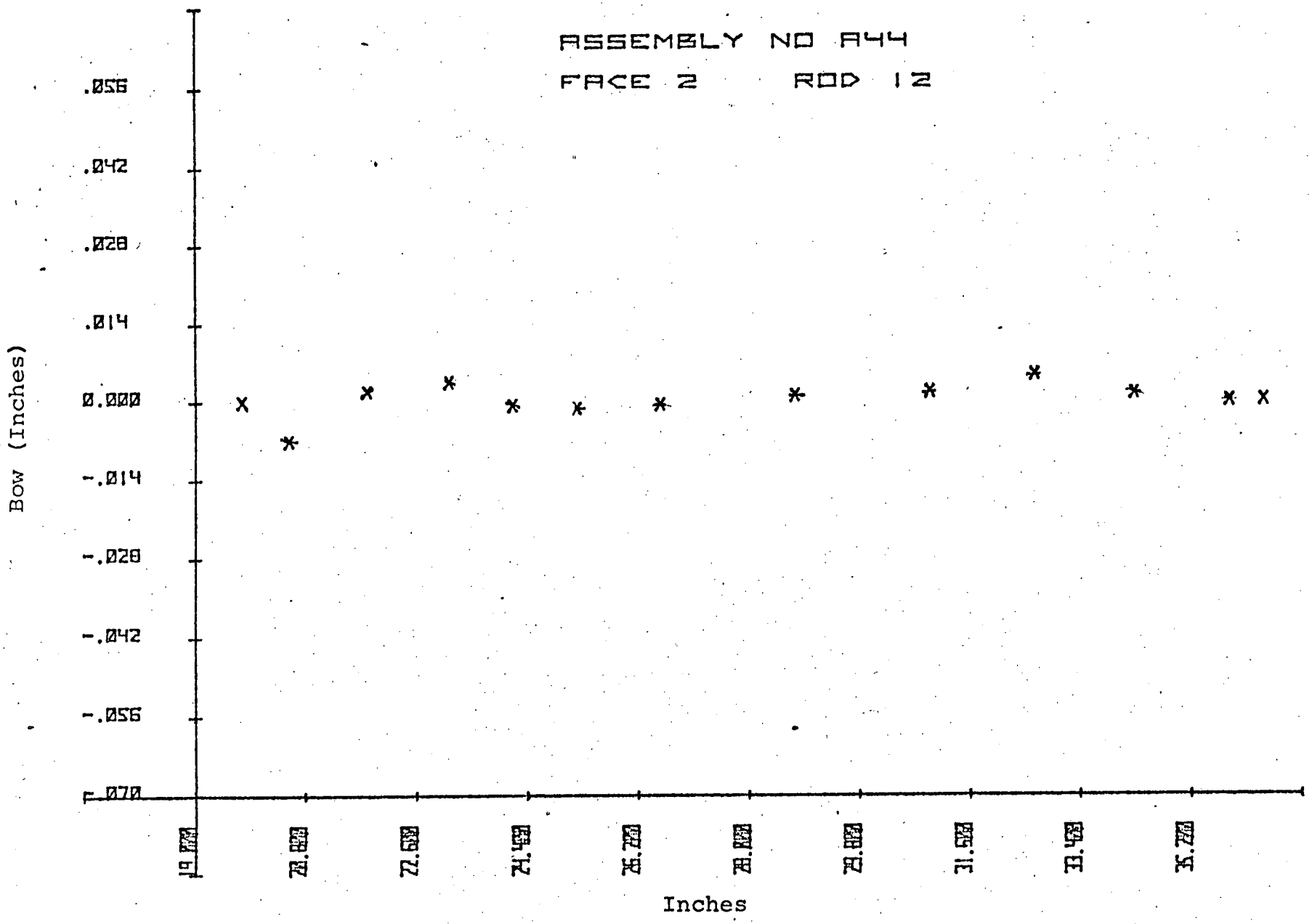

Figure 33 Bow of Rod 12, Face 2 of Assembly A-44 between Grids 2 and 3

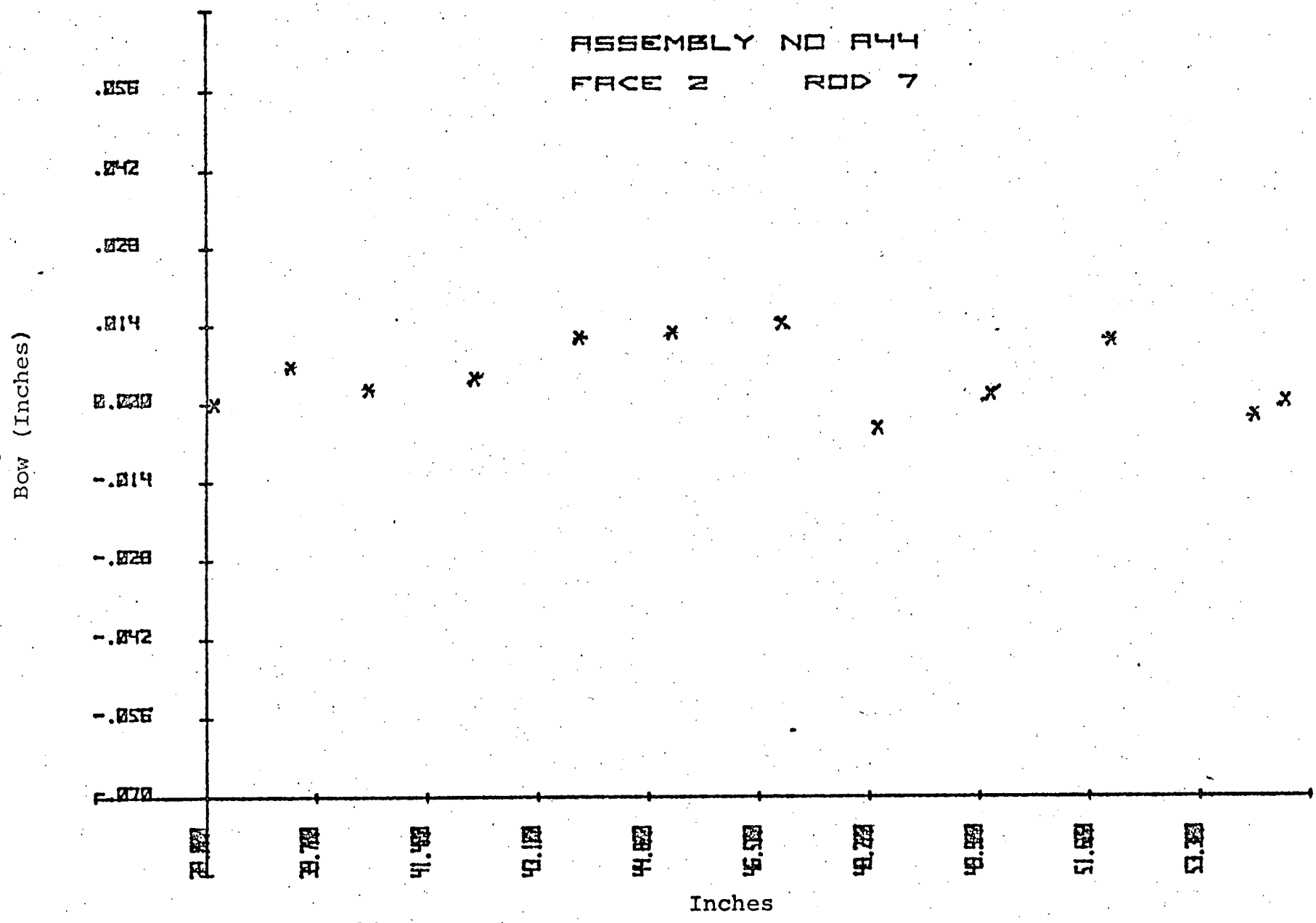

Figure 34 Bow of Rod 7, Face 2 of Assembly A-44 between Grids 3 and 4

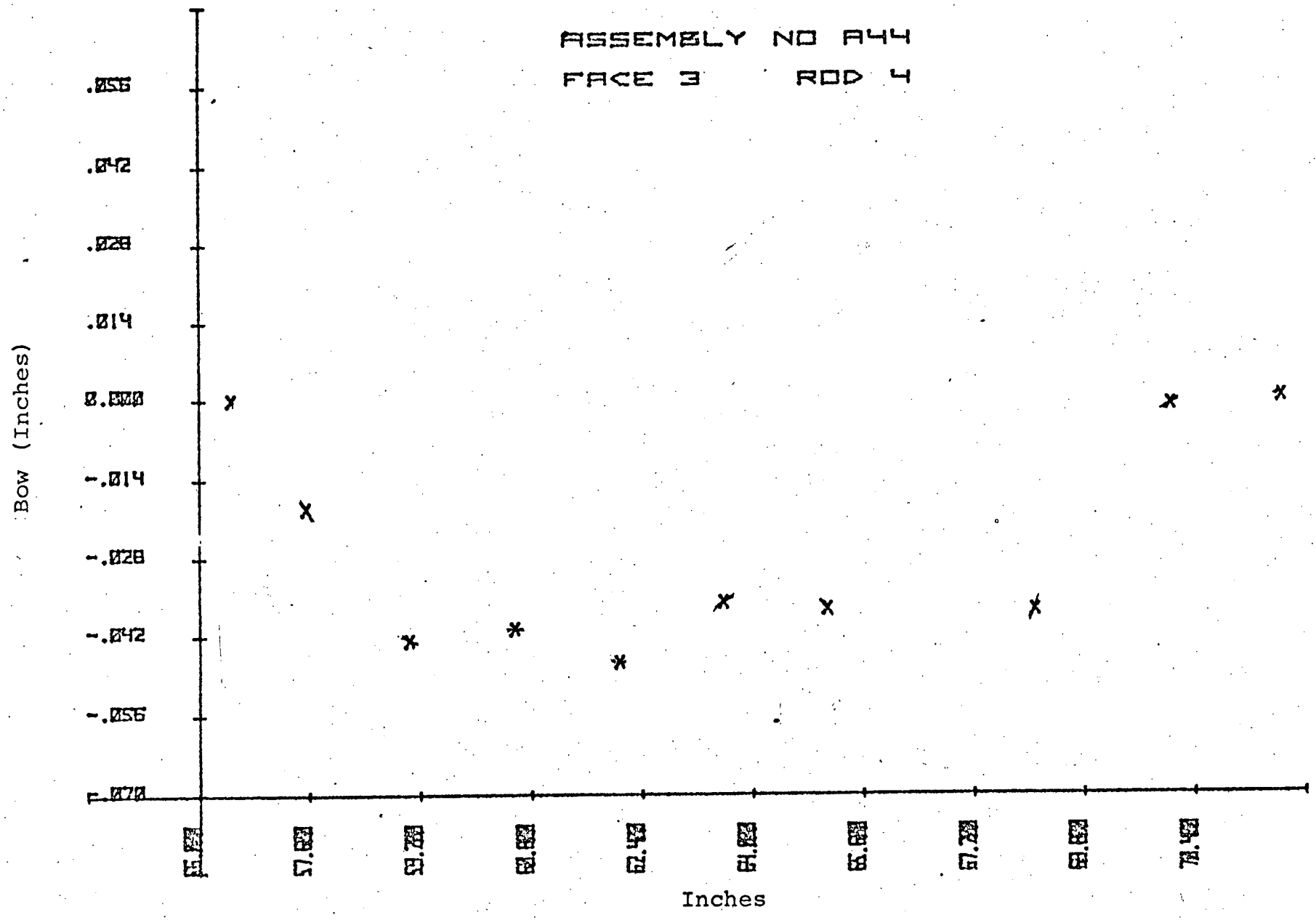

Figure 35 Bow of Rod 4, Face 3 of Assembly A-44 between Grids 4 and 5

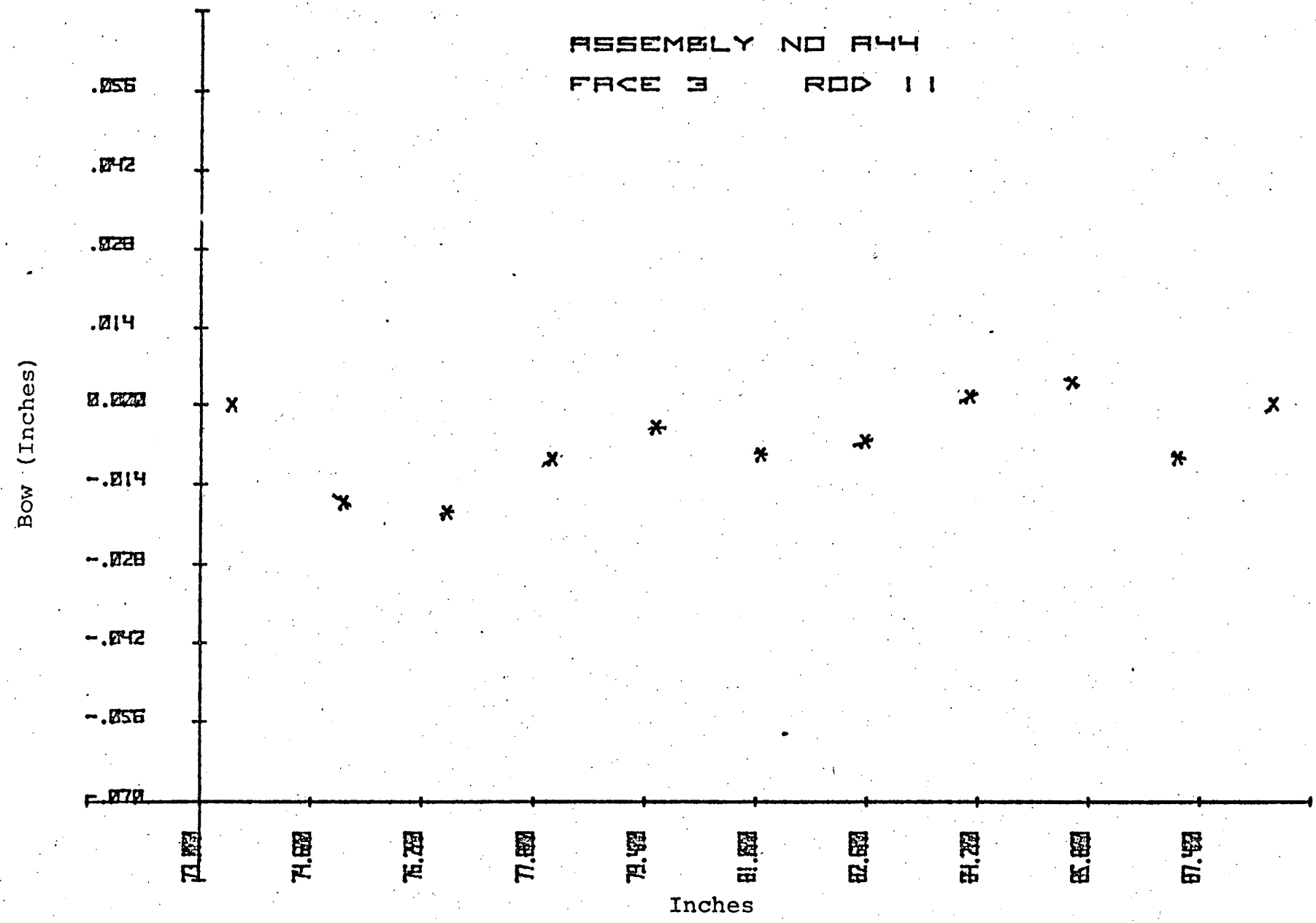

Figure 36 Bow of Rod 11, Face 3 of Assembly A-44 between Grids 5 and 6

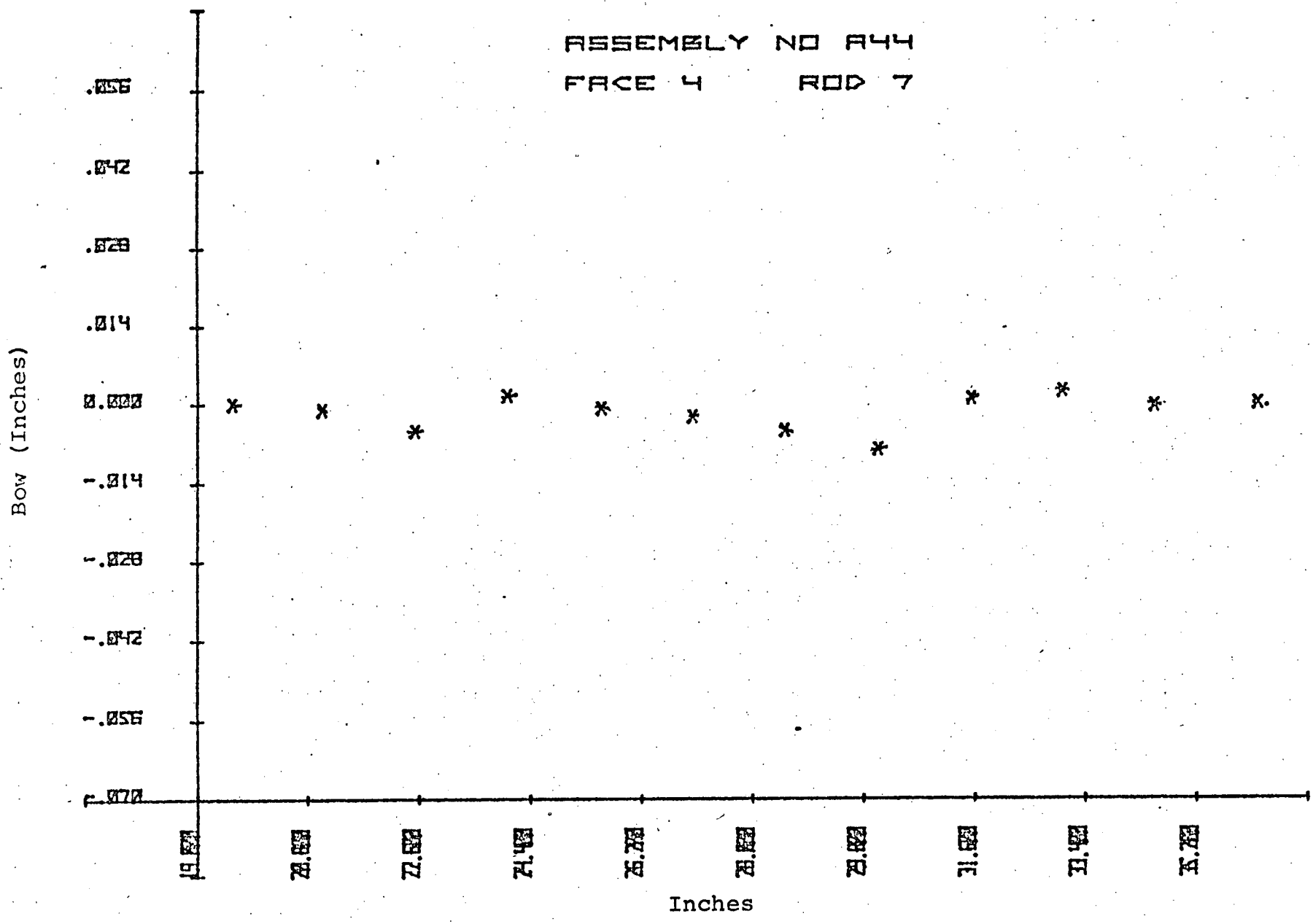

Figure 37 Bow of Rod 7, Face 4 of Assembly A-44 between Grids 2 and 3

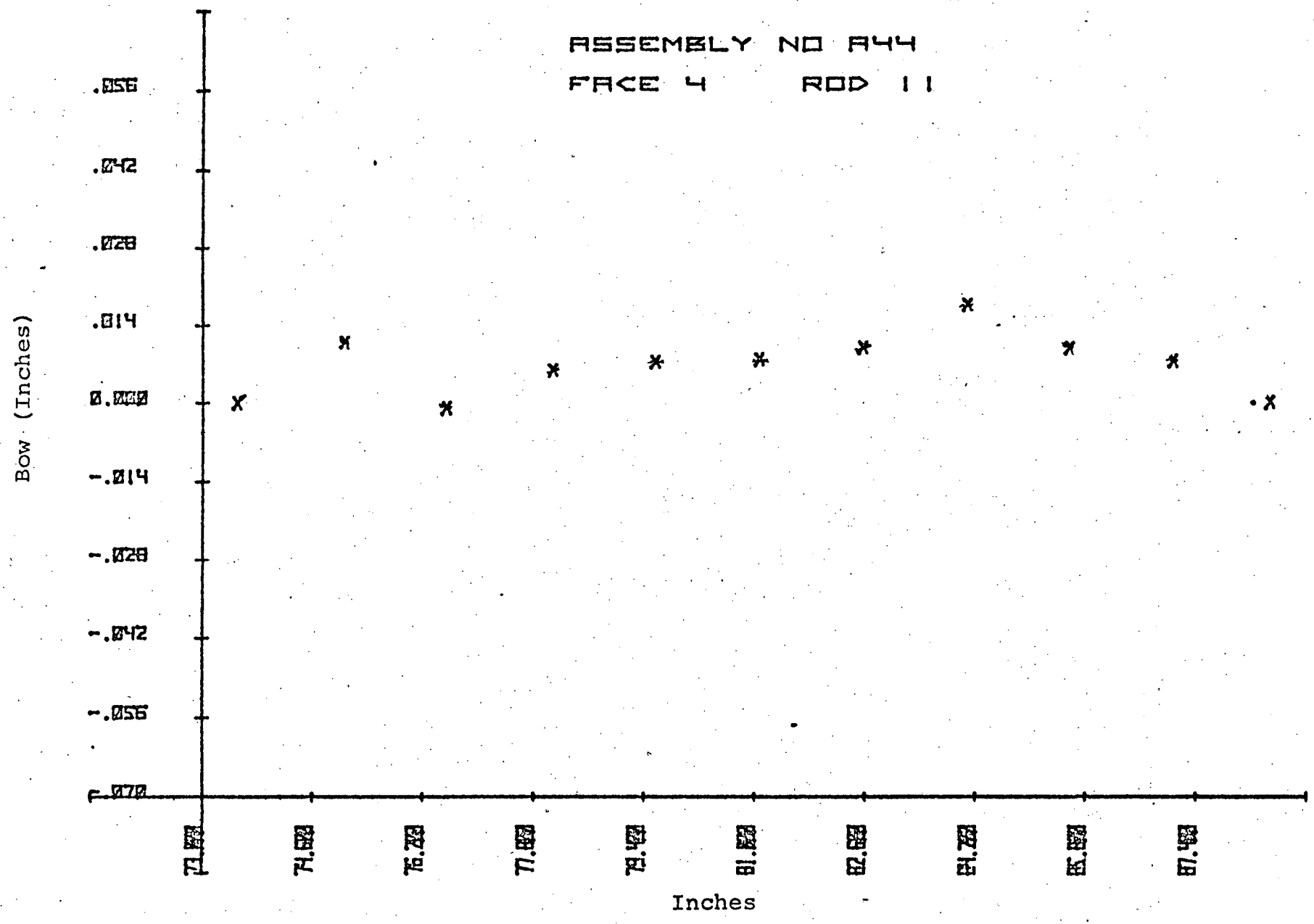

Figure 38 Bow of Rod 11, Face 4 of Assembly A-44 between Grids 5 and 6

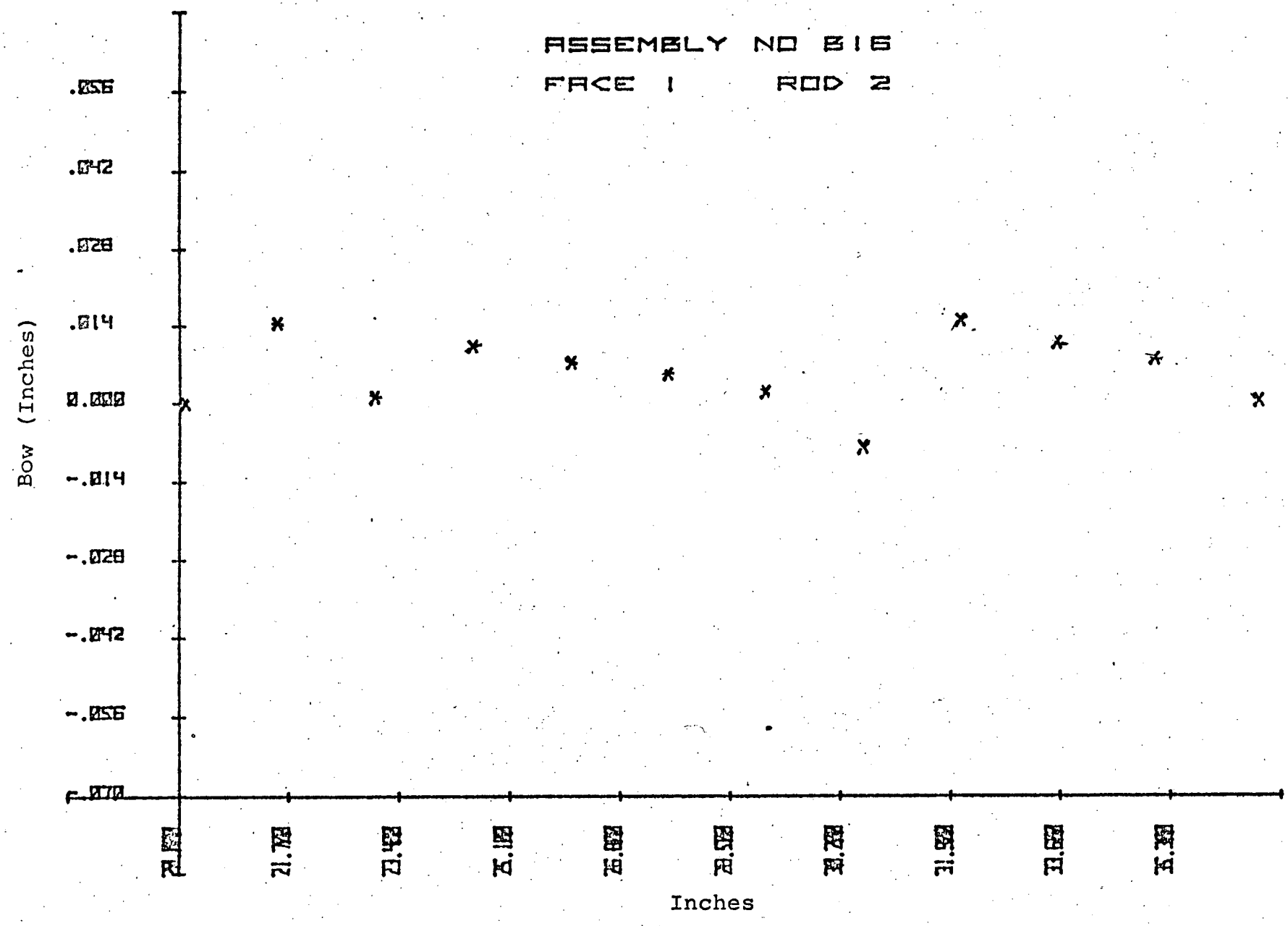

Figure 39 Bow of Rod 2, Face 1 of Assembly B-16 between Grids 2 and 3

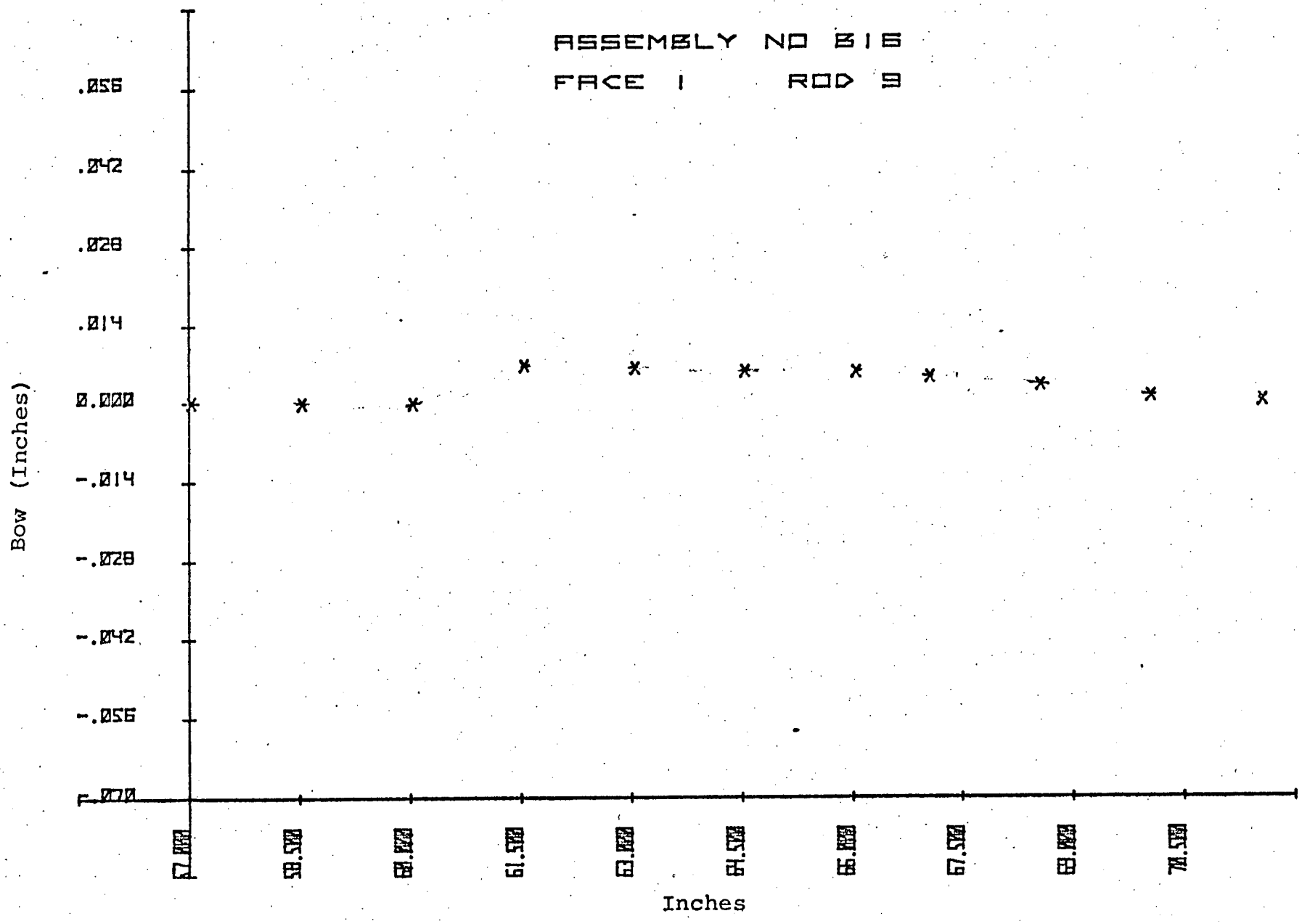

Figure 40 Bow of Rod 9, Face 1 of Assembly B-16 between Grids 4 and 5

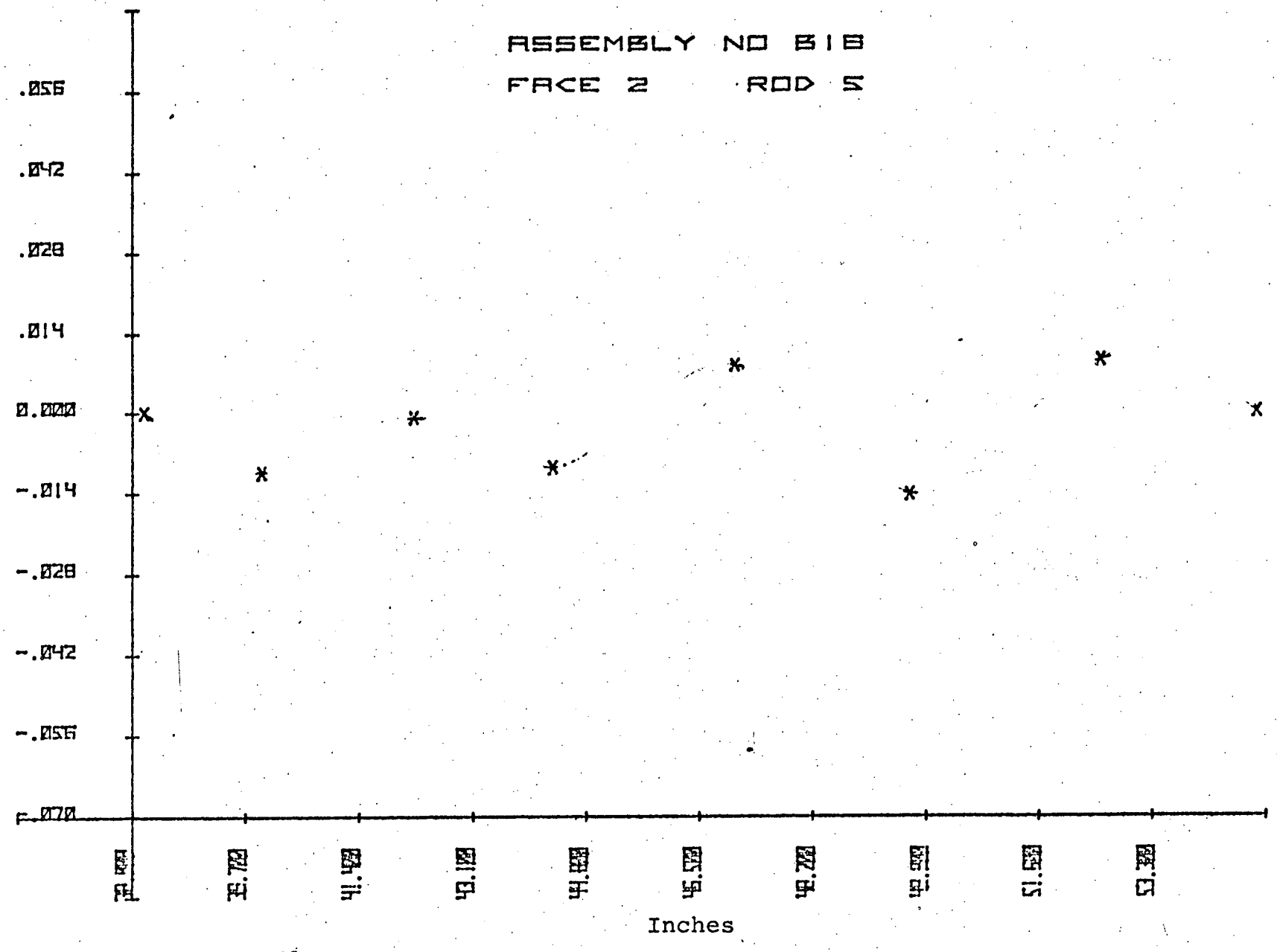

Figure 41 Bow of Rod 5, Face 2 of Assembly B-16 between Grids 3 and 4

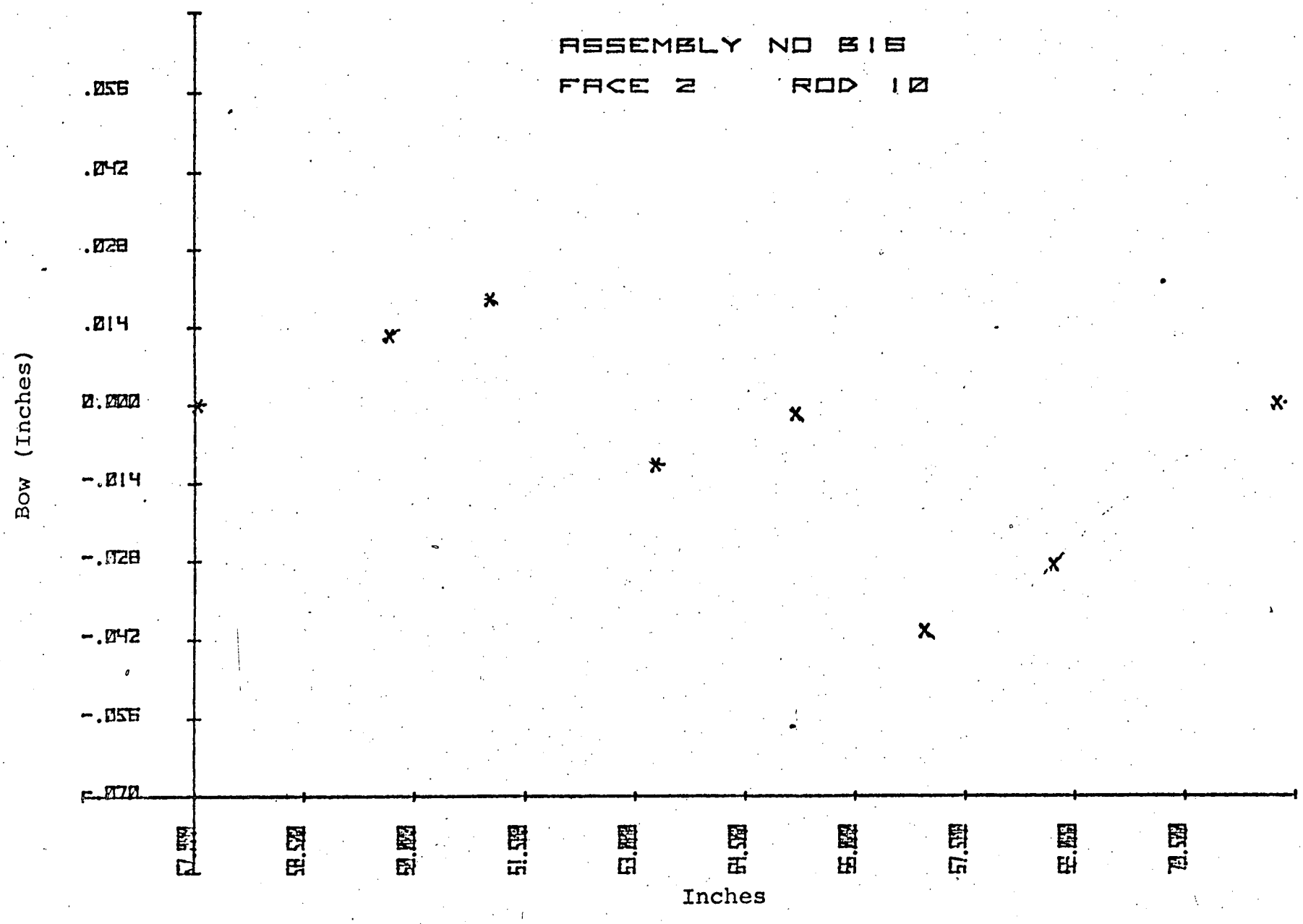

Figure 42 Bow of Rod 10, Face 2 of Assembly B-16 between Grids 4 and 5

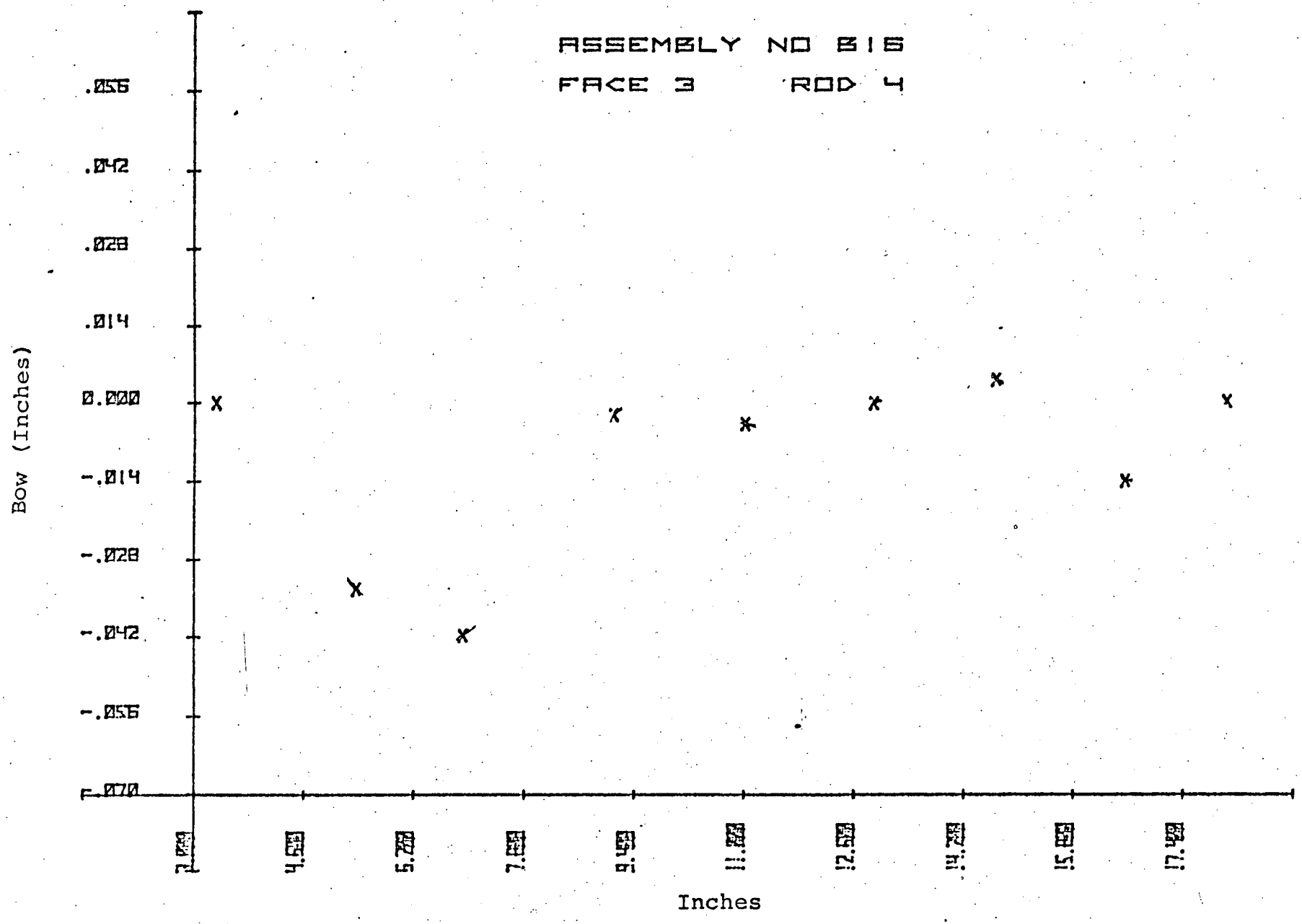

Figure 43 Bow of Rod 4, Face 3 of Assembly B-16 between Grids 1 and 2

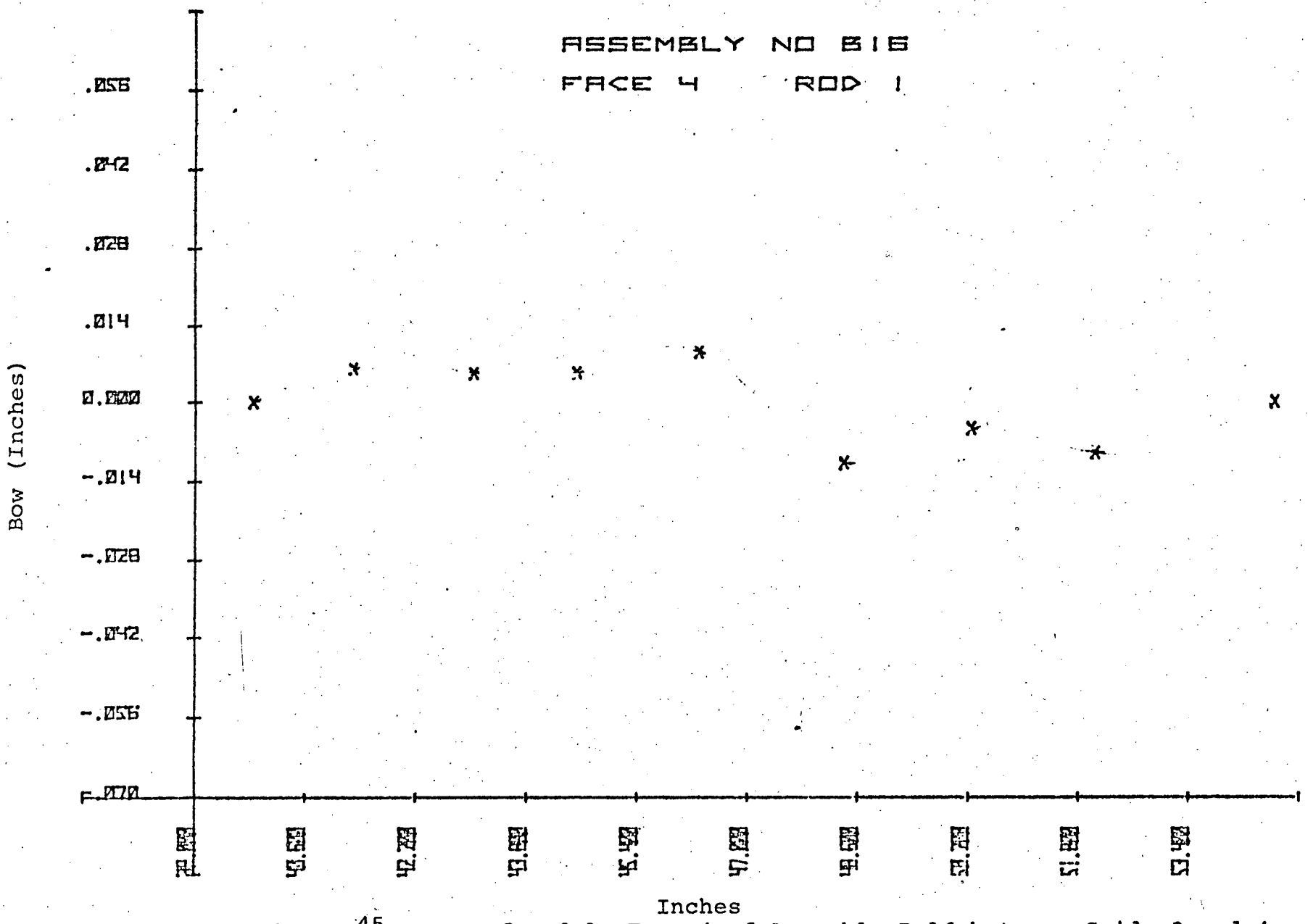

Figure 45 Bow of Rod 1, Face 4 of Assembly B-16 between Grids 3 and 4

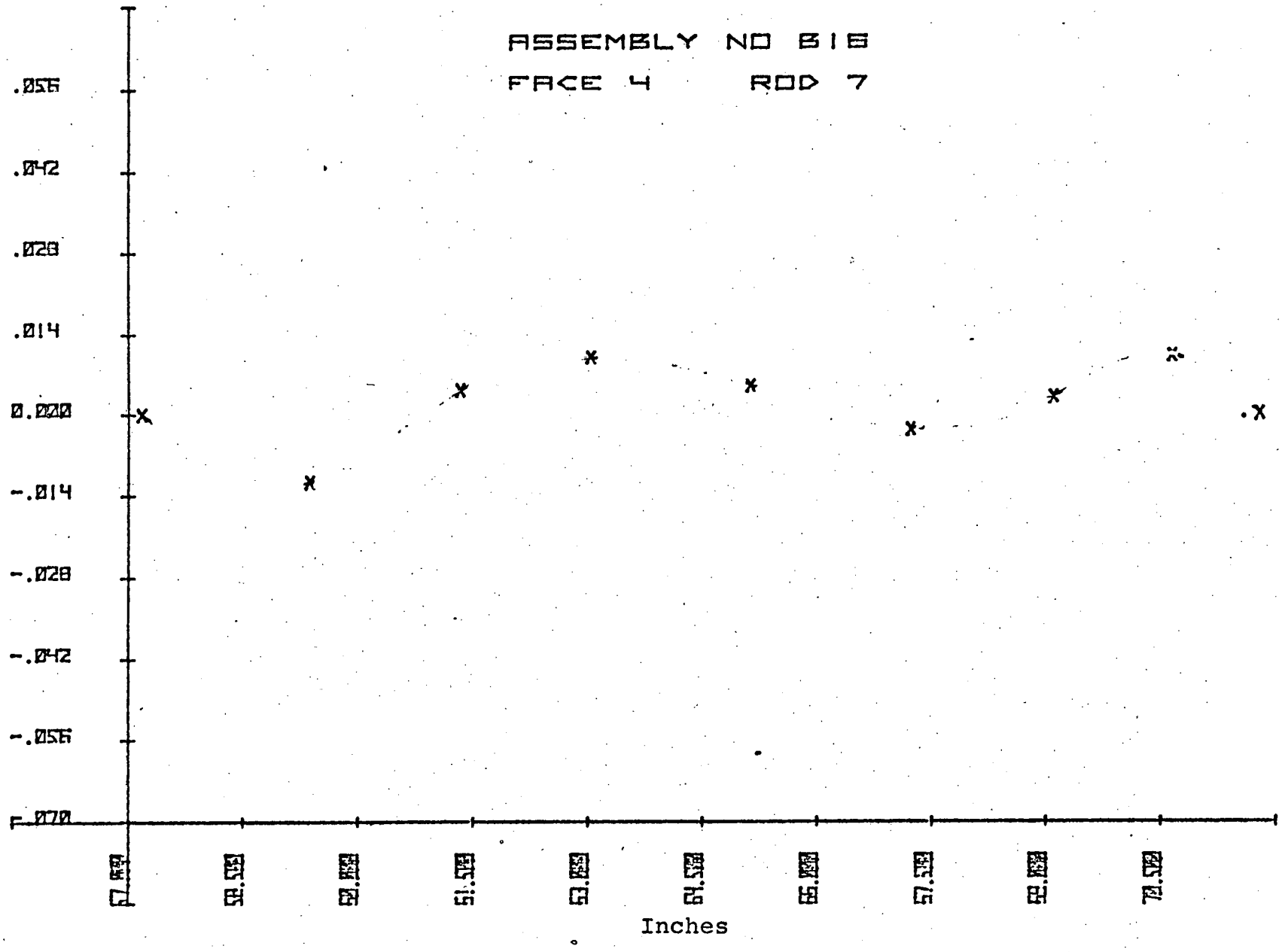

Figure 46 Bow of Rod 7, Face 4 of Assembly B-16 between Grids 5 and 6

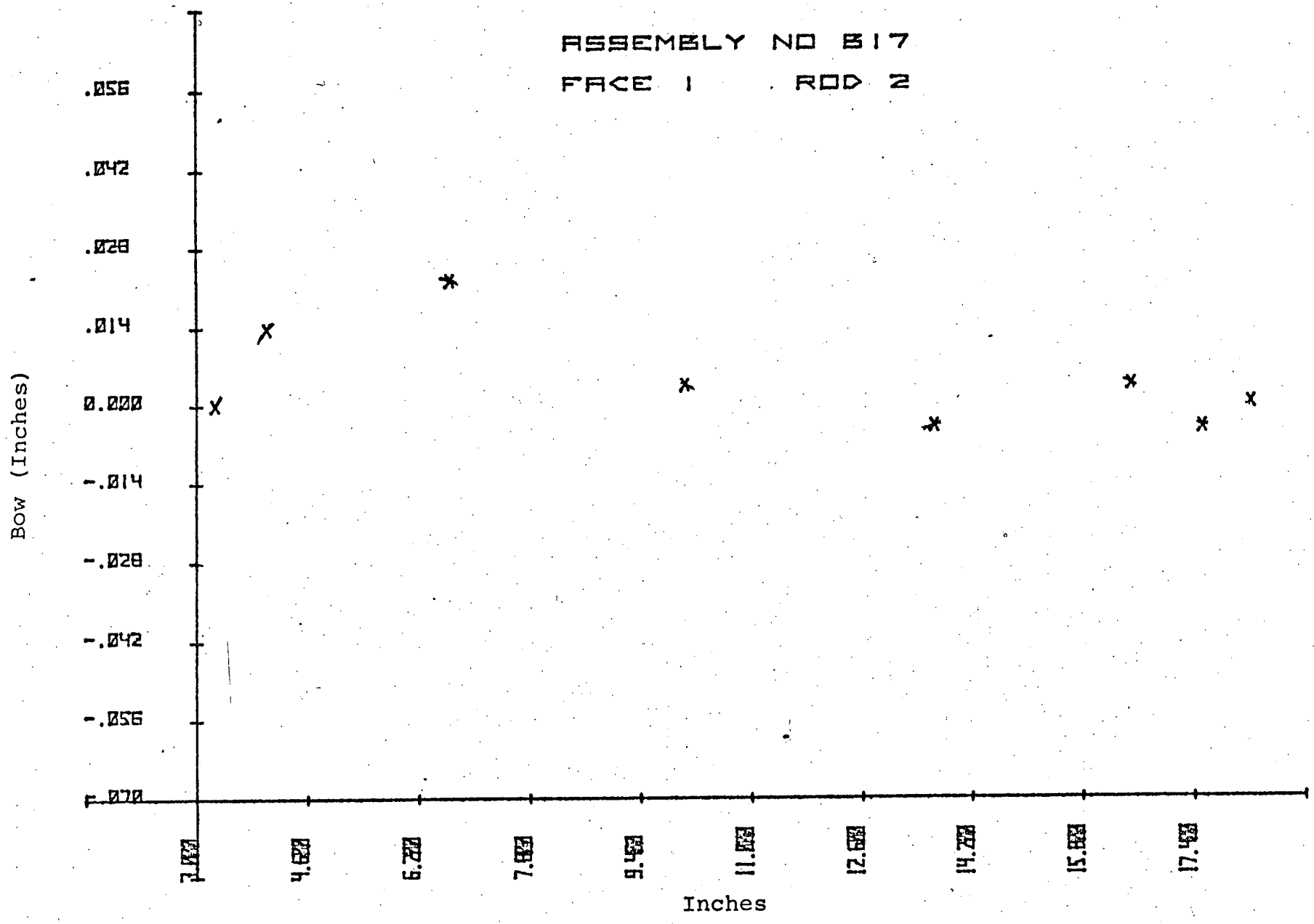

Figure 47 Bow of Rod 2, Face 1 of Assembly B-17 between Grids 1 and 2

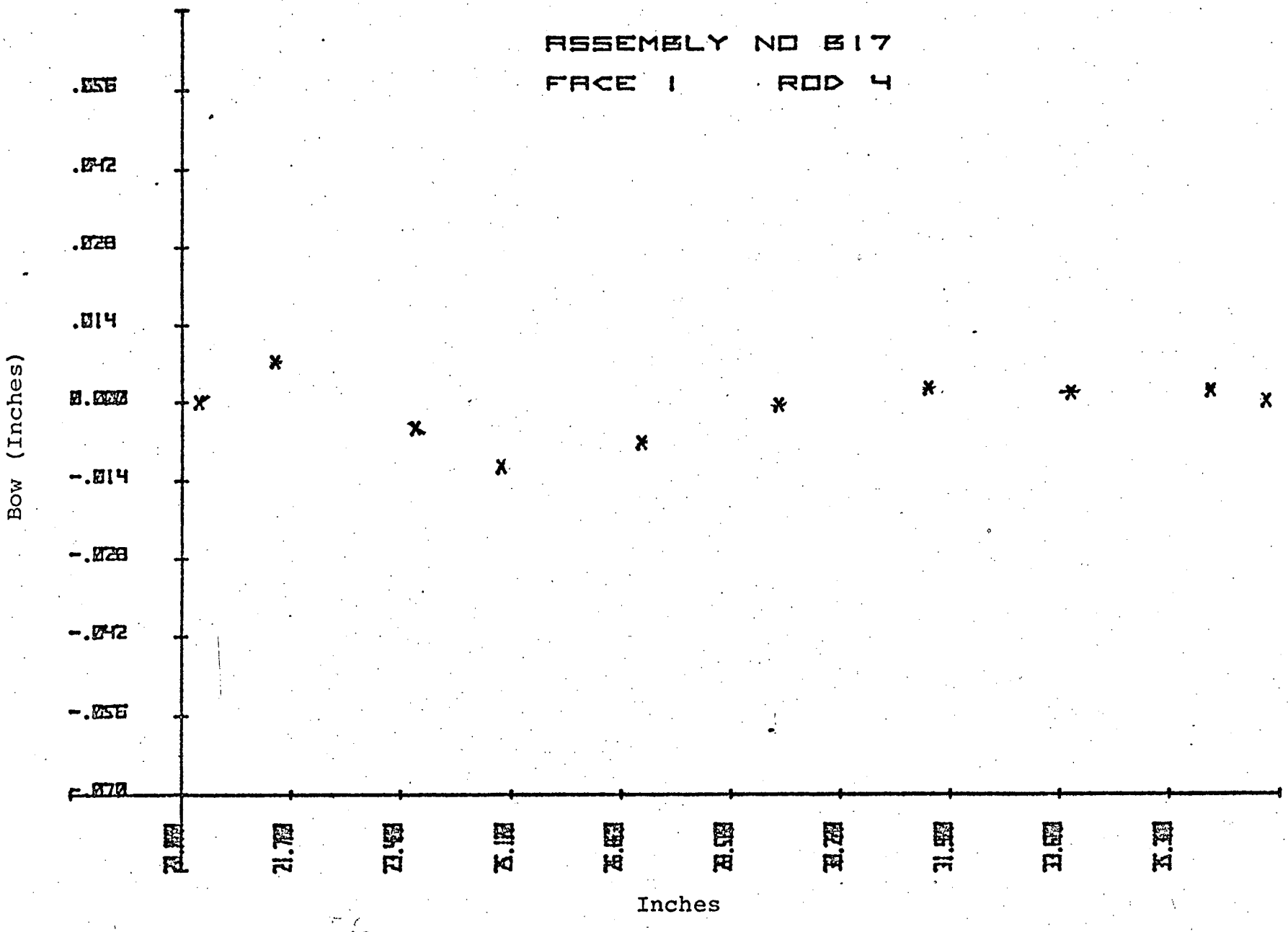

Figure 48 Bow of Rod 4, Face 1 of Assembly B-17 between Grids 2 and 3

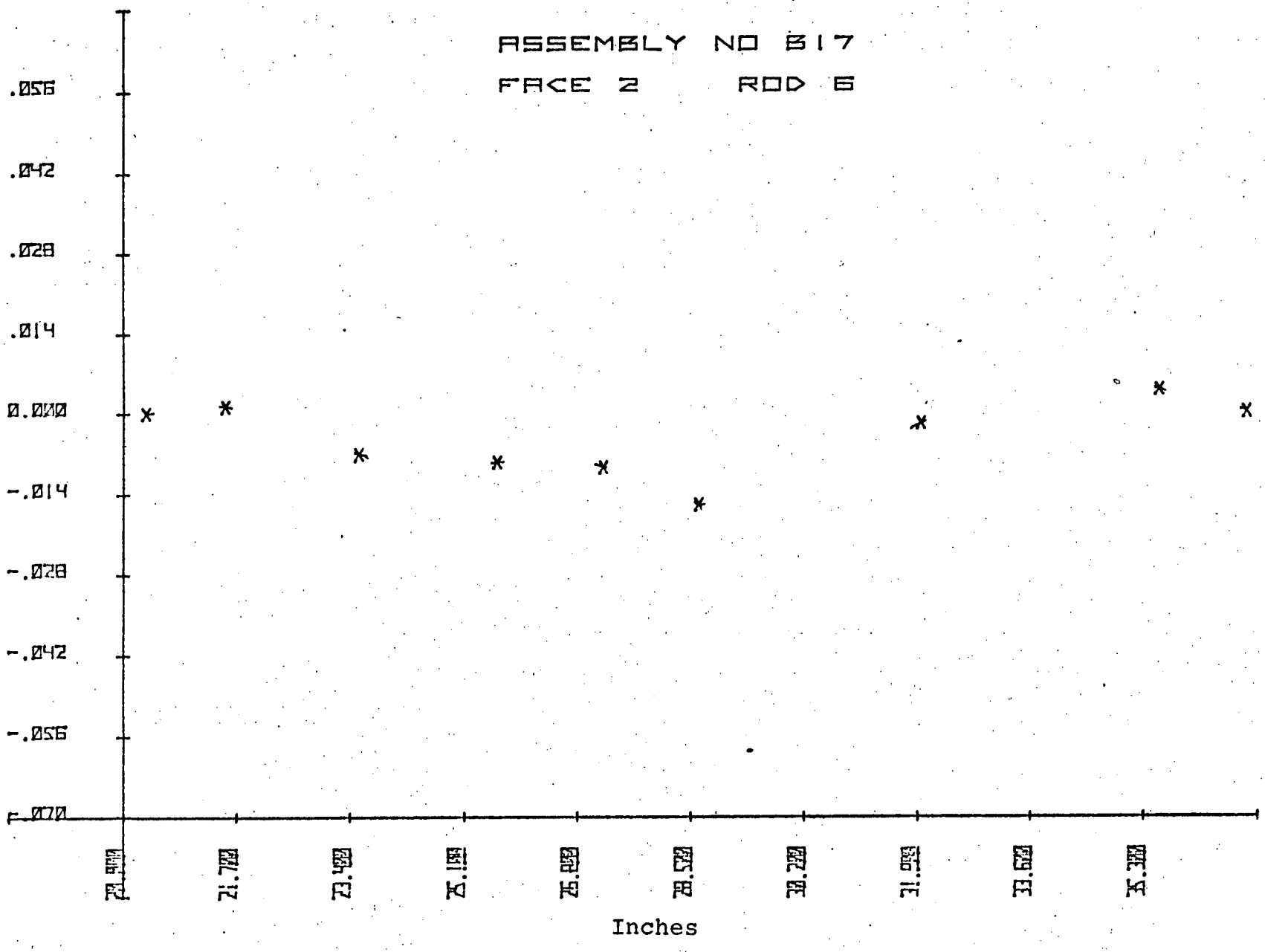

Figure 49 Bow of Rod 6, Face 2 of Assembly B-17 between Grids 2 and 3

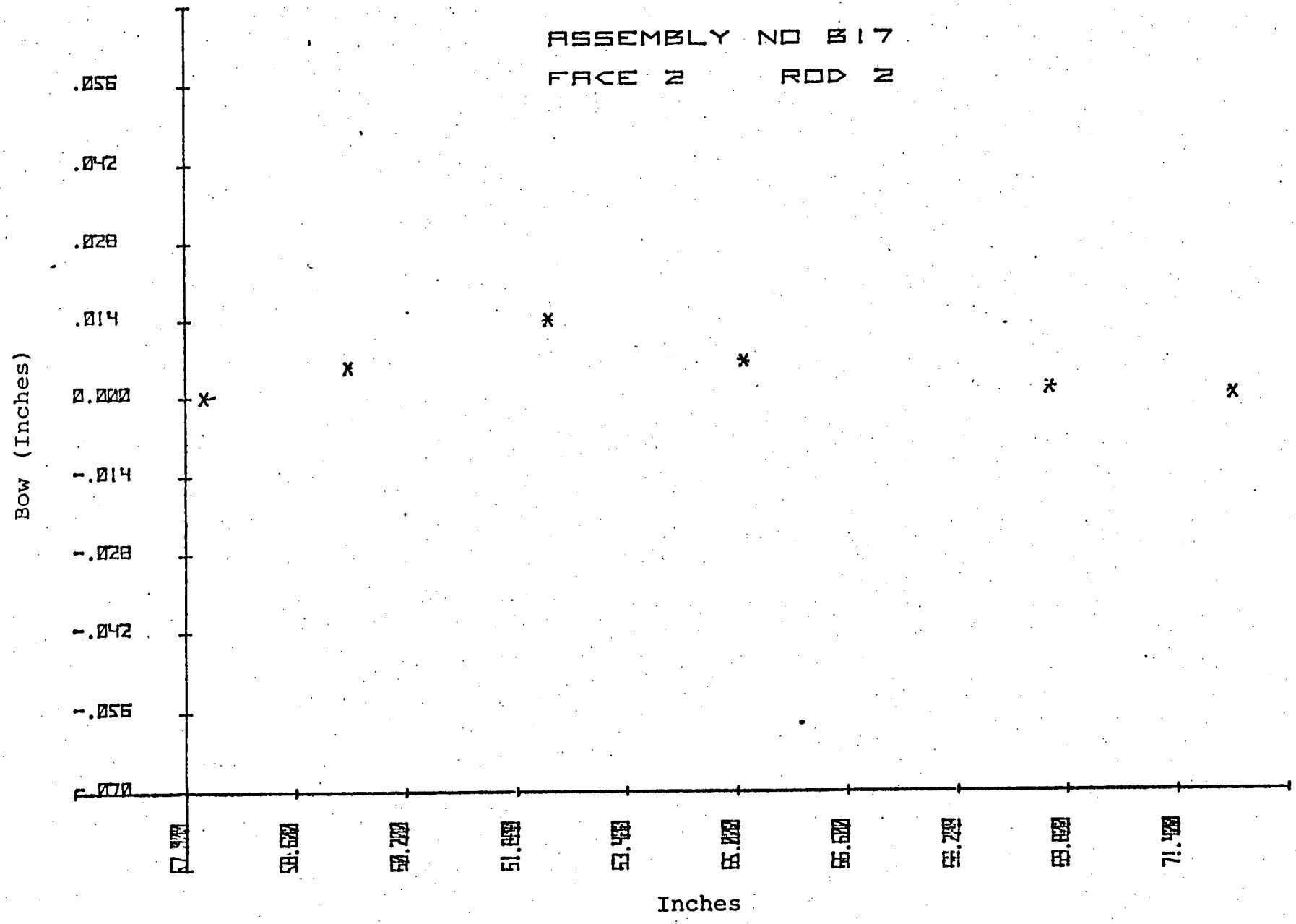

Figure 50 Bow of Rod 2, Face 2 of Assembly B-17 between Grids 4 and 5

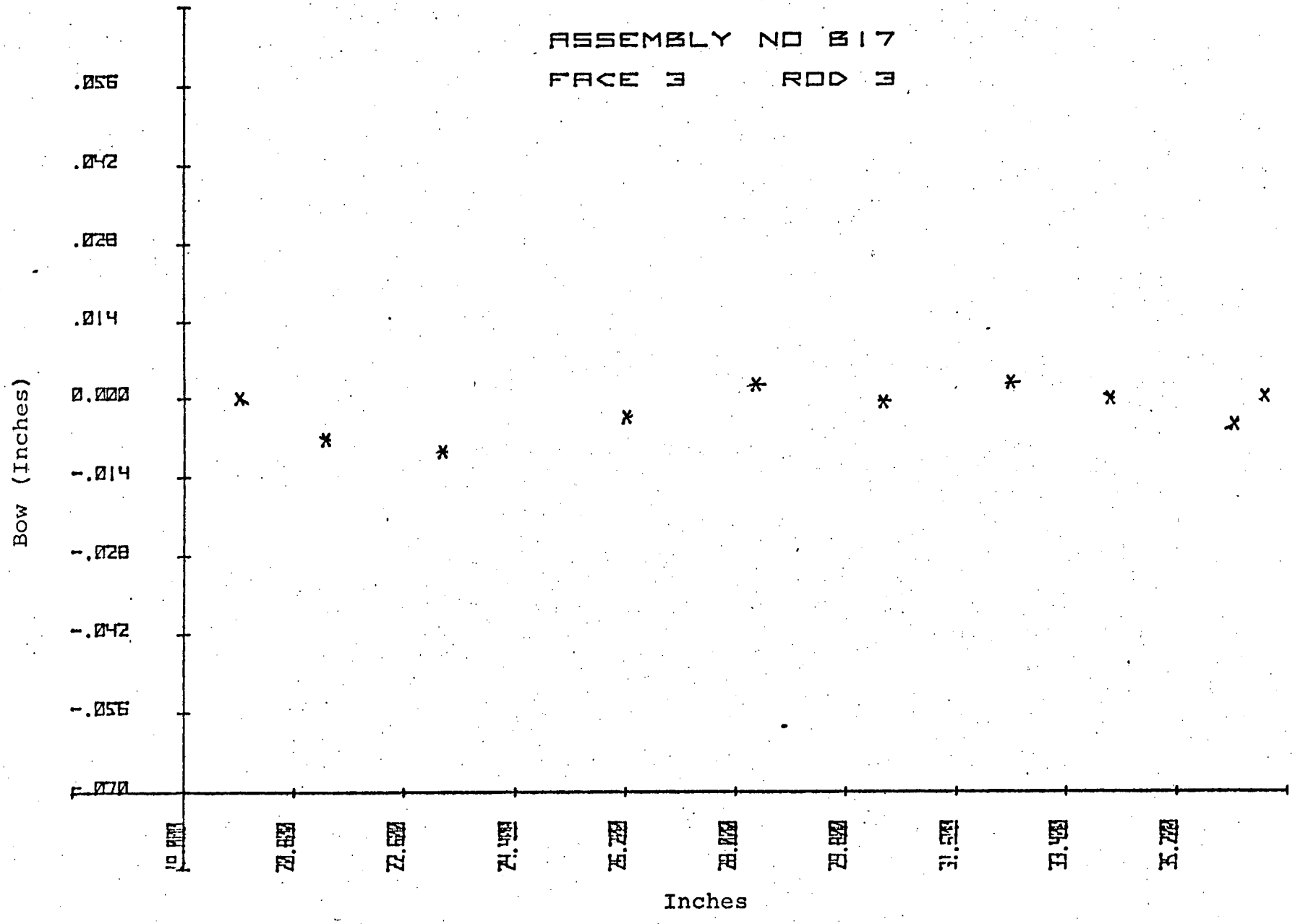

Figure 51 Bow of Rod 3, Face 3 of Assembly B-17 between Grids 2 and 3

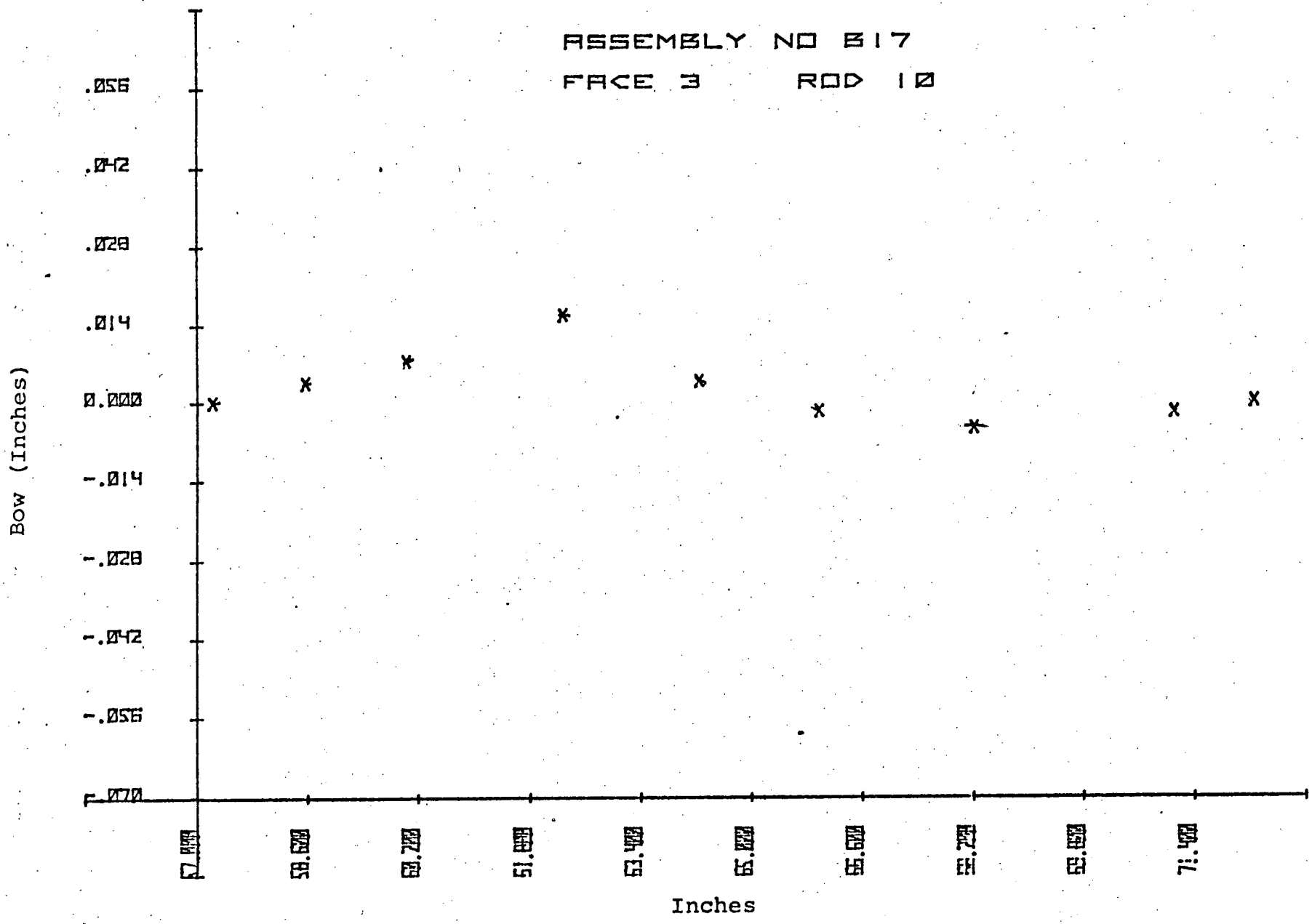

Figure 52 Bow of Rod 10, Face 3 of Assembly B-17 between Grids 4 and 5

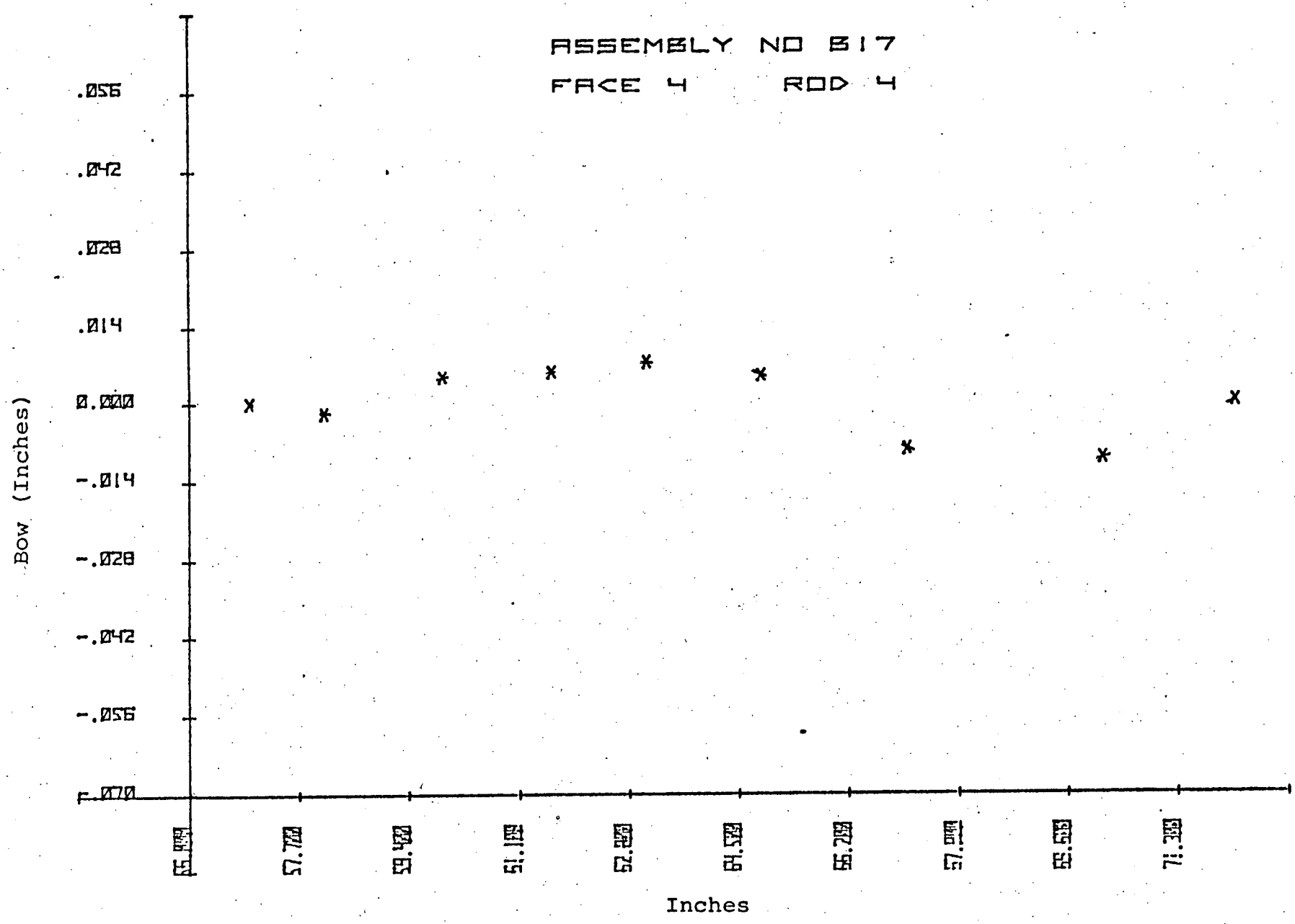

Figure 53 Bow of Rod 4, Face 4 of Assembly B-17 between Grids 4 and 5

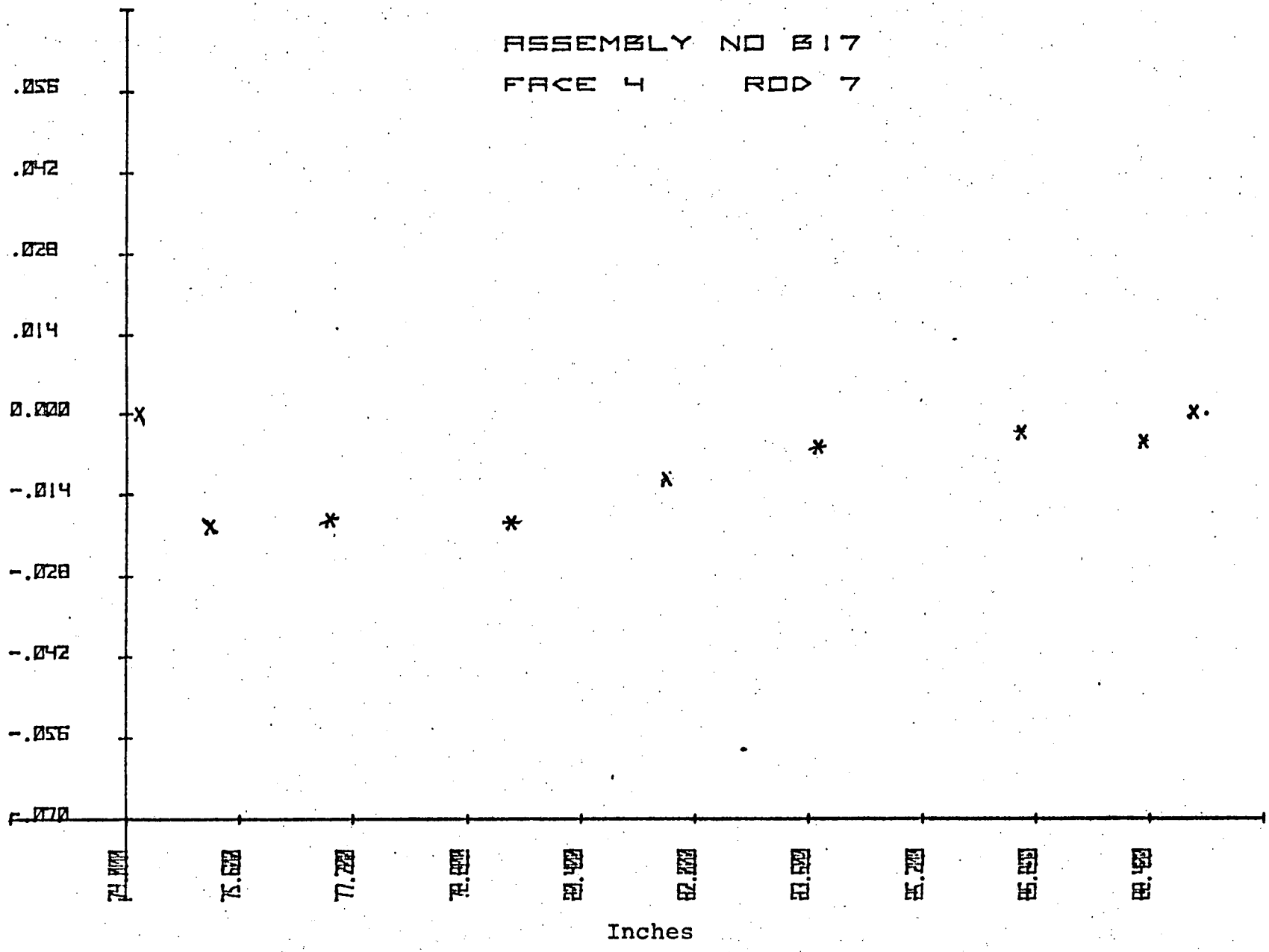

Figure 54 Bow of Rod 7, Face 4 of Assembly B-17 between Grids 5 and 6

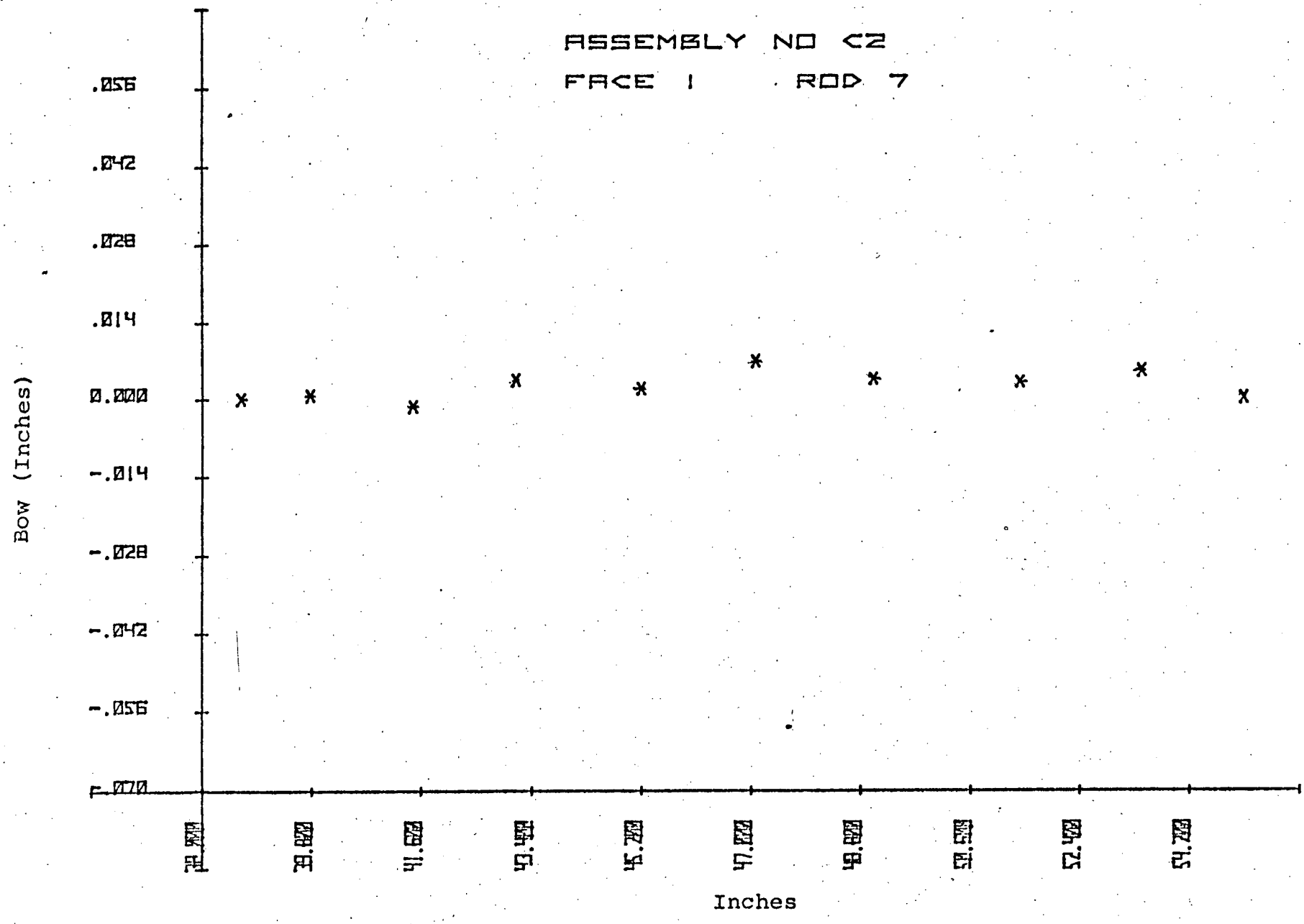

Figure 55 Bow of Rod 7, Face 1 of Assembly C-02 between Grids 3 and 4

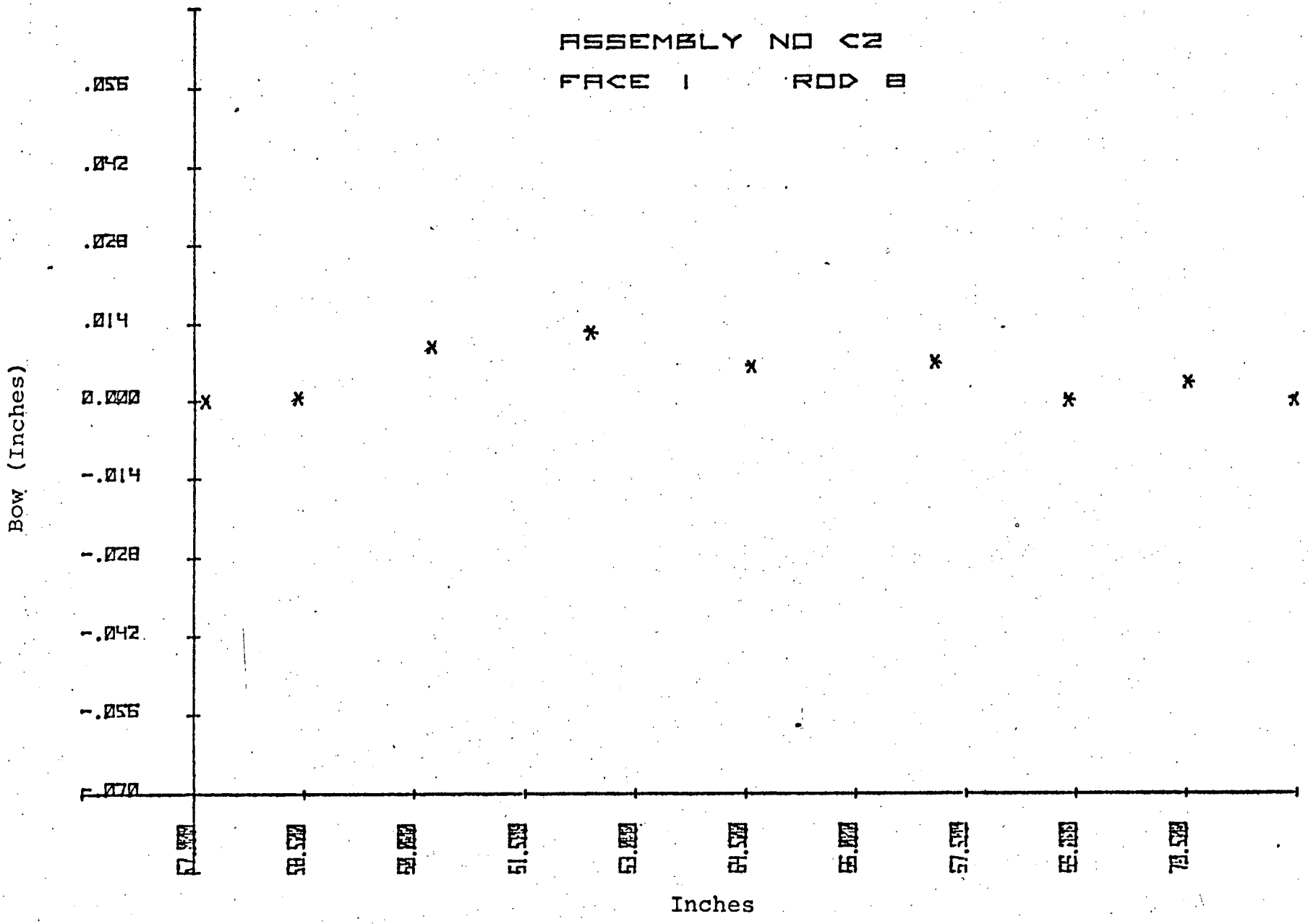

Figure 56 Bow of Rod 8, Face 1 of Assembly C-02 between Grids 4 and 5

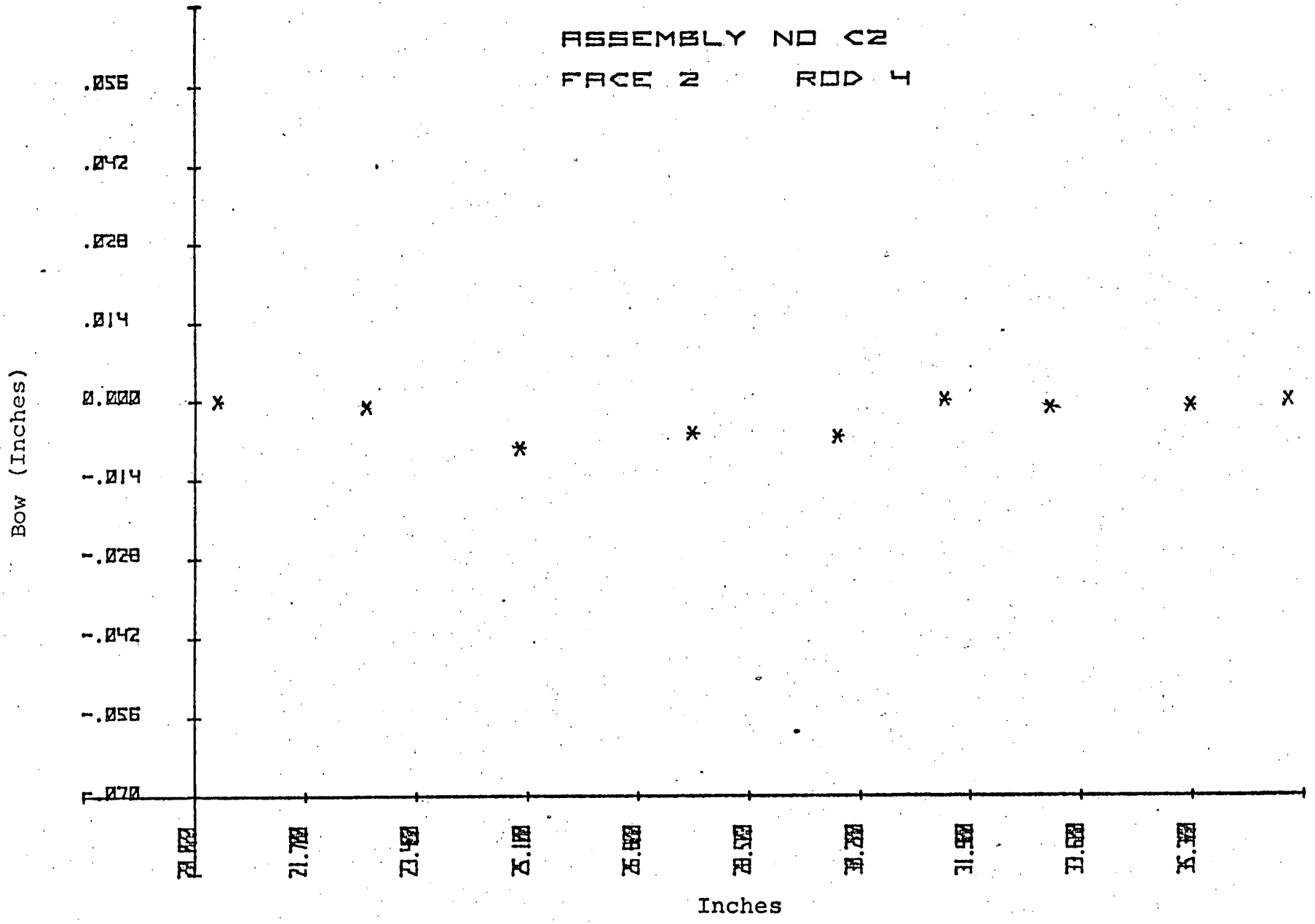

Figure 57 Bow of Rod 4, Face 2 of Assembly C-02 between Grids 2 and 3

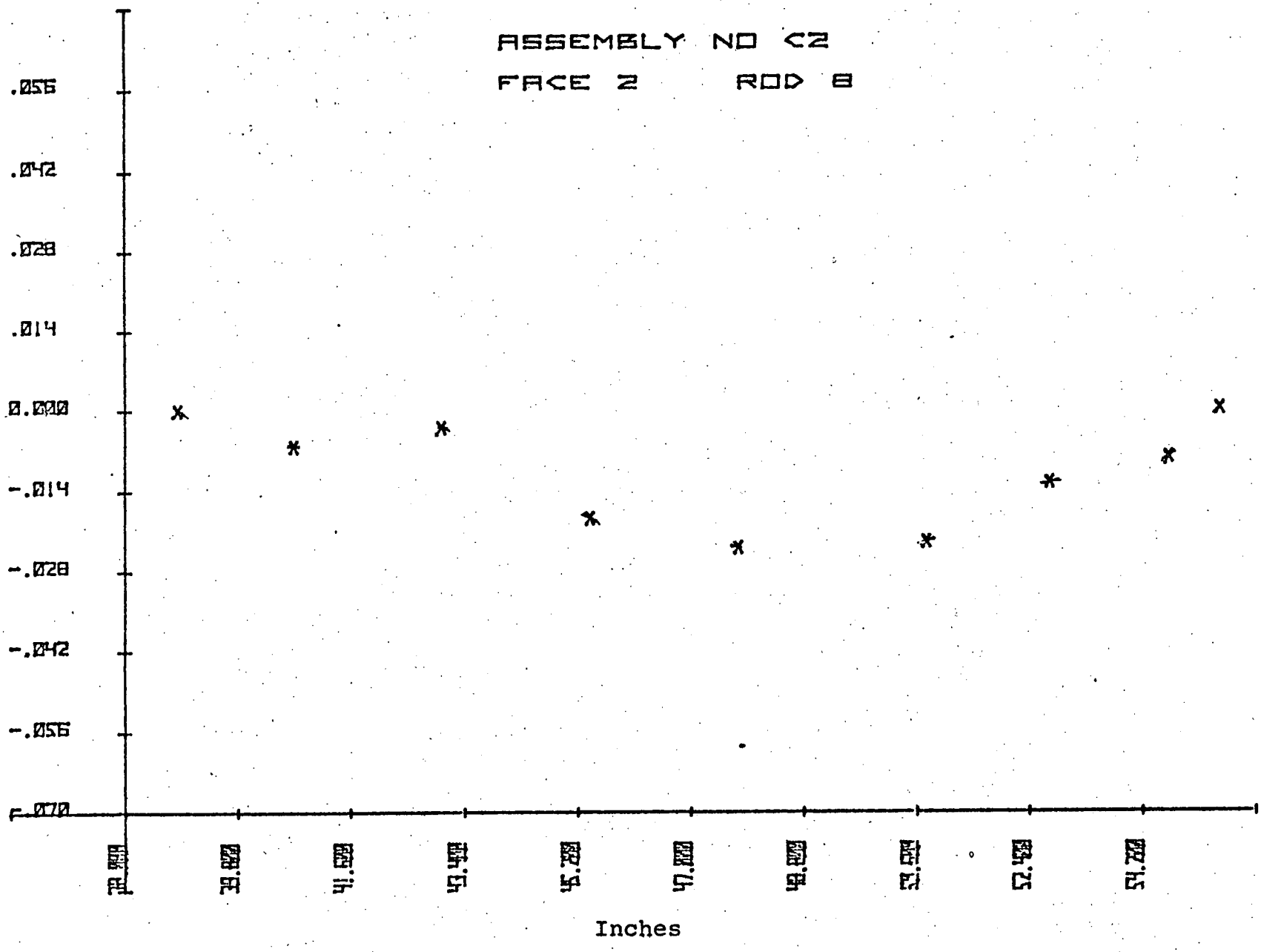

Figure 58 Bow of Rod 8, Face 2 of Assembly C-02 between Grids 3 and 4

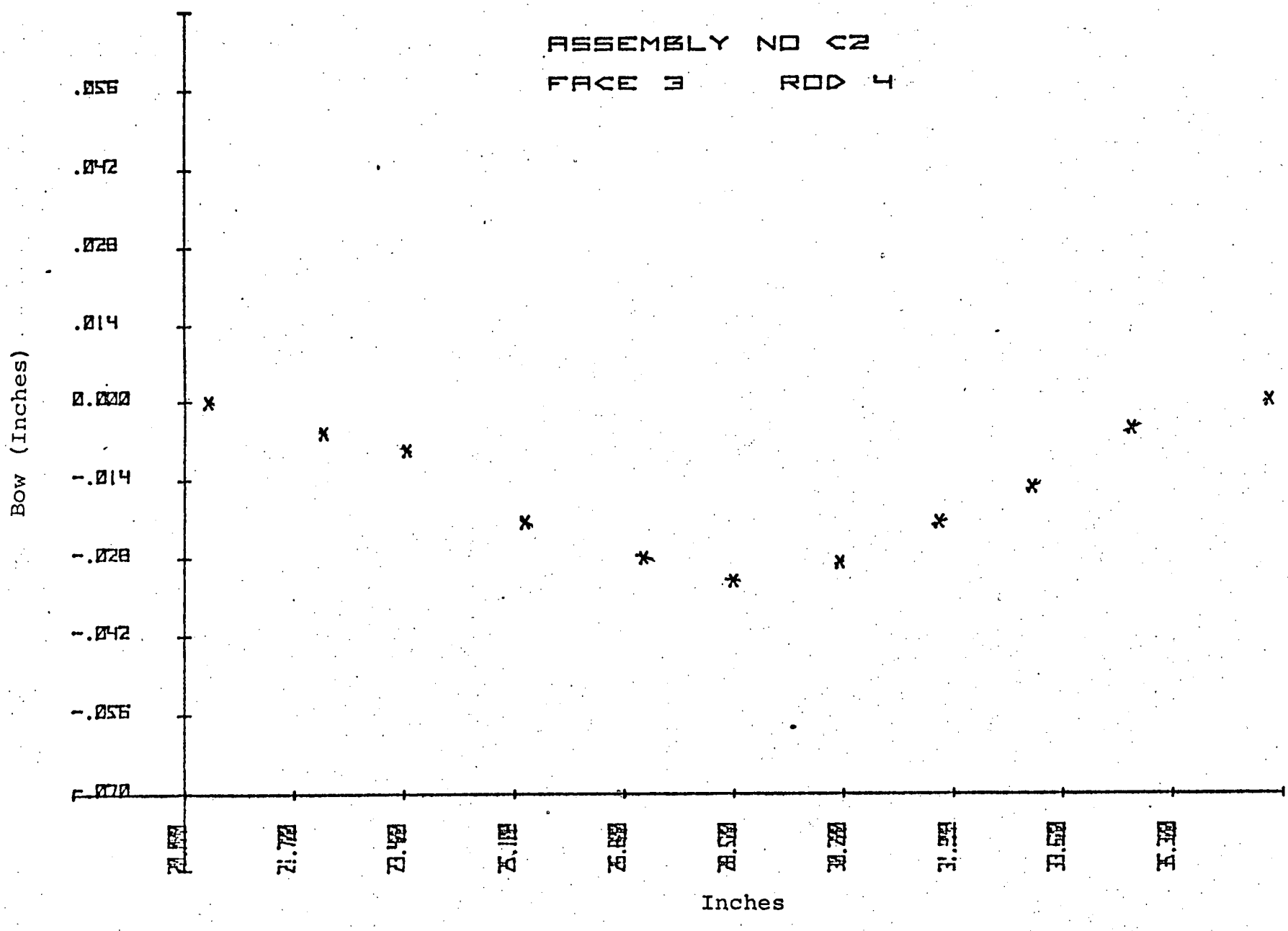

Figure 59 Bow of Rod 4, Face 3 of Assembly C-02 between Grids 2 and 3

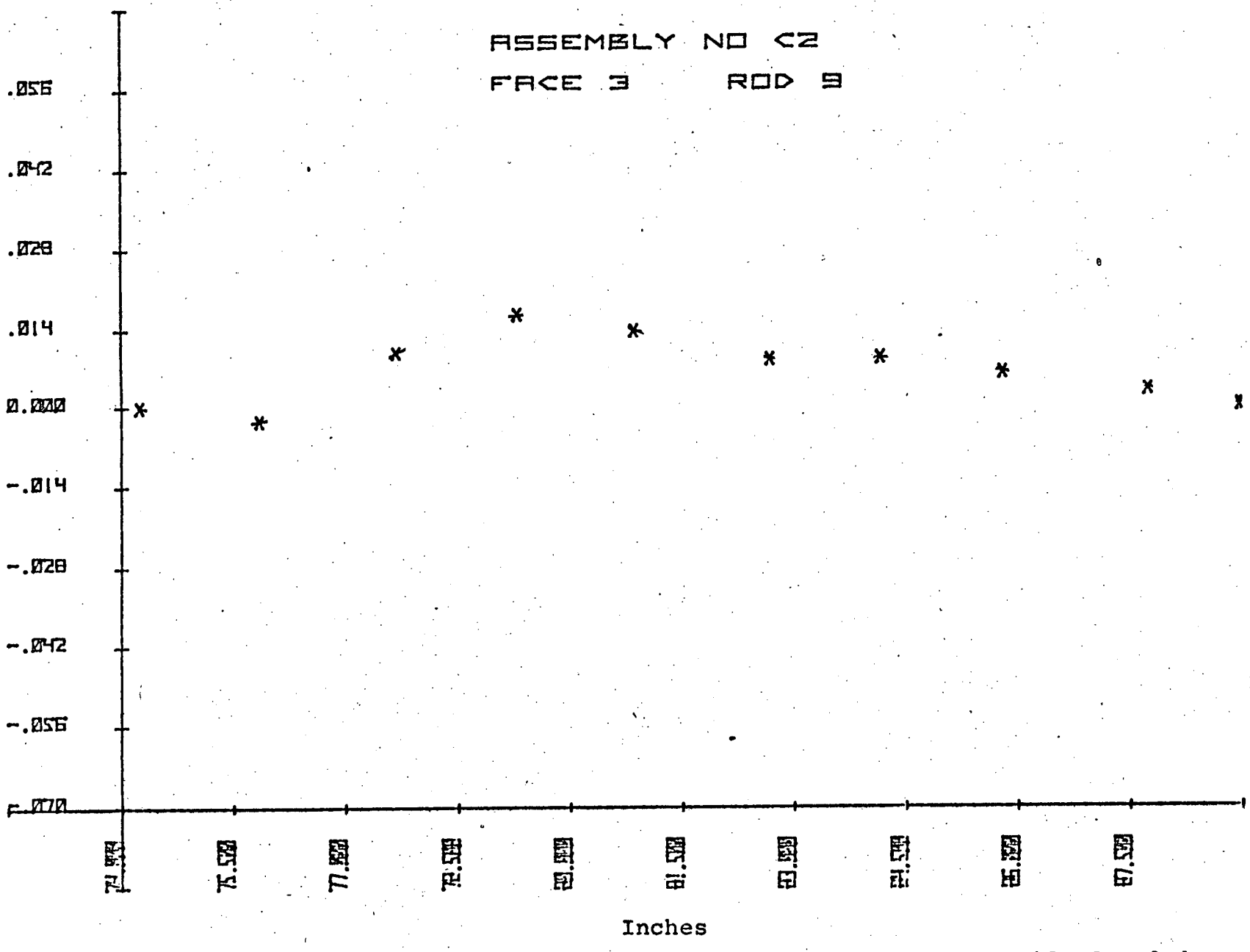

Figure 60 Bow of Rod 9, Face 3 of Assembly C-02 between Grids 5 and 6

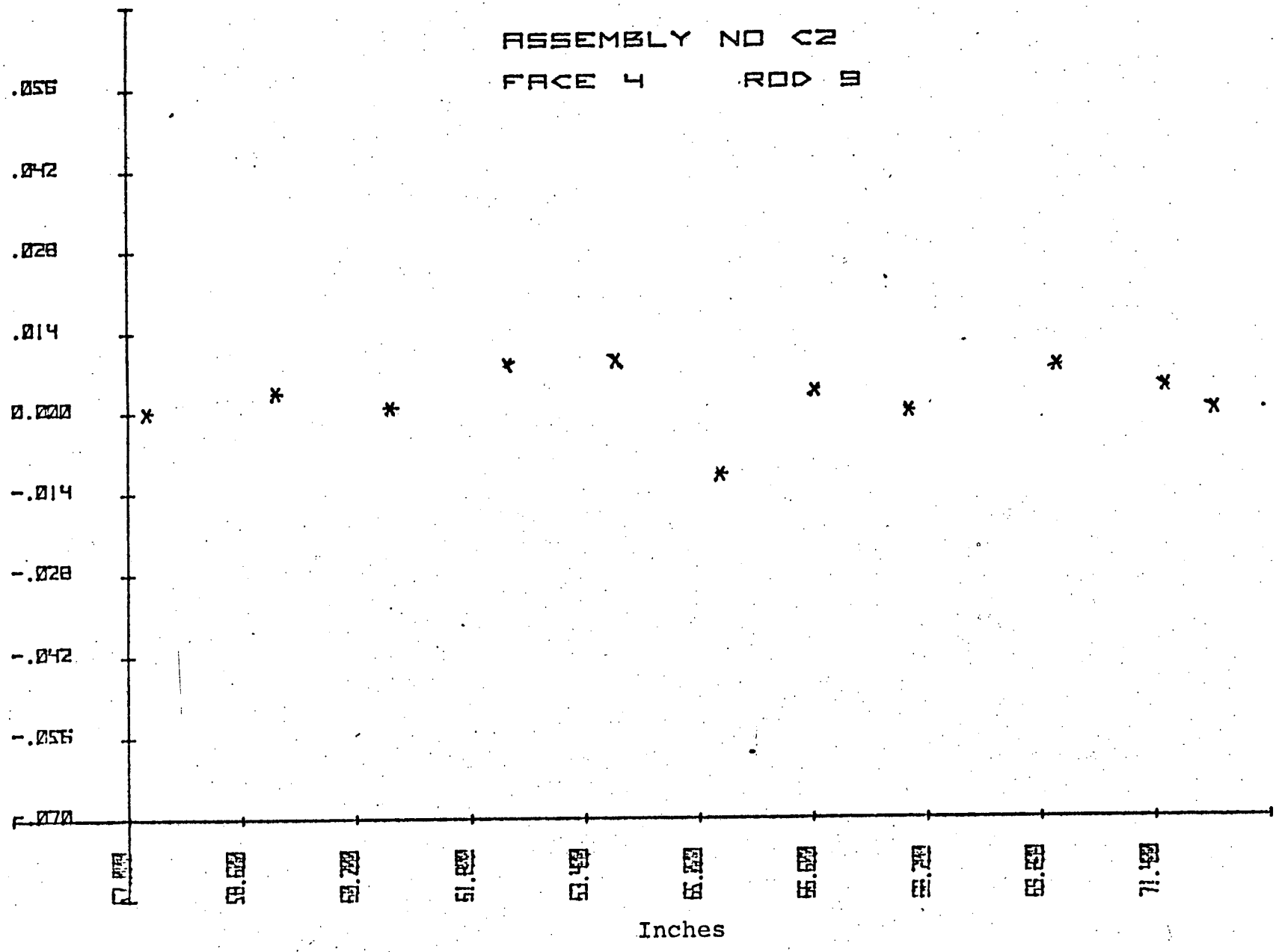

Figure 61 Bow of Rod 9, Face 4 of Assembly C-02 between Grids 5 and 6

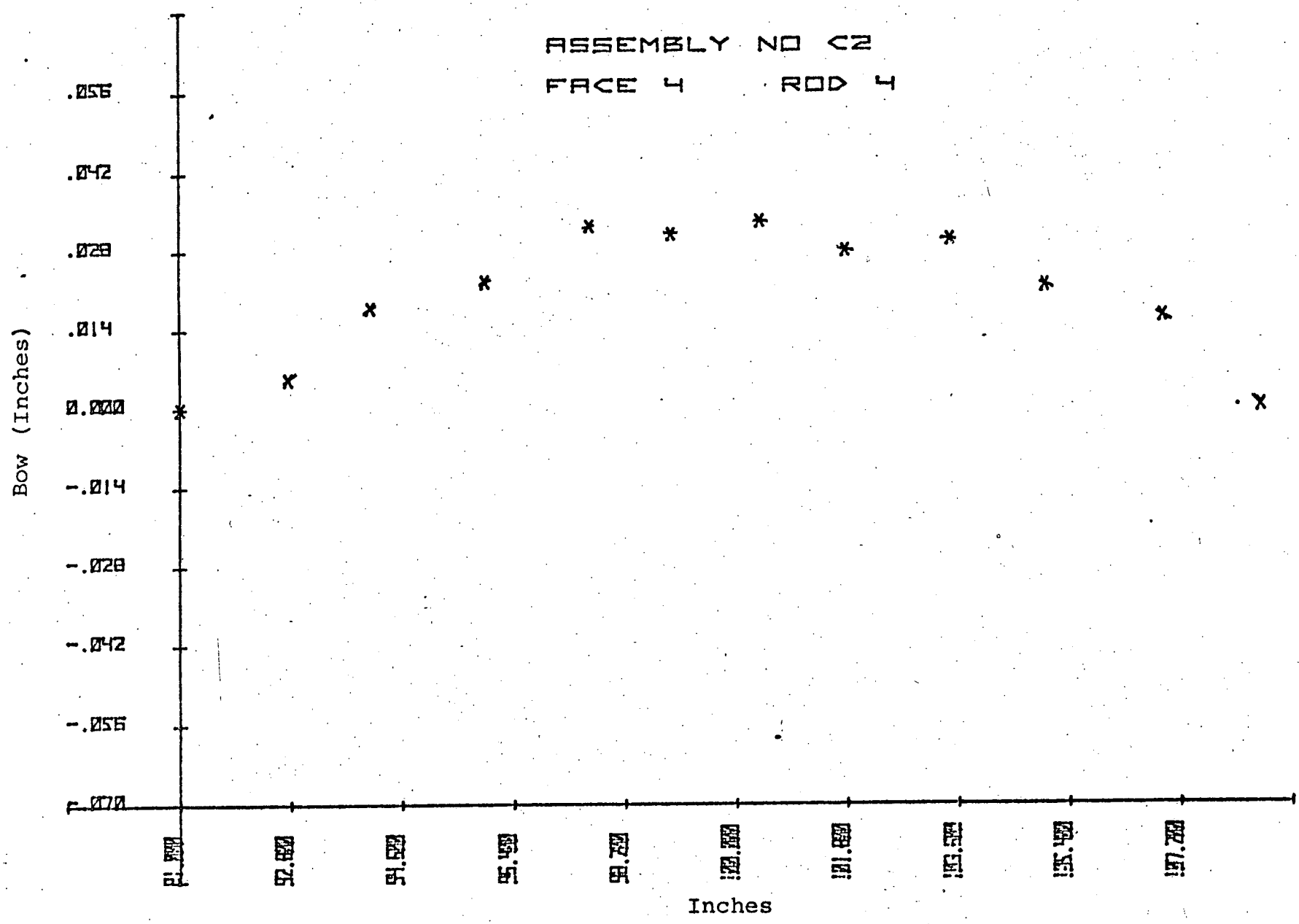

Figure 62 Bow of Rod 4, Face 4 of Assembly C-02 between Grids 6 and 7

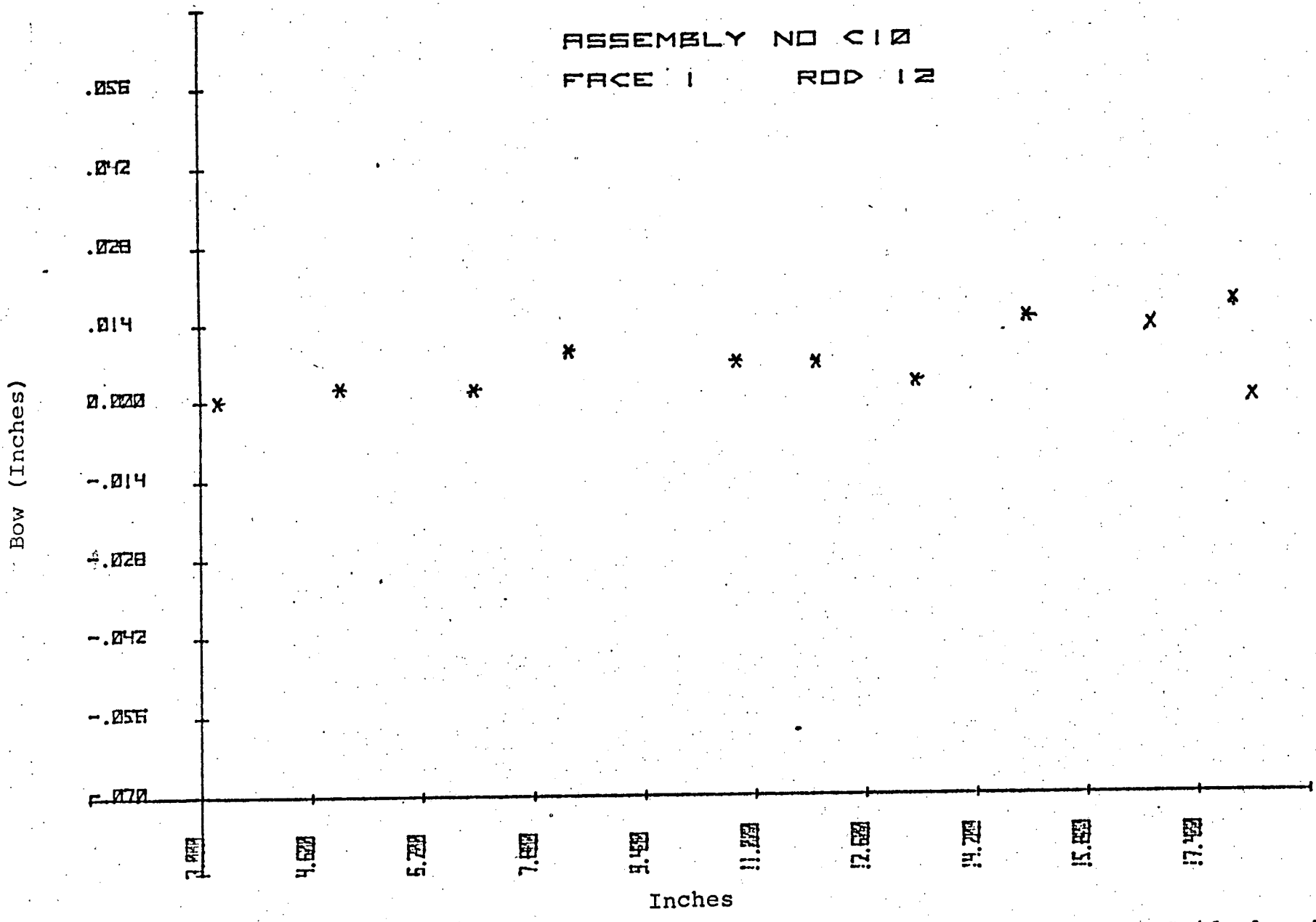

Figure 63 Bow of Rod 12, Face 1 of Assembly C-10 between Grids 1 and 2

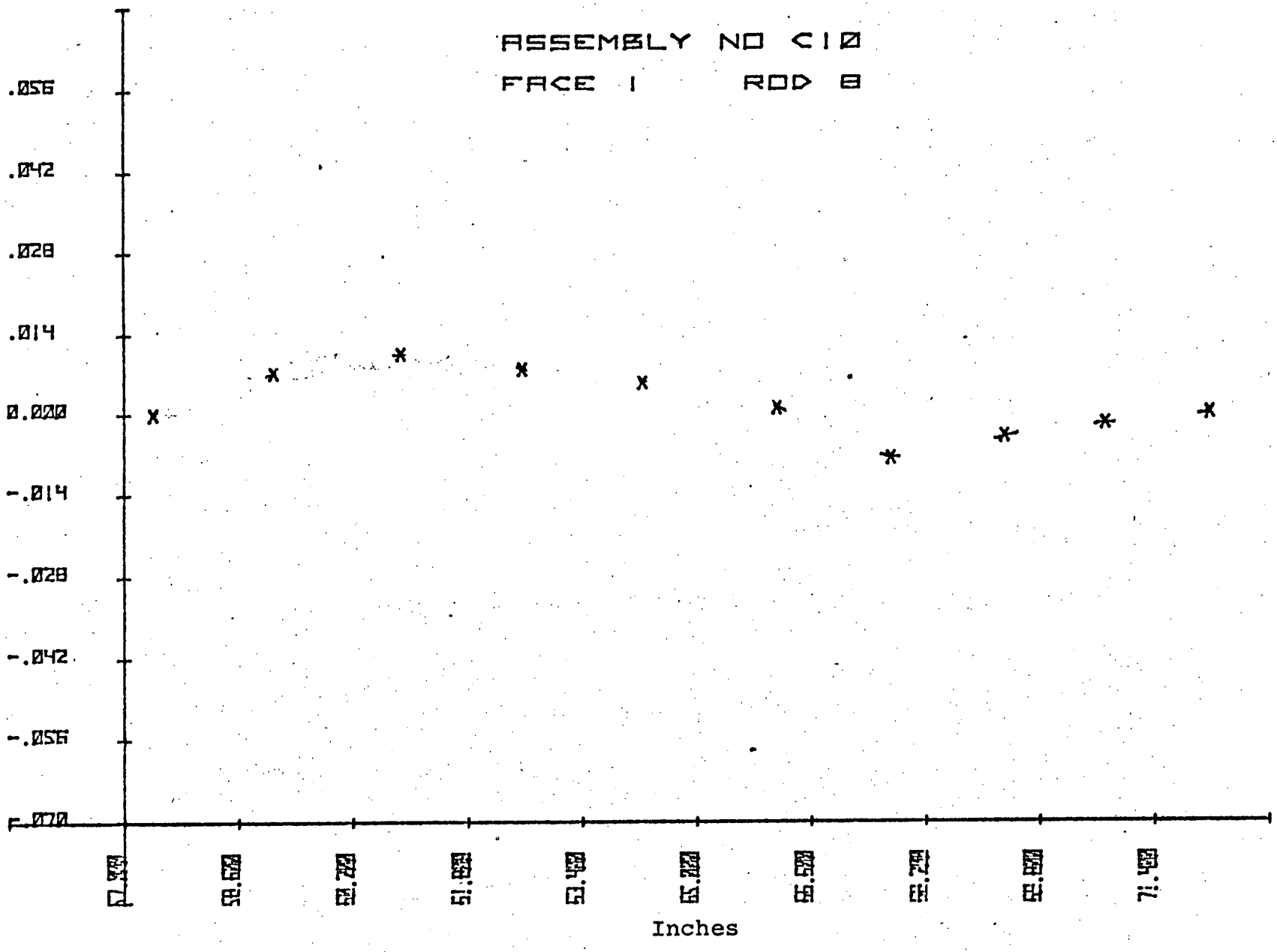

Figure 64 Bow of Rod 8, Face 1 of Assembly C-10 between Grids 4 and 5

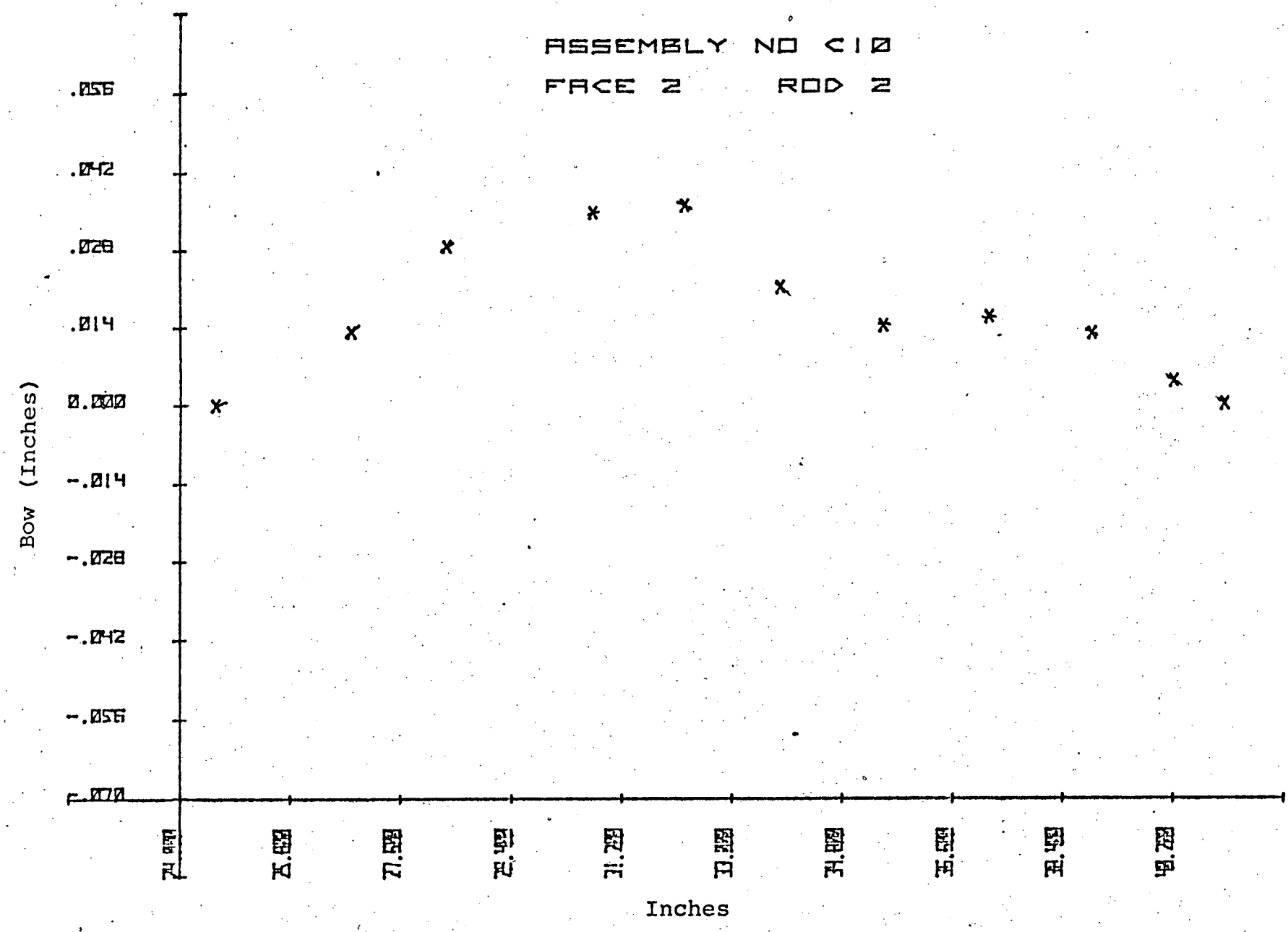

Figure 65 Bow of Rod 2, Face 2 of Assembly C-10 between Grids 2 and 3

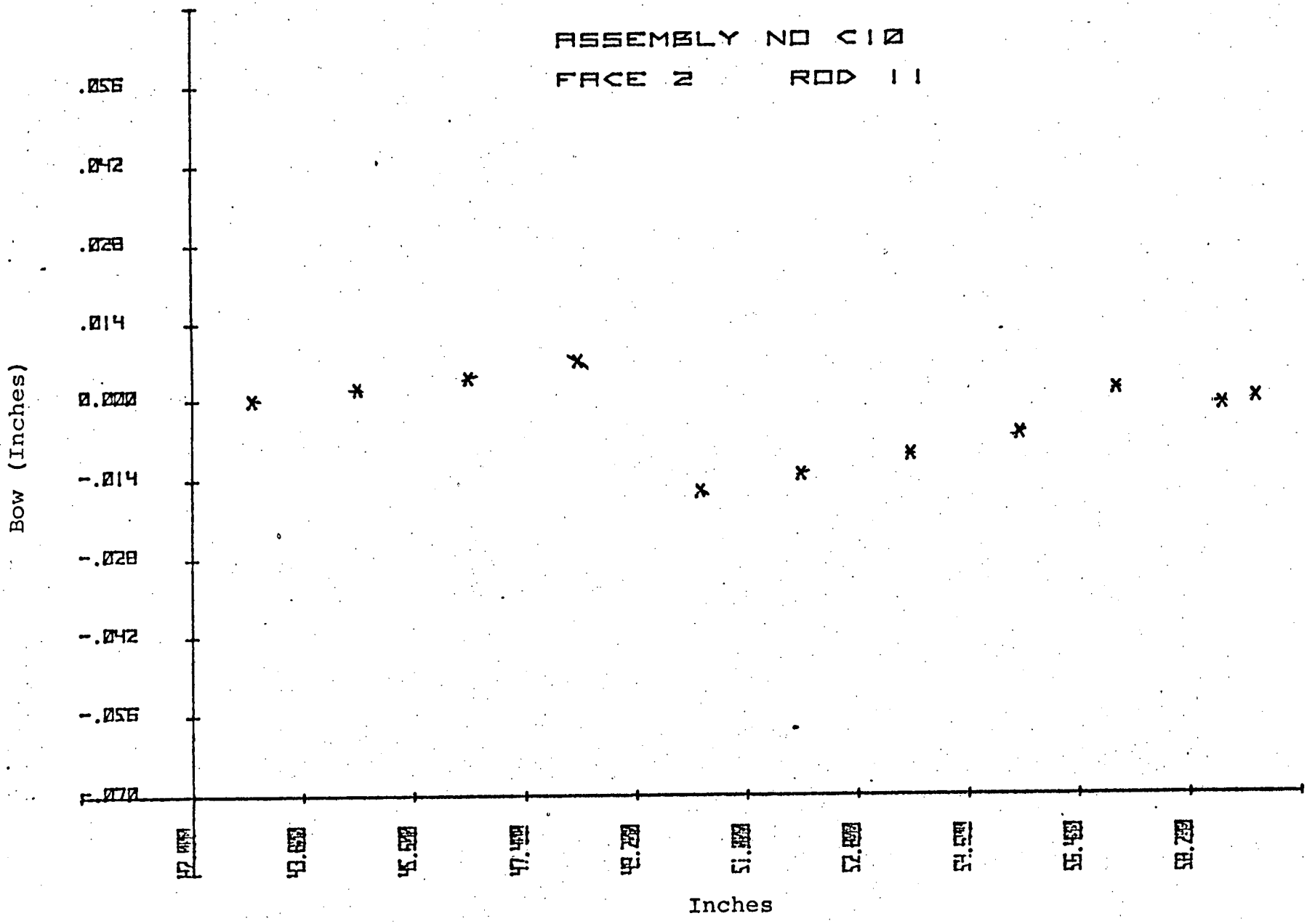

Figure 66 Bow of Rod 11, Face 2 of Assembly C-10 between Grids 3 and 4

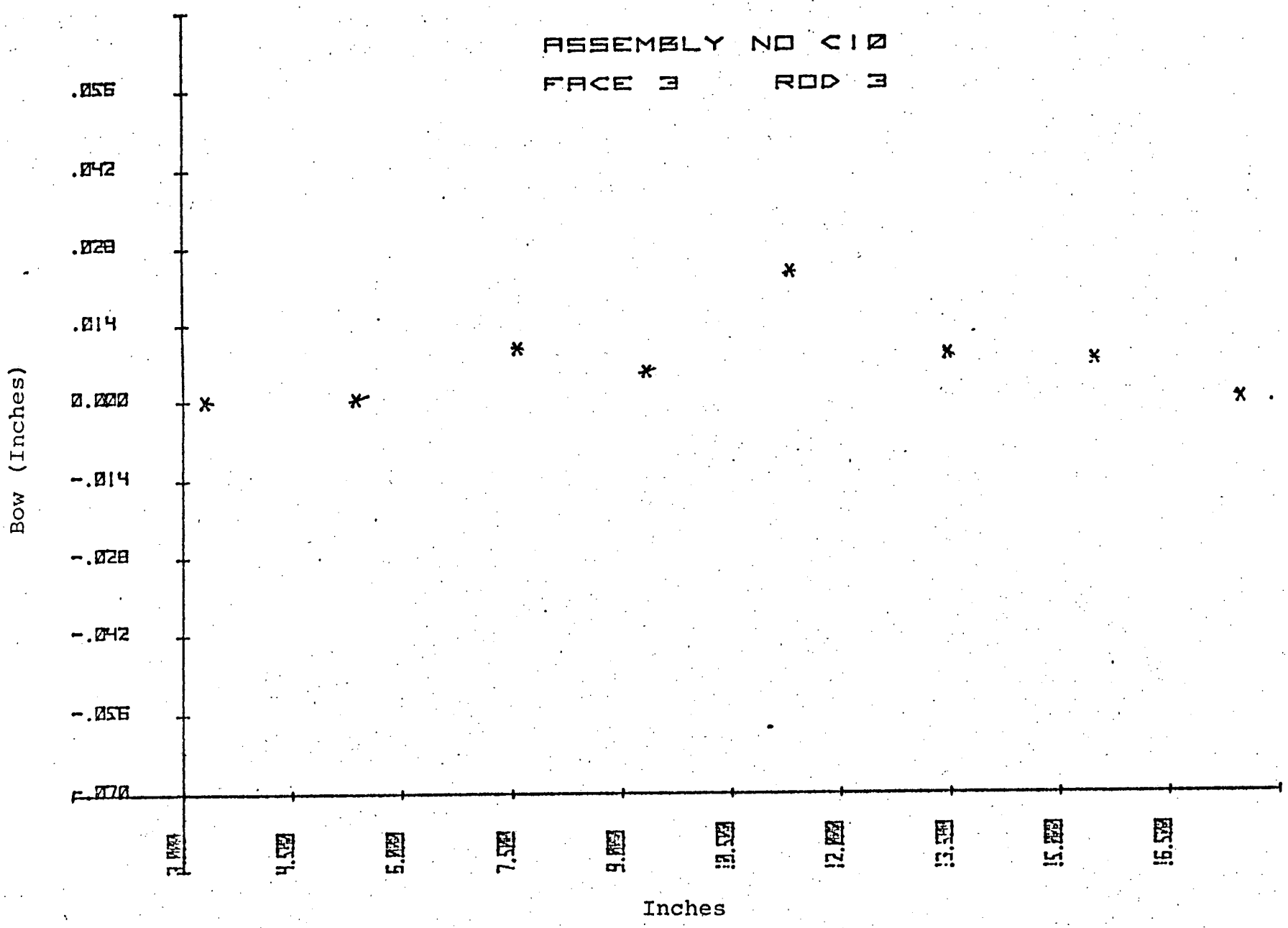

Figure 67 Bow of Rod 3, Face 3 of Assembly C-10 between Grids 1 and 2

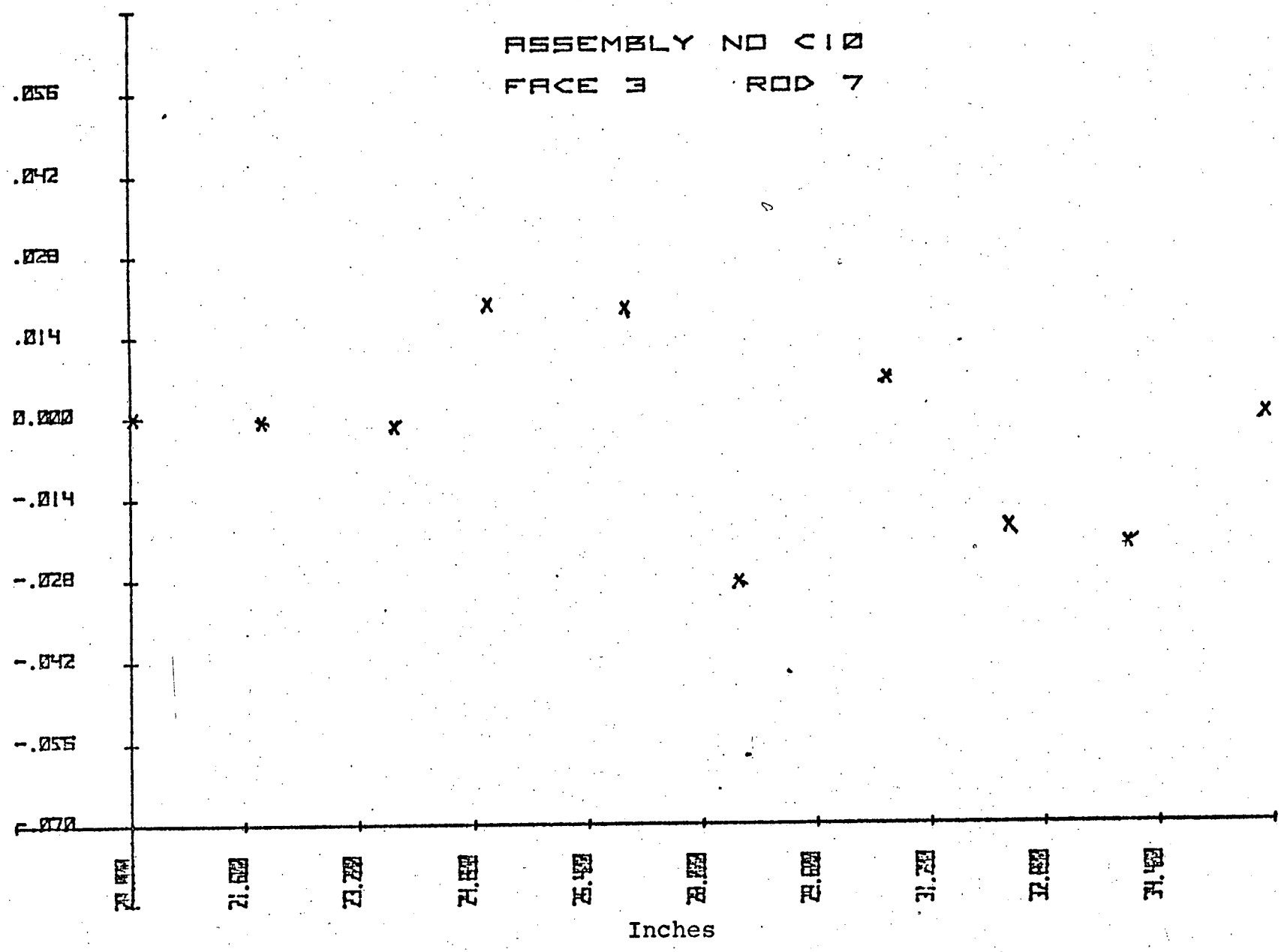

Figure 68 Bow of Rod 7, Face 3 of Assembly C-10 between Grids 2 and 3

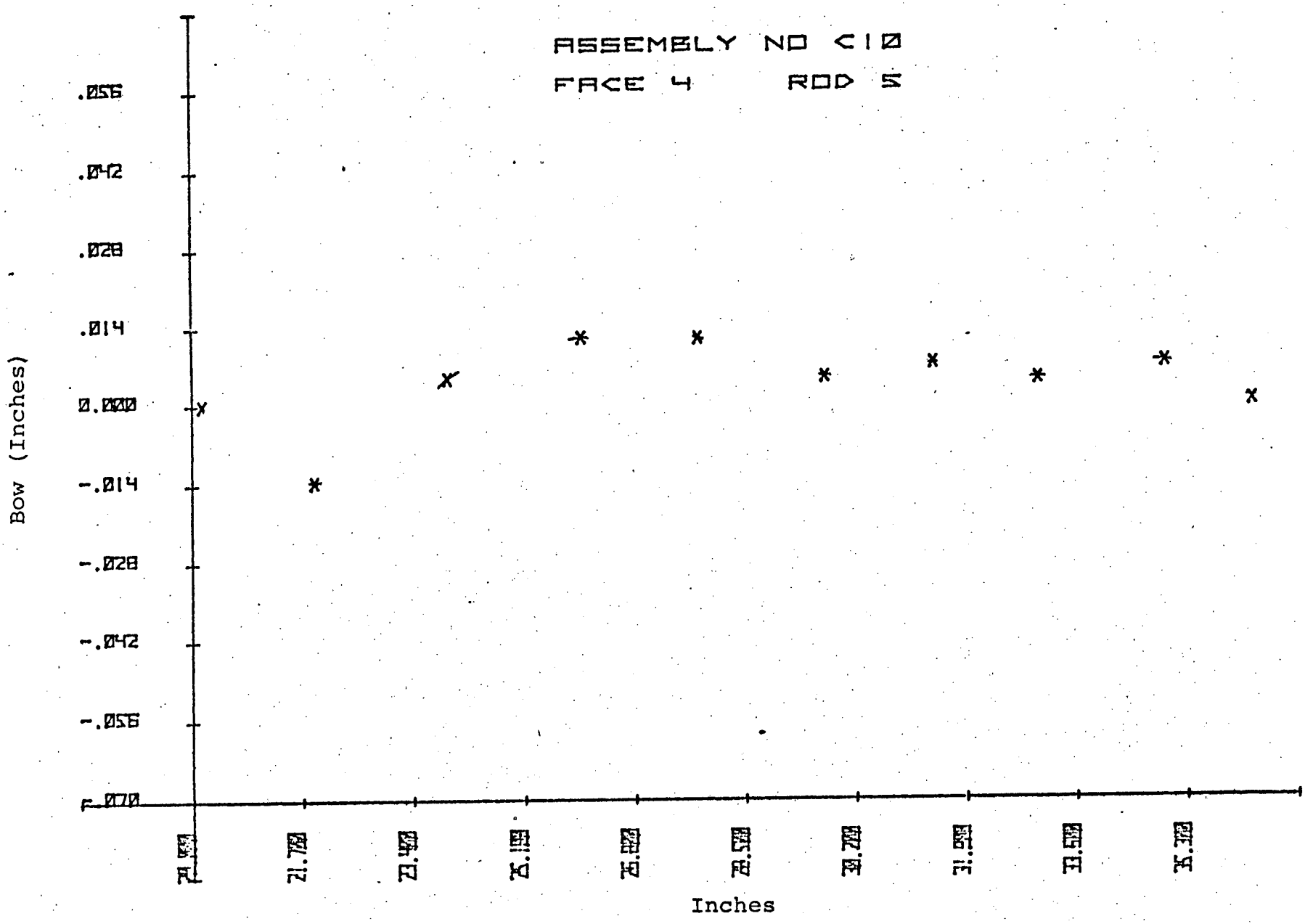

Figure 69 Bow of Rod 5, Face 4 of Assembly C-10 between Grids 2 and 3

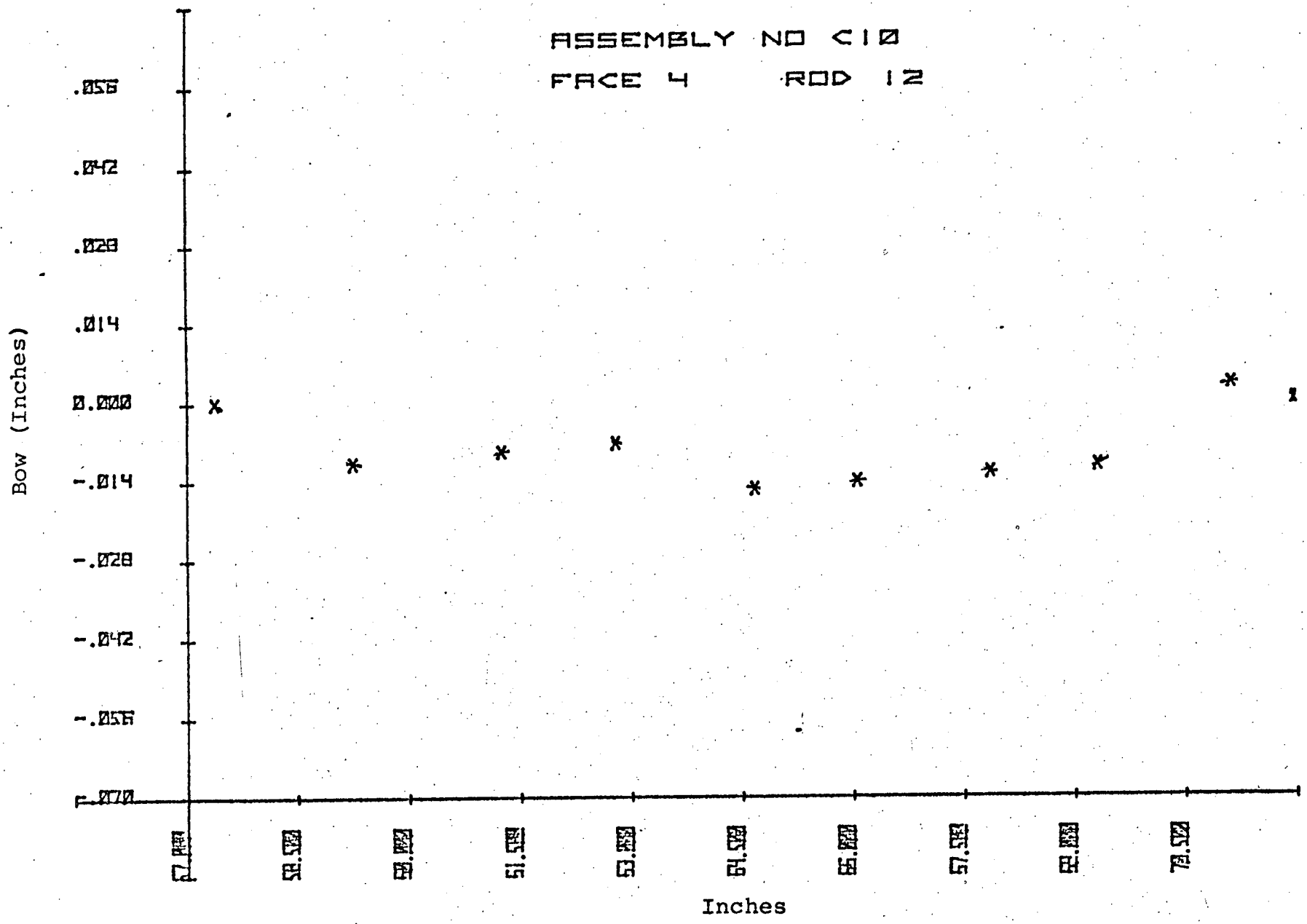

Figure 70 Bow of Rod 12, Face 4 of Assembly C-10 between Grids 4 and 5